



UNIVERSITA' DEGLI STUDI DI VERONA
Department of Neurosciences, Biomedicine and Movement Sciences

PHD SCHOOL OF LIFE AND HEALTH SCIENCES
Doctoral program in Neuroscience, Psychological and Psychiatric
Sciences, and Movement Sciences

CYCLE XXXV/2019




**IMMUNOPATHOLOGY OF INTRATHECAL
INFLAMMATION IN MULTIPLE SCLEROSIS: CLINICAL,
RADIOLOGICAL AND IMMUNOLOGICAL CORRELATES**
S.S.D. MED/26

Coordinator: Prof.ssa Rimondini Michela
Tutor: Prof. Calabrese Massimiliano
Dr.ssa Roberta Magliozzi

PhD candidate: Dr. Damiano Marastoni

This work is licensed under a Creative Commons Attribution-NonCommercial-NoDerivs 3.0 Unported License, Italy. To read a copy of the licence, visit the web page:

<http://creativecommons.org/licenses/by-nc-nd/3.0/>

-  **Attribution** — You must give appropriate credit, provide a link to the license, and indicate if changes were made. You may do so in any reasonable manner, but not in any way that suggests the licensor endorses you or your use.
-  **NonCommercial** — You may not use the material for commercial purposes.
-  **NoDerivatives** — If you remix, transform, or build upon the material, you may not distribute the modified material.

Immunopathology of intrathecal inflammation in multiple sclerosis: clinical and radiological correlates

Damiano Marastoni

PhD thesis

Verona, 24 September 2023

ISBN 12324-5678-910

INDEX

ABSTRACT

1. MULTIPLE SCLEROSIS _____ **7**

- 1.1 Historical Overview
- 1.2 Epidemiology
- 1.3 Risk Factors
- 1.4 Pathogenesis
- 1.5 Pathology of MS
- 1.6 Clinical manifestations
- 1.7 Disease course and phenotypic classification
- 1.8 Clinical and paraclinical assessments

2. INTRATHECAL INFLAMMATION IN MULTIPLE SCLEROSIS _____ **27**

- 2.1 Meningeal inflammation and cortical demyelination
- 2.2 Chronic active lesions
- 2.3 Axonal damage and neuronal loss

3. AIM OF STUDIES _____ **29**

4. CLINICAL CORRELATES: HIGH LEVELS OF PERIVASCULAR INFLAMMATION AND ACTIVE DEMYELINATING LESIONS AT TIME OF DEATH ASSOCIATED WITH RAPIDLY PROGRESSIVE MULTIPLE SCLEROSIS DISEASE COURSE: A RETROSPECTIVE POST-MORTEM COHORT STUDY _____ **30**

- 4.1 Introduction
- 4.2 Methods
- 4.3 Results
- 4.4 Discussion

5. RADIOLOGICAL CORRELATES: CORTICAL LESION LOAD AT DIAGNOSIS PREDICTS PROGRESSION INDEPENDENT OF DISEASE ACTIVITY AND LONG TERM DISABILITY ACCUMULATION IN MULTIPLE SCLEROSIS _____ **49**

- 5.1 Introduction

5.2 Methods

5.3 Results

5.4 Discussion

**6. MARKERS OF INTRATHECAL INFLAMMATION:
CSF LEVELS OF CXCL12 AND OSTEOPONTIN AS EARLY MARKERS
OF PRIMARY PROGRESSIVE MULTIPLE SCLEROSIS _____ 67**

6.1 Introduction

6.2 Methods

6.3 Results

6.4 Discussion

**7. CSF OSTEOPONTIN IS ASSOCIATED WITH CORTICAL DAMAGE
AND DISABILITY ACCUMULATION IN EARLY MULTIPLE
SCLEROSIS _____ 79**

7.1 Introduction

7.2 Methods

7.3 Results

7.4 Discussion

**8. INTRATHECAL INFLAMMATORY PROFILE PREDICT DISABILITY
PROGRESSION INDEPENDENT OF RELAPSE ACTIVITY IN EARLY
MULTIPLE SCLEROSIS _____ 94**

8.1 Introduction

8.2 Methods

8.3 Results

8.4 Discussion

9. CONCLUSIONS _____ 107

10. REFERENCES _____ 108

ABSTRACT

Intrathecal inflammation is a key factor that drives disability accumulation in Multiple Sclerosis (MS), since early disease phases. Clinical, radiological, and cerebrospinal fluid markers that correlate with chronic intrathecal inflammation are advocated.

i) To better clarify its clinical correlates, a post-mortem autopsy cohort study was performed on 269 progressive MS cases. The presence of early active lesions (EALs) and the extent of perivenular inflammation were examined. A subset of patients (n=87) already underwent characterization for the presence/absence of meningeal infiltrates and a detailed count of the CD20+ B cells and CD3+ T cells in perivenular infiltrates (n=22). EALs were detected in 22% of the examined cases, while high levels of perivascular inflammation were detected in 52% of cases. High levels of both active lesions and focal perivenular inflammation, enriched in B cells and associated with meningeal inflammation, within the white matter at post-mortem were associated with rapid disease evolution from onset and to the terminal stages.

ii) Several observations suggested that cortical lesions are a frequent and early phenomenon in MS and one of the major drivers of disability accumulation, being associated with chronic intrathecal inflammation. We evaluated 199 relapsing-remitting MS (RRMS) patients who underwent brain and spinal cord MRI examinations at the time of diagnosis, including assessment of cortical lesions (CLs) by Double Inversion Recovery sequences. All patients had regular clinical median follow-up for 18 years (range 15-22). Confirmed disability worsening (CDW) was assessed, based on EDSS increase by ≥ 1.5 , 1 or 0.5 points according to baseline EDSS (0, < 5.5 or ≥ 5.5 , respectively). Progression independent of relapse activity (PIRA) was referred as a 6-month CDW in which the Expanded Disability Status Scale (EDSS) worsening was sustained in all following assessments. The time to PIRA events, conversion to SPMS and to the EDSS score milestones of 4.0 and 6.0 was recorded. Eighty-three patients (41.7%) had PIRA after a mean of 7.6 ± 3.6 yrs. Patients with PIRA had increased CLn and volume compared to those without PIRA events. After random survival forest, higher CLn, CLv, and EDSS were factors best associated with the risk of experiencing PIRA. Multivariate regression (with MRI, demographics, clinical variables including therapies) confirmed a higher number of CLs, a larger CLv and higher EDSS as predictive of PIRA. Higher CLv, CLn, baseline EDSS and presence of SC lesions were best predictors of EDSS ≥ 4 and ≥ 6 with the above-mentioned models. ROC analysis estimated at least 3 CLs as the optimal cut-off to identify patients more likely to develop SPMS (≥ 3 , HR 12.2 [CI 3.55- 41.8], $p < 0.001$). Finally, 2-year accumulation of new CLs predicted SPMS (HR 1.3 [CI 1.1-1.5], $p < 0.001$), and achievement of EDSS ≥ 4 and ≥ 6 (HR 1.28 [CI 1.09-1.51], $p = 0.002$, and HR 1.39 [CI 1.12-1.73], $p = 0.003$, respectively). Concluding, early accumulation of focal cortical damage is an independent predictor of sustained disability progression and long-term disability.

iii) Candidate cerebrospinal fluid (CSF) markers of intrathecal inflammation are advocated. 67 CSF markers were evaluated at the time of diagnosis with Multiplex assay in patients with both primary progressive MS and RRMS.

CXCL12 and Osteopontin (OPN) revealed significantly increased in those patients experiencing a progressive course of the disease. OPN resulted best associated with accumulating cortical atrophy and confirmed disability worsening after two years of follow-up in a group of 107 patients with RRMS.

Finally, the predictive value of CSF markers on developing PIRA events was evaluated in a retrospective study. Many markers, particularly related to TNF superfamily (sTNFR1, LIGHT) as well as OPN were increased in those patients developing PIRA events (23 out of 80), and were confirmed in those with PIRA events and no radiological activity during the follow-up. This suggests that a specific intrathecal inflammatory profile characterizes patients at higher risk of PIRA since early disease phases. Further studies are needed to evaluate the efficacy of anti-inflammatory treatments, particularly those acting intrathecally, in preventing PIRA events and subsequent disability.

1.MULTIPLE SCLEROSIS

1.1 Historical overview

Self-reported descriptions of symptoms attributable to Multiple Sclerosis (MS) were offered by famous historical figures, such as Sir Augustus D’Este and Bruce Frederick Cummings (Pearce 2005). The first exhaustive description of MS is reported in a lecture held by Jean Martin Charcot (1825-1893, Figure 1.1) at the Salpêtrière university in Paris in 1868; he named the disease “sclérose en plaques” and identified the signs “intention tremor, nystagmus, and scanning speech” (known as Charcot’s triad) as pathognomonic of MS (Horwitz 1995).



Figure 1.1: Charcot examining a brain, depicted by this student Brissaud. Adapted from *Nouvelle Iconographie de la Salpêtrière*, Paris 1894.

In 1837 Sir Robert Carswell (1793–1857) depicted the anatomopathological features of MS plaques, without drawing any clinic-pathological correlations; in 1842 Jean Cruveilhier (1791–1874) independently described the anatomopathological appearance of MS lesions. Using Camillo Golgi and Santiago Ramon y Cajal’s, new staining techniques with silver and gold to enhance the microscopic visibility of neurones, James Dawson at Edinburgh in 1916 examined a series of MS brains and gave a full account of the neuropathology, describing the inflammatory damage to myelin and blood vessels.

1.2 Epidemiology

Recent estimates suggest that about 2.8 million people worldwide are affected by MS, with a global prevalence of 36 cases/100,000 people. MS is present in all the regions of the world, but its prevalence varies widely across countries, ranging from 336 and 303 cases/100,000 inhabitants for the areas with highest prevalence (San Marino and Germany respectively) to less than 40 cases/100,000 inhabitants for those with lowest prevalence. These differences might, at least in part, be attributed to potential report biases in some regions and to different opportunity for the resident population to access to care and to instrumental diagnostic tools. The presence of a different geographical distribution of MS was observed since the first epidemiological studies performed in the Twenties and it was speculated that it might be at least in part due to hereditary factors and migratory fluxes (Davenport, 1922). The concept of “latitudinal gradient” was used to indicate that people living at lower latitudes were at lower risk of MS compared to those living at higher latitudes. According to the latest Atlas of MS (3rd edition, September 2020), Europe and Americas show the highest estimated prevalence (133 and 112 cases/100,000 people respectively), while Africa and the West Pacific are the World Health Organization (WHO) regions with the lowest prevalence (5 cases /100,000 people). Italy is a high-risk area for MS and estimates of prevalence rates in 2015 ranged from 122 to 232 cases per 100,000 with an average of 176 per 100,000 in the mainland and Sicily, and from 280 to 317 with an average of 299 per 100,000 in Sardinia (Battaglia and Bezzini 2017). Females are more affected than males and the mean female to male ratio is 2.5:1 (Orton, Herrera et al. 2006). Disease onset typically occurs in the II-IV decades; incidence of MS is low in childhood and rapidly increases after adolescence, reaching a peak between 25 and 35 years, and then slowly declines (Koch- Henriksen 1999).

1.3 Risk factors

Although MS pathogenesis is still unknown, both environmental and genetic risk factors for the disease have been identified. A genetic predisposition to the disease was firstly suggested by epidemiological studies reporting heritability within families, with an increase in risk of MS proportional to the amount of the genetic background shared among individuals (Compston and Coles 2002). Accordingly, the risk of MS is highest in monozygotic twins of an affected individual, with rates of concordance of 25% (Hansen, Skytthe et al. 2005) in north Europe populations and of 10-15% in southern Europe regions (Ristori, Cannoni et al. 2006). The rates of concordance are progressively reduced to 5% in dizygotic twins and 3% in siblings (Ebers, Bulman et al. 1986, Willer, Dyment et al. 2003). The strongest genetic association with MS was identified in the major

histocompatibility complex (MHC) genes, located in chromosome 6p21.3. This area encodes for genes with a relevant role in the regulation of the immune system, included the transplantation human leukocyte antigen (HLA) genes encoding for membrane glycoproteins which have a role in the presentation of small peptide antigens to MHC-restricted T cells. The HLA locus accounts for 20–30% of genetic susceptibility in MS and the association was first identified in the 1970s (Jersild, Svejgaard et al. 1972); the main MS susceptibility maps to the HLA-DRB1 locus in the class II region of the MHC (Haines, Terwedow et al. 1998). Carriers of the HLA DRB1*15:01 allele show on average a threefold risk of developing MS compared to non-carriers, with a dose-response to the number of allele copies carried by the individual (Barcellos, Oksenberg et al. 2002).

Genome-wide association studies (GWAS) gave further insight into genetics of MS, uncovering more than 200 autosomal susceptibility variants outside the MHC, one chromosome X variant, and 32 independent associations within the extended MHC, which could jointly account for ~48% of the estimated heritability for MS (International Multiple Sclerosis Genetics 2019). Enrichment for MS susceptibility loci was apparent in many different immune cell types and tissues; amongst CNS cells, enrichment was detected in microglia. Such observations highlighted a potential role in MS pathogenesis of processes relating to the development, maturation, and terminal differentiation of B, T, natural killer, and myeloid cells. Single nucleotide polymorphisms associated to MS were detected in genes of interleukin (IL) 2 and 7 receptor alpha (IL2RA and IL7 RA) and CD58, TYK2, STAT3, TNFRSF1A (Sawcer, Franklin et al. 2014, Baranzini and Oksenberg 2017).

Besides genetic background, lifestyle and environmental risk factors can contribute to the development of MS. Well established risk factors include Epstein–Barr virus (EBV) infection (Bjornevik et al., 2022), smoking, lack of sun exposure or low levels of vitamin D, adolescent obesity. Exposure to organic solvents and working night shifts are less established risk factors (Olsson, Barcellos et al. 2017). Most of the environmental risk factors seem to have the greatest effect during adolescence, as suggested by migration studies which showed that individuals moving from a definite risk area to another geographical area bearing a different MS risk maintain the risk of the native region if the migration occurs after the adolescence (Cabre, Signate et al. 2005).

1.4 Pathogenesis

Th1 cells and Th17 cells appear the main CD4⁺ T cell subsets implicated in the disease, even if their relative importance in MS pathogenesis is still debated (Dendrou, Fugger et al. 2015). CD8⁺ T cells are found in higher frequency than CD4⁺ T cells in white matter and in grey matter demyelinating lesions, and their

numbers closely correlate with axonal damage (Frischer, Bramow et al. 2009). Up to a quarter of CD8⁺ T cells infiltrating active lesions of pwMS produce IL-17 and are thus thought to be mucosa-associated invariant T cells, MAIT (Willing, Leach et al. 2014).

Increasing evidence on the role of B cells in MS pathophysiology is emerging, as initially suggested by the effect of monoclonal antibodies targeting this cell population (Li, Patterson et al. 2018). Oligoclonal antibodies produced by intrathecal B cells are detectable in the CSF of pwMS and are of diagnostic value; moreover, clonally expanded B cells can be found in the meninges, parenchyma and CSF (Lovato, Willis et al. 2011). In the meninges of pw secondary-progressive (SP-) MS tertiary lymphoid structures of aggregated plasma cells, B cells, T cells and follicular dendritic cells were described (Howell, Reeves et al. 2011). Maturation of antigen-experienced B cells can occur in draining cervical lymph nodes before their transmigration to the CNS (Stern, Yaari et al. 2014), thus supporting the rationale of treatment targeting B cells in the peripheral compartment. Besides adaptive immune cells, invariant NK, γ/δ T cells and MAIT have been suggested to play a role in the pathogenesis of MS; a dysregulation of innate immunity may indeed promote pro-inflammatory differentiation of T cells or facilitate peripheral activation of autoreactive T cell clones, e.g. through priming induced by the release of extracellular traps from activated peripheral neutrophils (Tillack, Breiden et al. 2012). Furthermore, CNS resident innate immune cells switched into activated phenotypes might be directly responsible for neurodegenerative changes in progressive phases of the disease (Gandhi, Laroni et al. 2010).

All the aforementioned processes are predominant over the early phases of MS, which are characterized by extensive CNS inflammation with parenchymal immune cell infiltrates and leakage of the BBB. Over disease course, a progressive reduction of the extension of parenchymal infiltrates and formation of new lesions occurs, coupled with persistence of lymphomononuclear infiltrates surrounding blood vessel with intact BBB, this latter phenomenon referred to as compartmentalized inflammation (Meinl, Krumbholz et al. 2008). On the clinical ground, this phase of the disease (progressive MS) is characterized by a subtle and progressive accumulation of disability, occurring in a relapse-independent manner, which is no or only minimally halted by currently available disease modifying treatments (DMTs) that mainly target peripheral immune cell activation or block entering of activated cells into the CNS. In this latter phase, neurodegenerative phenomena appear to overwhelm inflammation and are presumed to be the main driver of irreversible disability accrual (Lassmann 2018).

It is still matter of debate whether neurodegeneration is a process separate from inflammation or not, (Hutchinson 2015, Louapre and Lubetzki 2015) and the

mutual relationship between these two processes is yet to be elucidated (Lassmann 2018). Moreover, recent observations suggest that brain atrophy and disability accrual start early on disease course and that in the relapsing MS progression of disability might occur even in the absence of relapse activity (“silent progression”) (University of California, Cree et al. 2019).

Direct cell to cell interaction and soluble factors released in the extracellular space might both contribute to the progressive tissue damage leading to neuronal death and oligodendrocyte disruption. Among these, reactive oxygen and nitrogen species (ROS and RNS) released in the CNS microenvironment by innate immune cells (oxidative burst) may be pivotal in inducing irreversible damage and degenerative processes; these phenomena might be further enhanced by the extracellular release of iron by disrupted astrocytes. Oxidative stress may induce accumulation of mutations in the mitochondrial DNA, thus resulting in mitochondrial dysfunction and energetic failure, that could exert an even more detrimental effect in partially demyelinated axons which underwent a redistribution of ionic channels with consequent intracellular accumulation of calcium and potentially pro-apoptotic changes (Lassmann and van Horssen 2011).

1.5 Pathology of MS

The anatomopathological hallmark of MS is the presence of large focal confluent lesions in the white (WM) and grey matter (GM) of the CNS characterized by primary demyelination and a variable extent of axonal loss, which were described since the first historical studies (Charcot 1877). In 1916, James Dawson reported that inflammation and myelin damage in MS brain were localized around blood vessels and described plaques expanding at their edges towards the surrounding normal-appearing white matter (NAWM) (Dawson 1916). A selective and primary perivenous demyelination with the destruction and loss of oligodendrocytes is typical of MS and is associated with activation of astrocytes followed by the formation of gliotic scars as the lesion becomes inactive (Lassmann 2018). Preservation of axons occurs at a larger extent than myelin loss, and the amount of axonal destruction is variable between different patients and even between lesions in the same patient (Lassmann 1999).

Inflammatory infiltrate consisting of T lymphocytes, B lymphocytes, and plasma cells is detected in and around MS plaques (including NAWM) and is described in all stages of the disease, even if it is most evident within actively demyelinating lesions (Frischer, Bramow et al. 2009). In 2000, 4 patterns of actively demyelinating lesions were defined (Lucchinetti, Bruck et al. 2000). In patterns I and II, active demyelination was associated with a T-lymphocyte- and macrophage- dominated inflammation. Pattern II lesions were characterized by a prominent deposition of immunoglobulins (mainly IgG) and complement C9neo

antigen at sites of active myelin destruction, which were not detected in pattern I lesions. Plaques showing pattern I or II were typically centred on small veins and venules and lesion edges were sharply demarcated. A variable loss of oligodendrocytes at the border of active pattern I and II lesions was described; reappearance of high numbers of oligodendrocytes in the inactive plaque centre was associated with a high incidence of remyelinated shadow plaques. Pattern III lesions also contained an inflammatory infiltrate (mainly T lymphocytes, with macrophages and activated microglia) without deposition of Ig and complement. Demyelination was not centred by veins and lesion edges were ill defined due to diffuse spread into the surrounding WM. The pattern of demyelination demonstrated a pronounced loss of oligodendrocytes at the active plaque border, with inactive centre almost completely devoid of oligodendrocytes. In pattern IV lesions an inflammatory infiltrate dominated by T lymphocytes and macrophages is also detected, again with absence of deposition of Igs and complement. Demyelination was associated with oligodendrocyte death and this generally was associated with a sharply demarcated plaque of demyelination with radial expansion of the lesion and a nearly complete loss of oligodendrocytes in active as well as inactive areas. Both pattern III and IV lesions were characterized by the absence of remyelinated shadow plaques. This latter two patterns were suggestive of a primary oligodendrocyte dystrophy, rather than autoimmunity. Heterogeneity of distribution of these patterns was observed between patients, while multiple active lesions from the same patient showed a homogeneous pattern. Lesions can be further classified based on the active/inactive status; MS pathology is heterogeneous and changes over time: active lesion patterns are typically observed in patients who had died in early disease stages, such as acute MS or relapsing remitting MS (Frischer, Weigand et al. 2015); on the other hand, brain from patients affected by progressive MS show mostly inactive or chronic active lesions. A recent consensus classification suggested classifying MS lesions as active, mixed active/inactive, or inactive, based on the presence/absence and distribution of macrophages/microglia (inflammatory activity) and the presence/absence of ongoing demyelination (demyelinating activity) (Kuhlmann, Ludwin et al. 2017, Figure 1.2). Active lesions are characterized by macrophages/microglia throughout the lesion area, whereas mixed active/inactive lesions have a hypocellular lesion centre with macrophages/microglia limited to the lesion border. Active and mixed active/ inactive lesions can be further subdivided into lesions with ongoing myelin destruction (demyelinating lesions, further divided into early and late demyelinating) and lesions in which the destruction of myelin has ceased, but macrophages are still present (post-demyelinating lesions). Inactive lesions are almost completely lacking macrophages/microglia.

Active demyelination is characterized by the presence of phagocytic cells showing

a morphological phenotype of activated microglia, most of them showing a foamy morphology, with presence of myelin degradation products within the cytoplasm of macrophages/microglia (Prineas 1985, Bruck, Porada et al. 1995). Staging of the activity of a demyelinating lesion is defined by the immunocytochemical profile of different minor and major myelin proteins within the degradation products deriving from remnants of the destroyed myelin sheaths contained in macrophages (Bruck, Porada et al. 1995).

Slowly expanding lesions or smoldering lesions (SELs) were included among mixed active/inactive lesions. SELs are characterized by a hypo-cellular core with paucity of inflammatory infiltrates and a rim of iron-laden macrophages/activated microglia at the lesion's edges, and are supposed to progressively expand towards the surrounding white matter. The rim of iron-laden macrophages has been suggested as a potential hallmark of chronic active vs inactive lesions. No leakage of the BBB is detectable in chronic active lesions and the ongoing inflammatory process acting beyond a "closed" or repaired BBB is considered the pathological correlate of compartmentalized inflammation (Meinl, Krumbholz et al. 2008). Proportion of SELs increases over time during disease course and is higher in progressive vs relapsing disease: an anatomopathological study on 120 MS brain donors showed that SELs were rare in the acute monophasic disease and in the RR phase, whilst they represented around 20% of the lesions analysed in SP-MS and PP-MS cases or in cases with disease duration longer than 30 years (23%) (Frischer, Weigand et al. 2015). Another study on 182 MS brain donors confirmed that the frequency of chronic active lesions was higher in progressive vs relapsing form of the disease and that patients who had a more severe disease course showed a higher proportion of mixed active/inactive lesions and a higher lesion load at the time of death (Luchetti, Fransen et al. 2018). These observations suggested that SELs might be the anatomopathological hallmark of progression independent from relapse activity (PIRA).

Inactive lesions are the most abundant lesion in MS brains and are characterized by a sharply demarcated border and primary demyelination, with partial axonal preservation and reactive gliosis. A variable degree of microglia activation is present in the periplaque white matter, whereas the number of microglia is profoundly reduced in the centre of the demyelinated plaque and fibrillary scar tissue fills the spaces between demyelinated axons (Hametner, Wimmer et al. 2013). Recruitment and differentiation of oligodendrocyte progenitor cells may induce partial remyelination of demyelinated MS lesions (Prineas, Barnard et al. 1993), but efficiency of the remyelination process is variable and seems to be influenced by several factors, such as the presence of progenitor cells and their potential of differentiation into mature myelinating oligodendrocytes (Chang, Tourtellotte et al. 2002), the presence and functional properties of axons, the

occurrence of repeated demyelination of remyelinated areas (Bramow, Frischer et al. 2010), age and disease progression (Goldschmidt, Antel et al. 2009). Even if MS has been traditionally considered a WM disease, also grey matter (GM) is heavily affected by and GM damage starts early in the disease and substantially affects clinic and cognitive functioning (Geurts and Barkhof 2008). Cortical lesions can be classified into 4 categories, according to the extension of involvement of the cortex (Bø, Vedeler et al. 2003). Type 1 lesions are present at the cortico- subcortical border and affect the grey as well as the white matter (cortical/juxta-CL lesions). Type 2 lesions are small peri-venous intracortical lesions. Type 3 lesions are located in the subpial layers of the cortex and are associated with inflammation in the meninges and they expand from the pial surface into the deeper cortical layers (Howell, Reeves et al. 2011). A type 4 lesion affects the entire cortex but does not extend beyond the grey-white matter junction. Both cortical and subcortical GM are involved, and MS lesions were described also in cerebellar cortex (Kutzelnigg, Faber-Rod et al. 2007), deep GM nuclei (Vercellino, Masera et al. 2009), and GM of the spinal cord (Lassmann 2018).

Infiltrates of inflammatory cells, mainly T and B lymphocytes and plasma cells, have been described in the leptomeninges of pwMS (Bø, Vedeler et al. 2003). Accumulation of B cells in the context of ectopic tertiary lymphoid structures, morphologically resembling secondary lymphoid follicles, have been demonstrated within the inflamed meninges of a subgroup of post-mortem acute and progressive MS cases with more rapid and severe disease progression (Serafini, Rosicarelli et al. 2004, Bevan, Evans et al. 2018). Approximately 40% of all examined SPMS cases harboured at least one detectable lymphoid- like structure in their forebrain meninges, mainly containing aggregates of B cells interacting with a network of follicular dendritic cells, and with T cells and plasma cells (Aloisi and Pujol-Borrell 2006). The presence of follicle-like structures in pwMS correlates with the extent of the adjacent subpial cortical grey matter demyelination, with a “surface-in” gradient of subpial cortical neurodegeneration and microglia activation, and with a more severe and rapid disease progression (Magliozzi, Howell et al. 2010, Howell, Reeves et al. 2011, Bevan, Evans et al. 2018).

Diffuse injury in the NAWM is prominent in MS, mostly in patients in the progressive stages of the disease. It consists of small perivascular inflammatory infiltrates, some diffuse infiltration of the tissue (mainly CD8+ T cells), diffuse axonal injury with secondary demyelination, reactive astrocytic scarring and global microglia activation. The presence of ongoing axonal damage in the absence of actively demyelinating lesions may reflect secondary anterograde or retrograde degeneration due to axonal or neuronal damage, that has occurred even

months before (Singh, Dallenga et al. 2017, Lassmann 2018). Inflammation in the meninges could contribute to diffuse axonal damage in the NAWM of the spinal cord, and a similar process may trigger neuronal loss in the normal appearing cortex (Androdias, Reynolds et al. 2010).

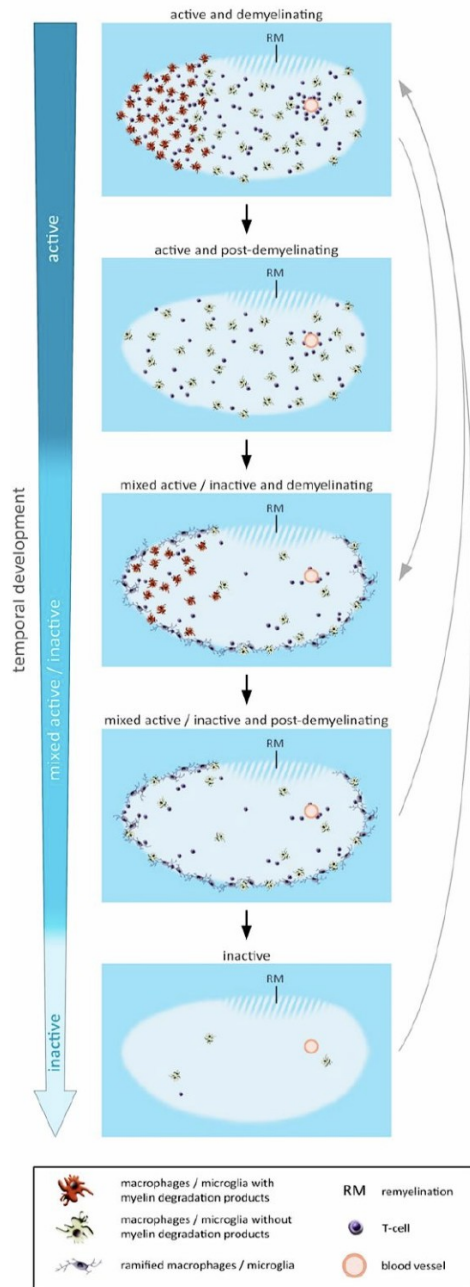


Figure 1.2: Schematic diagram summarizing the temporal development of MS lesions. Reproduced from ref. Kuhlmann, Ludwin et al. 2017.

1.6 Clinical manifestations and diagnosis

Onset of MS

Clinical presentation of MS is heterogenous, being potentially affected every area of the CNS. However, the frequent involvement of a few areas allows the identification of a few clinical pictures recognized as typical demyelinating episodes. The first clinical manifestation consistent with a typical demyelinating episode is named clinically isolated syndrome (CIS): a monophasic episode of neurological syndrome with acute/subacute onset showing clinical features which are characteristic of a typical inflammatory demyelinating event (e.g. optic neuritis, transverse myelitis, brainstem or cerebellar syndrome). CIS shares epidemiological features with MS (female predominance, age at onset 20-40 years in most of the cases) and the risk of conversion to clinically definite MS varies according to clinical and paraclinical factors, such as presenting symptoms, presence of oligoclonal bands (OCBs) in the CSF, number and distribution of demyelinating lesions at brain MRI. Follow-up studies on patients with CIS showed rate of conversion to MS of 10-85% for cases with optic neuritis, 41-61% for myelitis and 53-60% for brainstem presentations (Miller, Chard et al. 2012).

Main clinical manifestations

Typical neurological manifestations of CIS could occur over disease course and are defined as relapses once the diagnosis of clinically definite MS has been made. A relapse is defined as monophasic clinical episode with patient-reported symptoms and objective findings typical of multiple sclerosis, reflecting a focal or multifocal inflammatory demyelinating event in the CNS, developing acutely or sub-acutely, with a duration of at least 24 h, with or without recovery, and in the absence of fever or infection. Attack, relapse and exacerbation are synonyms (Thompson, Banwell et al. 2018).

Other symptoms typically experienced by pwMS include fatigue and cognitive impairment. Fatigue is disabling symptom experienced by 50-80% of pwMS, mainly in progressive forms, and it affects quality of life of the individual due to the potential impairment of sleep and mood. Fatigue is defined as a reversible motor and cognitive impairment, with reduced motivation and desire to rest. It could appear spontaneously or may be brought on by mental or physical activity, humidity, acute infection and food ingestion. It is relieved by daytime sleep or rest without sleep. It could occur at any time but is usually worse in the afternoon (Mills and Young 2008). Cognitive impairment is reported in 40-60% of pwMS and the main domains involved are complex attention, executive functions and

long-term memory. The most common clinical picture is characterized by a mild cognitive impairment, while severe impairment or dementia are rarely reported (Chiaravalloti and DeLuca 2008). Lesion load and distribution and brain atrophy correlate with cognitive dysfunction (Korakas and Tsolaki 2016).

Diagnosis of MS

Diagnostic criteria

Diagnosis of MS is formulated based on clinical grounds with support of MRI and other paraclinical parameters. Diagnostic criteria were firstly suggested by Allison and Millar in 1954 and standardized by Schumacher in 1965, when MS was defined as “symptoms and signs of neurological dysfunction indicating multiple and separate lesions in the central nervous system. Symptoms appear longitudinally” (Schumacher, Beebe et al. 1965). This introduced the concepts of dissemination in space (DIS) and in time (DIT) of disease activity and gave a definition of relapse; the need for the exclusion of other potential causes of the disease (“no better explanation” criteria) was also suggested. With the revision of the criteria performed in 1983 by Poser et al. (Poser, Paty et al. 1983), paraclinical tests such as evoked potential and CSF analysis were introduced to detect an asymptomatic involvement of the CNS which might allow to meet the DIS and DIT criteria; this could anticipate MS diagnosis even in case of a single clinical episode, if evidence for CIS and DIT was provided. Detection of oligoclonal bands (OCBs) in the CSF was considered as a laboratoristic support for the diagnosis of MS. Evidence of demyelinating lesions detectable with MRI was added as supportive criteria in the 2001 revision of diagnostic criteria (McDonald, Compston et al. 2001). Further revisions were made in 2005 (Polman, Reingold et al. 2005) and 2010 (Polman, Reingold et al. 2011), mainly consisting in modification of the radiological criteria and of the role of CSF.

In 2016, the MAGMINS (Magnetic resonance imaging in MS) study group suggested a further revision of the MRI criteria, taking into consideration newly emerging MRI techniques (Filippi, Rocca et al. 2016). The suggested modifications included: extension of CNS area adopted for the DIS criteria to include also cortical regions and optic nerve; requirement of at least 3 lesions in the peri-ventricular area; abolition of any differences between symptomatic and asymptomatic lesions for the DIT criteria; adoption of the same DIS criteria for the diagnosis of both relapsing and progressive forms of disease. The adoption of the central vein sign as a marker of MS in the differential diagnosis with white matter lesions of other aetiology was hypothesized, but considered not yet applicable in clinical setting. These suggestions were partially included in the last revision of the criteria, published in 2017, Table 1.1 (Thompson, Banwell et al. 2018).

Diagnostic criteria for patients with an attack at onset		
	Number of lesions with objective clinical evidence	Additional data needed for a diagnosis of MS
≥ 2 clinical attacks	≥ 2	None*
≥ 2 clinical attacks	1 (as well as clear-cut historical evidence of a previous attack involving a lesion in a distinct anatomical location†)	None*
≥ 2 clinical attacks	1	Dissemination in space demonstrated by an additional clinical attack implicating a different CNS site OR by MRI‡
1 clinical attack	≥ 2	Dissemination in time demonstrated by an additional clinical attack OR By MRI§ OR demonstration of CSF-specific oligoclonal bands¶
1 clinical attack	1	Dissemination in space as defined above AND Dissemination in time as defined above

Diagnostic criteria for patients with a disease course characterised by progression from onset (PP-MS)	
1 year of disability progression (retrospectively or prospectively determined) independent of clinical relapse	<p>Plus two of the following criteria:</p> <ul style="list-style-type: none"> • One or more T2-hyperintense lesions° characteristic of MS in one or more of the following brain regions: periventricular, cortical or juxtacortical, or infratentorial • Two or more T2-hyperintense lesions° in the spinal cord • Presence of CSF-specific oligoclonal bands
<p>*No additional tests are required to demonstrate dissemination in space and time. However, unless MRI is not possible, brain MRI should be obtained in all patients in whom the diagnosis of MS is being considered. In addition, spinal cord MRI or CSF examination should be considered in patients with insufficient clinical and MRI evidence supporting MS, with a presentation other than a typical clinically isolated syndrome, or with atypical features. If imaging or other tests (eg, CSF) are undertaken and are negative, caution needs to be taken before making a diagnosis of MS, and alternative diagnoses should be considered.</p> <p>†Clinical diagnosis based on objective clinical findings for two attacks is most secure. Reasonable historical evidence for one past attack, in the absence of documented objective neurological findings, can include historical events with symptoms and evolution characteristic for a previous inflammatory demyelinating attack; at least one attack, however, must be supported by objective findings. In the absence of residual objective evidence, caution is needed. ‡The MRI criteria for dissemination in space are described in panel 5.</p> <p>§The MRI criteria for dissemination in time are described in Table 1-4.</p> <p>¶The presence of CSF-specific oligoclonal bands does not demonstrate dissemination in time per se but can substitute for the requirement for demonstration of this measure.</p> <p>°Unlike the 2010 McDonald criteria, no distinction between symptomatic and asymptomatic MRI lesions is required.</p>	

Table 1.1. The 2017 revision of McDonald criteria for the diagnosis of MS. Adapted from ref. (Thompson, Banwell et al. 2018)

The diagnosis of MS can be formulated if the 2017 McDonald Criteria are fulfilled and there is no better explanation for the clinical presentation. If MS is suspected by virtue of a CIS but the 2017 McDonald Criteria are not completely met, the diagnosis is possible MS. The last revision of the McDonald criteria was developed to facilitate earlier diagnosis of MS in patients presenting with typical demyelinating syndromes, rather than differentiate MS from other conditions, and therefore should be applied only in typical presentations. In patients presenting with atypical or nonspecific neurologic syndromes, or typical syndromes with concurrent red flags of possible better explanation (Miller, Weinshenker et al. 2008), accuracy of diagnostic criteria is reduced and additional clinical and radiographic monitoring are necessary before making a definitive diagnosis of MS (Solomon, Naismith et al. 2019).

1.7 Disease course and phenotypic classification

The first classification of disease course was published in 1996, and four disease courses were identified, according to the occurrence of relapses and/or disability progression: relapsing-remitting (RR), secondary progressive (SP), primary progressive (PP) and progressive-relapsing (PR) (Lublin and Reingold 1996).

A relapse is defined as a worsening of neurological impairment or an appearance of a new symptom or abnormality attributable to MS, lasting at least 24 hours and preceded by stability of at least 1 month (Poser, Paty et al. 1983). RRMS is the presenting form of MS in about 85% of the cases; it is characterized by alternating periods of neurological dysfunction (relapses) and relative clinical stability free of new neurological symptoms (i.e. remission),

Natural history studies on MS suggest that between one-third and one-half of patients will enter the SP phase 15 years after disease onset (Confavreux, Vukusic et al. 2000).

SPMS is defined as a phase characterized by an objective worsening of neurological impairment without any recovery detected over a defined timeframe (e.g. 6 or 12 months), associated or not with relapse activity; periods characterized by fluctuation of symptoms or stability might occur in the progressive phases (Lublin, Reingold et al. 2014). The diagnosis of transition to SP-MS phase is most often established retrospectively, after a period of uncertainty which is reported to last 2.9 ± 0.8 years on average in one examined population; this is mainly due to the subtle and often fluctuating initial symptoms of early progression, coupled with a sort of reluctance to establish a diagnosis of progressive disease from the clinician, in the lack of approved therapies for this stage of the disease (Katz Sand, Krieger et al. 2014). This phenomenon might be attributable, at least in part, also to the difficulties in defining the transition to progressive disease; among

different definitions of SP phase, an analysis of the MSBase cohort study suggested to adopt the following one: disability progression by 1 EDSS step in patients with EDSS ≤ 5.5 or 0.5 EDSS steps in patients with EDSS ≥ 6 in the absence of a relapse, a minimum EDSS score of 4 and pyramidal functional system (FS) score of 2 and confirmed progression over ≥ 3 months, including confirmation within the leading FS (Lorscheider, Buzzard et al. 2016). This objective definition was more sensitive but less specific than the retrospective physicians' diagnosis and enabled the diagnosis of SP-MS more than 3 years earlier than the diagnosis date assigned by the treating physicians. The estimated mean period between disease onset and SP phase was of 21.4 (95% CI 19.5 to 23.1) years in a large cohort database study and by 6 and 15 (median time) years from disease onset 25% and 50% pwMS respectively, had SP-MS (Scalfari, Neuhaus et al. 2014). The rate of conversion to SP-MS was much higher during the first 15 years (25.8 patients/year) of disease duration than during the following 15 years (8.1 patients/year). More recent studies evaluating transition to SPMS during treatment era showed that this event occurs in between 15% and 30% of cases over long term follow-up (University of California, Cree et al. 2016). A few factors have been identified as predictor of earlier conversion to SP-MS; among these, male sex, older age at disease onset, higher relapse frequency in the first 2 years and extension of cortical pathology (Calabrese, Romualdi et al. 2013, Scalfari, Neuhaus et al. 2014, Scalfari, Romualdi et al. 2018). Natural history studies showed that about 50% of pwMS achieves EDSS of 3.0, 4.0 and 6.0 and SP phase after 20, 26, 30 and 23 years respectively since disease onset (Manouchehrinia, Beiki et al. 2017).

In 2010, a model of a two-stage disability progression was suggested by Leray et al. (Leray, Yaouanq et al. 2010), with a first stage probably dependant on focal inflammation and a second stage probably independent of current focal inflammation. This concept has currently changed: in a subgroup of pwRR-MS disability progression occurred independently from relapses or MRI activity (defined silent progression) to indicate an underlying neurodegenerative process with subtle emergence over the course of RR-MS (University of California, Cree et al. 2019). This process might act since the early stages of the disease, as supported by evidence of accelerated brain atrophy in those cases experiencing silent progression; moreover, it seems likely that the same process underlying silent progression is responsible also for transition to SPMS when the march of clinical worsening is more evident.

About 15% of pwMS develop a progressive accrual of disability since disease onset and are identified as PP-MS. Likely SP-MS, the rate of disability accrual is not uniform in PP-MS, and superimposed relapses as well as periods of relative disease stability might occur (Miller and Leary 2007). A fourth MS form named

PRMS was defined as presence of clinical relapses superimposed over a PP course. Whether progressive phase in SP-MS and PP-MS share similar pathophysiological mechanisms is matter of debate and increasing clinical, imaging, and genetic data suggest that differences between these two entities are more of a quantitative than qualitative nature. This might suggest that the different phenotypes are part of a disease spectrum modulated by individual genetic predisposition and environmental influences (Antel, Antel et al. 2012). Increased understanding of MS and its pathology, together with general concern that abovementioned clinical descriptors may no longer adequately reflect recently identified clinical aspects of the disease, prompted a re-examination of MS disease phenotypes, leading to a revision of their classification in 2013 (Lublin, Reingold et al. 2014). According to this latter, two main clinical courses were identified: relapsing and progressive, based on the presence of either relapse activity or disability progression. Relapsing phenotype is further divided into active and inactive form, being the first one characterized by the occurrence of clinical (e.g. relapses) and/or radiological (e.g. new/enlarging T2 lesions and/or gd enhancing lesions) signs of inflammatory disease activity. Progressive phenotype is characterized by disability progression determined on clinical examinations, and is further divided into 4 subgroups according to the presence of disease activity (as defined above) and/or disability progression: active and with progression, active but without progression, not active but with progression, not active and without progression (i.e. stable disease). The progressive phenotype encompasses both SP and PP course, while the PR-MS subtype was eliminated, as this latter was included in PP-MS phenotype with disease activity.

1.8 Clinical and paraclinical assessment

Disability scoring systems

The Expanded Disability Status Scale (EDSS) score is the most commonly used tool to evaluate the accumulation of disability and response to treatment in pwMS (Kurtzke 1983). The scale ranges from 0 (no neurological signs) to 10 (death due to MS), by 0.5 point steps (Figure 1.3). The score is determined by the combination of a set of sub-scores deriving from the assessment of 8 functional systems (FS: pyramidal, cerebellar, brainstem, sensory, bowel and bladder, visual, cerebral and other) and to the ambulation index. This latter is determined by the distance that the patient is able to walk without aid or rest (up to EDSS 4.0), the needing of assistance to walk (EDSS 6.0 e 6.5) or the restriction to a wheelchair (EDSS 7.0). Scores above 8 are determined by further disability which makes the patient dependent in daily living, up to death due to MS (EDSS 10). The not linearity of the scale, the overwhelming effect of pyramidal dysfunction and ambulation impairment over the other FS and the lack of an accurate exploration of the cognitive functions are known limitation of this tool. EDSS has therefore

only moderate accuracy in the representation of the clinical picture of a patient.

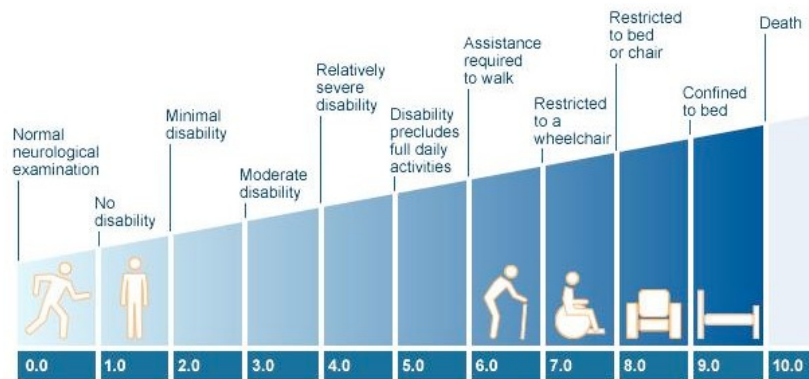


Figure 1.3: The Expanded Disability Status Scale (EDSS) score, the most commonly used tool to assess disability in pwMS. EDSS score ranges from 0 (absence of any neurological signs or symptoms) to 10 (death due to MS), by 0.5 point steps. EDSS is a not linear scale; up to score of 4, ambulation is not affected. Scores higher than 4 are determined by a restriction in ambulation, up to requirement of assistance (EDSS 6.0) and wheelchair (EDSS 7).

Magnetic resonance imaging

MRI is a useful tool in the diagnosis of MS, allowing the in vivo visualisation of demyelinating lesions and aiding in excluding other neurological diseases. As described above, demonstration of dissemination in time and space by MRI is adopted in the diagnostic criteria. MRI can provide valuable information at disease onset, (e.g. correlations between lesion load and prognosis), and over follow-up, e.g. to assess treatment response and to diagnose treatment-related adverse events, such as progressive multifocal leukoencephalopathy under natalizumab treatment (Wattjes, Rovira et al. 2015). Demyelinating WM lesions of MS show a round-ovoid shape with sharply demarcated borders and tend to confluence over time. Periventricular and juxta-cortical WM are typically affected, as well as the optic nerve, infratentorial regions and spinal cord (Figure 1.4). Active lesions are characterized by gadolinium enhancement, reflecting BBB disruption which is usually associated with new lesions formation (Brück, Bitsch et al. 1997, Lassmann 2008). According to MAGNIMS consensus guidelines on the use of MRI in MS, brain MRI should be ideally performed on the same MRI system and using the same imaging protocol as the reference (baseline) scan (Wattjes, Rovira et al. 2015). Contrast-enhanced T1 weighted sequences are recommended to detect acute inflammation, but also demonstration of active (new or enlarging) T2 lesions can deliver sufficient information about subclinical disease activity and disease progression.

Several MRI markers provide information on focal neurodegeneration, such as chronic T1 hypointense lesions ('black holes') and brain atrophy. Reduced intensity of MS lesions in T1-weighted sequences was correlated to the extent of demyelination and axonal loss in biopsy specimens (Bitsch, Kuhlmann et al.

2001), and T1 hypo-intense lesion load and accumulation of black holes were correlated with disability and disease progression (Truyen, van Waesberghe et al. 1996). People with MS show rates of brain volume loss (BVL) higher than healthy individuals since the early stages of the disease, and rates of BVL and grey matter loss predict the conversion from CIS to clinically definite MS (Calabrese, Rinaldi et al. 2011). Furthermore, Double Inversion Recovery allow the detection of cortical lesions (Calabrese 2013). T2* weighted images allow the detection of hypo-intense signal of a vein centred in a lesion and has been proposed as a marker for differential diagnosis between MS and other inflammatory CNS diseases (Maggi, Absinta et al. 2018), although it has not yet been endorsed by the current diagnostic criteria. Recently, the identification of a paramagnetic rim in susceptibility-weighted images has been suggested as a potential biomarker of compartmentalized disease activity, and possibly of treatment response. Anatomopathological studies showed that those lesions characterized by the presence of a rim of iron- laden macrophages at their edge (slowly expanding lesions, SELs) can be identified as phase-rim positive (rim+) lesions using susceptibility-weighted images at brain MRI with 7T field (Dal-Bianco, Grabner et al. 2017). These data have been replicated also with 3T MRI (Absinta, Sati et al. 2018), allowing the evaluation of this putative biomarker also in clinical settings. Evidence on a correlation between rim+ lesions and both progressive forms of MS and high disability has recently been provided, and SELs were detected across different treatment groups with a trend towards a higher prevalence of rim+ lesions in patients treated with second line DMTs (Absinta, Sati et al. 2019). Quantitative MRI techniques, including magnetization transfer and diffusion tensor imaging, can measure the extent of structural changes that occur within and outside focal lesions in white and grey matter. These techniques can characterize the extent and distribution of MS-related damage within focal lesions or in normal-appearing white and grey and correlative histopathological–MRI studies have shown that can characterize the pathological nature of these changes (Wattjes, Rovira et al. 2015).

CSF analysis

A lumbar puncture is routinely performed in the diagnostic workout of pw suspected MS. CSF analysis is pivotal in excluding potential alternative diagnosis, mostly in atypical presentations and in the presence of red flags of possible better explanation. Routine CSF analysis includes chemic-physical examination and evaluation of oligoclonal bands (OCBs). Cytological examination shows a normal cell count in 50% of the cases and a modest mononuclear pleocytosis in the remaining, with only 1% of the cases showing >35 cells/ μ l (Andersson, Alvarez-Cermeno et al. 1994). For OCBs evaluation, a quantitative measurements of immunoglobulins (Ig) and albumin and a qualitative analysis of CSF Ig in

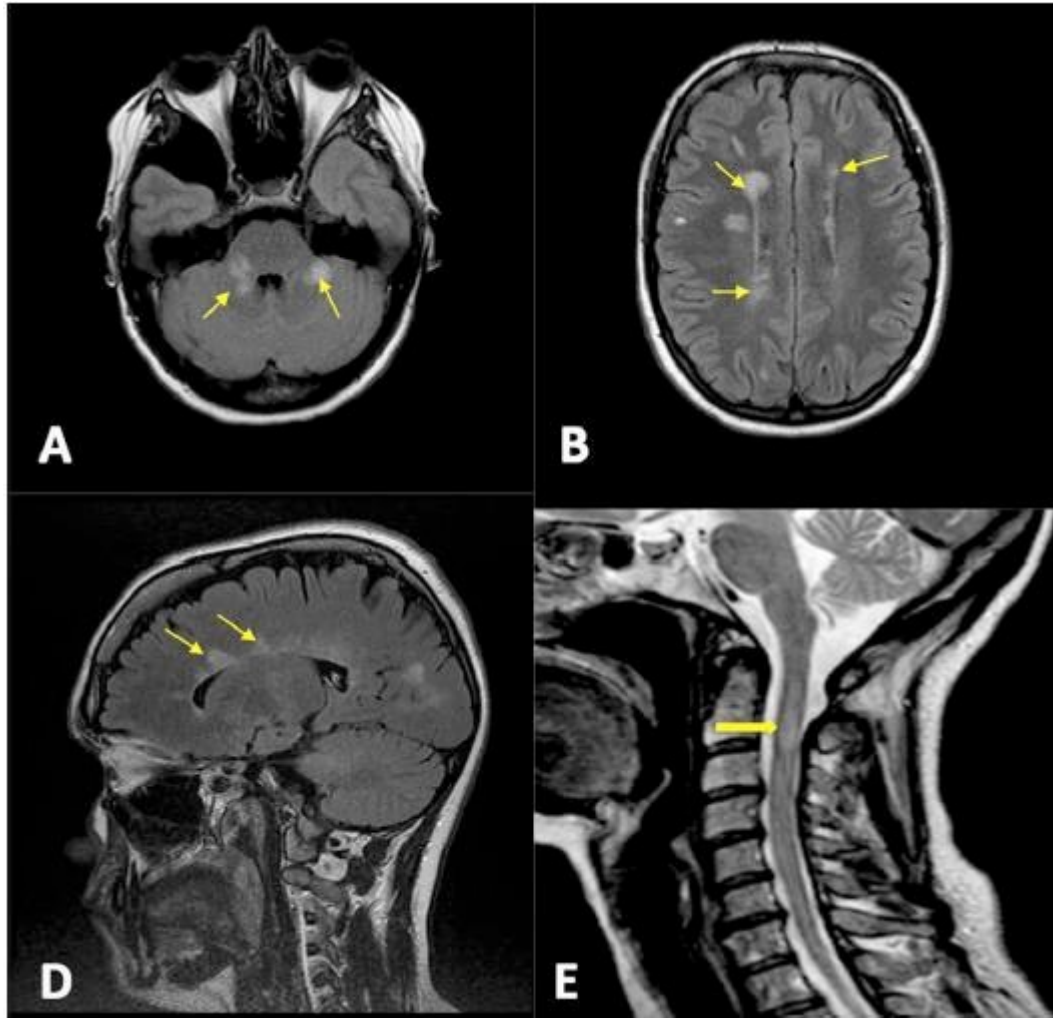


Figure 1.4: Examples of T2-weighted lesions in a person with RRMS that fulfill criteria for dissemination in space. A. Axial fluid-attenuated inversion recovery (FLAIR) brain scan showing infra-tentorial lesions. B. Axial FLAIR brain scan demonstrating periventricular lesions. C. Axial FLAIR brain scan demonstrating a juxtacortical lesion. D. Sagittal FLAIR brain scan demonstrating callosal lesions ('Dawson's fingers'). E. Sagittal T2-weighted scan of the cervical spinal cord demonstrating a focal lesion. Reproduced from ref. (Kearney, Cahalane et al. 2018).

comparison with serum Ig are performed. Intrathecal synthesis of IgG is determined by the presence of a specific IgG oligoclonal profile in CSF, not observed in serum. The typical MS pattern is the detection of at least two OCBs in the CSF which are not associated to corresponding OCBs in serum. OCBs are one of the diagnostic hallmark of MS, detectable in up to 95% of pwMS in northern Europe populations, even if the specificity is low (Link and Huang 2006). Presence of OCBs in people with CIS is an independent predictor for conversion to clinically definite MS (Arrambide, Tintore et al. 2018); OCBs at MS onset may be associated with a more severe disease course and were associated with more severe GM pathology and with a more severe physical disability and cognitive impairment in another study (Farina, Magliozzi et al. 2017). Quantification of the

kappa free light chain and the λ free light chain in CSF and kappa index [(CSFFLC/SerumFLC)/(CSFAlbumin/SerumAlbumin)] have been recently proposed as a diagnostic sensitive alternative to OCBs, and further evaluations are ongoing (Valencia-Vera, Garcia-Ripoll et al. 2018). Furthermore, serum Neurofilaments (sNfL) levels have been suggested as a biomarker of disease activity and monitoring of treatment- response (Leppert and Kuhle 2020). SNfL concentrations predict disability accrual and accelerated brain and spinal cord atrophy in pwMS (Barro, Benkert et al. 2018). Finally, in research setting, many potential CSF and serum biomarkers (such as GFAP, TNF- α , CXCL8, IL-15, IL-12p40, CXCL13, CXCL12) as well as metabolomics are currently under investigations and show promising correlation with MS types and long-term prognosis; however, their application in clinical setting and actual role in daily practice has yet to be elucidated (Bhargava and Calabresi 2016; Magliozzi 2018; Magliozzi 2020).

Treatments

Treatments for MS are classified into acute phase treatments, e.g. treatments administered in the event of relapse, and disease modifying treatments (DMTs). Whereas treatment of the acute phase is based mainly on corticosteroids, many different DMTs have been approved in the last two decades and were demonstrated to be effective in reduction of disease activity and long-term accrual of disability, even if each at different extent.

Acute phase treatments

First choice treatment for MS relapses are high dosage corticosteroids, which are typically administered by intravenous route (e.g. methylprednisolone, MP, 1 gr/day for 5 days). Adrenocorticotrophic hormone (ACTH) might also be administered, by intramuscular or subcutaneous injections (Berkovich 2016). In case of disabling relapses or no response to MP, plasma-exchange or immunoabsorption (5 to 10 treatment performed every other day) might be considered, and were reported to be effective in up to 72% of the treated patients (Cortese, Chaudhry et al. 2011).

Disease modifying treatments

The therapeutic scenario of MS has greatly evolved over the last decade and more than 10 disease DMTs are approved to date. Mechanism of action of such DMTs is based on the modulation of the immune system in order to reduce inflammation and subsequent CNS damage. Most of DMTs act on the peripheral compartment, reducing or preventing activation of immune cells, blocking CNS trafficking or egress from lymphoid organs of activated lymphocytes. Due to the mechanism of

action, DMTs are effective in the early phase of MS, where inflammation is the main driver of disease activity. On the other hand, the treatment of progressive MS is more difficult, with few treatments available and with disability accrual that is probably promoted by many different pathogenetic mechanisms. According to recent guidelines, initiation of treatment with DMTs is recommended as soon as possible once MS diagnosis is established (Montalban, Gold et al. 2018). The choice of the appropriate DMT should be tailored on patient's characteristics, including disease activity and tolerability to potential side effects. Approved DMTs are classified, in Italy, into first line and second line treatments, according to the safety profile of each drug and the subsequent benefit/risk ratio. Most commonly adopted and licensed drugs are Interferons (IFNs), Glatiramer-acetate, Teriflunomide, Dimethyl-fumarate (first line) and Natalizumab, S1PR inhibitors (Fingolimod, Siponimod, Ozanimod), anti-CD20 B-cell depleting monoclonal antibodies (Ocrelizumab, Ofatumumab), Cladribine and Alemtuzumab (second line).

2. INTRATHECAL INFLAMMATION IN MULTIPLE SCLEROSIS

2.1 Meningeal inflammation and cortical demyelination

Grey matter (GM) demyelination can be more extensive than WM lesions. Lesions can be detected through cortical, deep (Magliozzi 2022, Cooze 2022) and spinal cord (Reali 2020) GM and are a typical finding of MS. The most common pattern is the so-called type III, with extensive subpial demyelination, but type II (intracortical) and type I (leukocortical) lesions can be frequently found (Peterson 2001, Magliozzi 2007). These lesions are characterized by little parenchymal or perivascular immune cell infiltration (Peterson 2001) and there is no clear association between infiltrates and demyelination. On the contrary, demyelination associates with inflammatory infiltrates in the adjacent meningeal spaces (Howell 2011) and an ‘outside-in’ gradient of tissue damage with microglia activation and neuronal and axonal loss can be noticed, both in the subpial cortical and in the deep GM (Magliozzi 2010, 2022). Meningeal T and B cells inflammatory infiltrates often assume the aspect of tertiary lymphoid structures (Magliozzi 2007, Serafini 2004), suggested to provide cytotoxic mediators that can diffuse into the underlying tissues (Gardner 2013, James 2020, James 2022, James 2020). In particular, infiltrates are enriched in B cells that may contribute to compartmentalised inflammation not only by a continuing humoral immune response but also by antigen presentation and production of proinflammatory and cytotoxic mediators (Lisak 2012, 2017). Furthermore, increasing evidence from the peripheral blood, the CSF, and meningeal follicles hints at a key pathological role of the crosstalk between proinflammatory memory B cells and plasmablasts on one side and memory CD4⁺ T cells with a Th1/Th1* phenotype on the other (Jelcic 2018, van Langelaar 2019). These CSF-infiltrating T cells may respond to multiple autoantigens i.e. HLA-DR15 (Jelcic 2018), myelin oligodendrocyte glycoprotein (MOG) (Bielekova 2004), Ras guanyl-releasing protein 2 (Jelcic 2018), GDP L-fucose synthase (Planas 2018), among others. Notably, the degree of immune cell infiltration in the meninges also associates with increased WM lesion number and activity, particularly in the spinal cord (Androdias 2010, Reali 2020), but also in the subcortical WM (Ahmed 2022), suggesting a similar mechanism of compartmentalised inflammation-induced pathology in both the WM and GM.

2.2 Chronic active lesions

The proportion of chronic active lesions strongly correlated with disease severity in a large retrospective autopsy cohort study (Luchetti et al., 2018). These lesions are characterized by a rim of activated myeloid phagocytes (microglia and macrophages) with occasional myelin degradation products as a sign of continuous low-level demyelination (Heß). CD3⁺ T cells are sparse, while

myeloid phagocytes at their rims accumulate iron and frequently adopt a senescent morphology (DalBianco 2017, Bunyan 2011, Bagnato 2013). Most of myeloid cells show an activated phenotype (Dal Bianco 2017, Absinta 2021, Zrzavy 2017, Jäckle 2020), that associates with APP+ axonal spheroids that are found at the slowly expanding rims (Dal Bianco 2021, Maggi 2021). These lesions can be detected in vivo with MRI (Absinta 2016) and positron emission tomography (PET) imaging using a TSPO-specific tracer (Kaunzner 2019). In addition to axonal damage, chronic lesion activity associates with a remyelination failure, possibly mediated by T cells-secreted IFN γ (Starost 2020).

2.3 Axonal damage and neuronal loss

Neuroaxonal loss, rather than demyelination, is likely to be one of the main determinants of GM atrophy (Carassiti 2018, Mahajan 2020). Neuroaxonal loss is probably related to both lesion-dependent and lesion-independent mechanisms and involves all GM structures (Vercellino 2005, Trapp 2018, Schirmer 2009). Similarly, a diffuse synaptic loss characterizes MS brains and can be related to both lesion-dependent and lesion-independent mechanisms. Notably, acute synaptic loss is associated with phenotypic changes in cortical microglia induced by meningeal inflammation (van Olst 2021) and inflammatory cytokines (such as TNF, IL-1, IFN γ) have been shown to induce synaptic alterations (Mandolesi 2012).

3. AIM OF THE STUDIES

Many evidence support the key role of intrathecal inflammation in driving disability accumulation in multiple sclerosis.

The current studies aim to better characterize the impact of intrathecal compartmentalized inflammation on disability outcomes, as well as characterize its basis and define potential biomarkers to be applied in clinical practice.

i. In the first study we assessed in a post-mortem cohort the correlation between inflammatory cells compartmentalized in perivenular spaces, an hallmark of MS pathology, on disease outcomes. This approach involved a retrospective analysis, aimed to characterize the association with disability progression both in the first years after a diagnosis of MS and in the last year of disease. Notably, due to the available information about presence of meningeal infiltrates, sometimes aggregates in the context of tertiary lymphoid structures, we were able to also evaluate the correlation between subarachnoidal compartmentalized inflammation, parenchymal lesions and disease outcome.

ii. Among MRI markers that associated with a severe disease course at least in the short term follow-up, cortical lesions gained increasing attention. They represent a good imaging surrogate of chronic inflammation and, even not all, they can be detected with the application of sequences (i.e. Double Inversion Recovery) that could be introduced in clinical practice. The availability of an almost 20-years follow-up permitted to validate the impact of focal cortical pathology on clinical outcome, confirming the predictive role of early accumulation of cortical damage on long-term disability accumulation.

iii. Cerebrospinal fluid correlates of intrathecal inflammatory processes are advocated. They could provide additional markers to be tested in larger cohorts and introduced in clinical practice as well as provide insight into MS specific pathogenetic processes. The application of Multiplex assay permitted to test several inflammatory markers, representative of intrathecal inflammation, and to evaluate their prognostic value. Such prognostic value has been evaluated on both clinical aspects (capability to identify patients with primary progressive MS, prediction of progression independent of relapse activity) and radiological markers of disease severity as cortical thinning accumulation

4. HIGH LEVELS OF PERIVASCULAR INFLAMMATION AND ACTIVE DEMYELINATING LESIONS AT TIME OF DEATH ASSOCIATED WITH RAPIDLY PROGRESSIVE MULTIPLE SCLEROSIS DISEASE COURSE: A RETROSPECTIVE POST-MORTEM COHORT STUDY.

Manuscript under review, *Ann Neurol*.

Authors contributions: Richard Nicholas^{1,2*}, Roberta Magliozzi^{2,3*}, Damiano Marastoni^{3*}, Owain Howell^{2,4*}, Federico Roncaroli⁵, Paolo Muraro², Richard Reynolds², Tim Friede⁶.

¹ Imperial College Healthcare NHS Trust, London, UK

² Department of Brain Sciences, UK Multiple Sclerosis Society Tissue Bank, Faculty of Medicine, Imperial College London, Hammersmith Hospital Campus, London, UK

³ Dept. of Neurosciences, Biomedicine and Movement Sciences, University of Verona, Italy

⁴ Institute for Life Sciences, Swansea University, Swansea, Wales.

⁵ Division of Neuroscience and Experimental Psychology, University of Manchester, Manchester, UK.

⁶ Dept. of Medical Statistics, University Medical Center Göttingen, Göttingen, Germany

*These authors equally contributed

4.1 INTRODUCTION

Inflammation is thought to be the fundamental driver of the pathology in multiple sclerosis (MS) at all stages of the disease course, giving rise to demyelination and axonal and neuronal loss and this combined pathology results in the characteristic symptoms experienced by people with MS (Reynolds et al., 2011, Kutzelnigg & Lassmann, 2014, Steinman & Zamvill, 2016). In individuals the manifestations are highly variable but are characterised by two dominant clinical events: relapses, transient periods of neurological deterioration with variable recovery; and progression, characterised by the gradual accumulation of disability that leads to the major personal and societal cost of MS (Olesen et al., 2014). Relapses have proven amenable to therapy but progression has thus far been resistant to treatment leading to a major unmet need (Humphries, 2012). Thus, despite extensive pathological evidence for inflammation in progressive MS (Reynolds et al., 2011; Frischer et al., 2009), no immunomodulatory treatment that has been shown to suppress relapses and gadolinium MRI activity has had a major impact on the progressive course (Montalban et al., 2017; Kappos et al., 2018). This may be due to the dominant type of intrathecal compartmentalized inflammation in progression being ‘hidden’ behind the blood brain barrier or due to alternative mechanisms, such as cortical pathology and slowly expanding lesions (Mahad et al., 2015; Lassmann et al., 2019; Monaco et al., 2020; Haider et al., 2021; Absinta et al., 2016). Furthermore, although MS is a highly heterogeneous disease, characterized by large inter-individual differences in disease course, several lines of evidence from both MRI and pathological assessment (biopsies and autopsies) indicate that the immunologic pattern of tissue pathology in MS characterizes

each MS patient from the initial disease phase (Lucchinetti et al., 2000; Metz et al., 2014; Luchetti et al., 2018).

The UK MS Society Tissue Bank (UKMSTB) post-mortem MS cohort offers a unique opportunity to investigate how inflammation evident at time of death reflects the lifetime course of MS, offering pathological confirmation of MS in concert with a clinical history and standardised pathological assessment in a large community-based cohort. This resource has contributed to our understanding of the impact of meningeal B-cell inflammation on subpial grey matter (GM) demyelination and immune-pathological cell and molecular alterations that in turn may lead to a more rapid and severe disease progression (Magliozzi et al., 2007; Howell et al., 2011; Bevan et al., 2018; Picon et al., 2021).

To determine whether there are any other pathological features of inflammation, in addition to meningeal infiltration, that could be related to the time of the progressive phase in subjects with MS, we examined two aspects of inflammation in post-mortem tissue in well characterised cases: active and demyelinating/early active lesions (Brück et al., 1995, Reynolds et al., 2011; Kuhlmann et al., 2017) and the perivenular infiltrates (Reynolds et al., 2011, Frischer et al., 2009; Luchetti et al., 2018). Active lesions (AL) are classified by the presence of inflammation with evidence of recent myelin breakdown indicating that they have been present for only 3 months (Brück et al., 1995). Perivenular inflammation is an infiltration of lymphocytes into the venule outside the blood brain barrier producing thickening of the venule wall (Charcot, 1869, Frischer et al., 2009; Luchetti et al., 2018). Both these features are distributed throughout the brain in MS, requiring widespread sampling to confirm or refute their presence. The extensive and reproducible assessment of brain tissue used in the UKMSTB allows the consistent identification of these inflammatory processes, if present. The possible association between early active plaques, perivenular inflammation (PVI) and clinical outcome has therefore been examined in detail in a large MS cohort to determine whether variations in clinical milestones in MS were associated with the prevalence of these inflammatory lesions in post-mortem tissue.

4.2 METHODS

UKMSTB cohort

The UKMSTB operates a nationwide community-based donor scheme of people, with and without MS, who register to donate their brain and spinal cord after death. After donation donor histories, where available, are summarised by a neurologist prior to the neuropathological analysis (Reynolds et al., 2011). All tissues were collected with fully informed consent via a prospective donor scheme with ethical approval by the National Research Ethics Committee (08/MRE09/31). Donor brain and spinal cord are examined by a neuropathologist according to standardised criteria (BrainNet Europe: <http://www.brainnet-europe.org>).

This analysis focused on a group of 269 MS donors, who died between 2004 and 2012, where it was possible to clearly characterize the disease course with sufficient clinical records to provide information on the key clinical milestones: age at disease onset, an estimate of the time to onset of progression, the time at which a wheelchair was required or not and the age at death. In brief the history was summarised by a neurologist blinded to the neuropathological findings to determine the key clinical milestones above, but also the number of relapses in the first two years of disease (n=260), the time at which a wheelchair was required (n=220), and the occurrence of progression during terminal illness (n=239), defined by accumulation of disability in the last months prior to death. The examined cohort closely reflects the UK MS population and the range and ratio of PPMS and SPMS cases in the UK (Reynolds et al., 2011).

All demographic and clinical characteristics of the cohort are described in Table 4.1. All donor brains had been examined for the presence or not of early active lesions and perivenular inflammation (graded 0-5) as this formed the focus of this investigation (Reynolds et al., 2011). Perivenular inflammation was scored as the highest degree of severity seen in this assessment. Further information available included: gender and the number and nature of clinical relapses. In addition, the examined cohort includes a subset of brains (87 out of 269) previously investigated for the presence of meningeal inflammation and associated subpial cortical demyelination (Howell et al., 2011).

Neuropathology examination

Donor brain and spinal cord were examined by a neuropathologist according to standardised criteria (BrainNet Europe: <http://www.brainet-europe.org>). Tissue blocks (2x2x1cm) were prepared from whole coronal slices dissected immediately on brain retrieval and fixed in 4% paraformaldehyde for a minimum of 12 hours and processed for paraffin embedding or rapid freezing. This study focussed on the standardised set of paraffin embedded blocks that are prepared for diagnostic confirmation. Paraffin serial sections (7 µm) from each block were stained with haematoxylin–eosin, Luxol Fast Blue/Periodic Acid-Schiff (LFB/PAS) and Luxol Fast Blue/Major Histocompatibility Complex class II (LFB/MHC class II) antigen, with additional histochemical and immunohistochemical stains performed when required for diagnosis (Reynolds et al., 2011). The classification of plaques used at the UKMSTB has been proposed by Professor I. Allen (<http://www.ICDNS.org>), and referred to the first stage of inflammation and myelin breakdown as AL, characterized by hypercellularity with microglial activation throughout the lesion, signs of myelin phagocytosis and degradation with LFB fragments of myelin within macrophagic cells (Reynolds et al., 2011), similarly to what recently described as ‘active and demyelinating lesions’ (Kuhlmann et al., 2017).

Parameter	Total MS	Female	Male	SPMS	PPMS
Number of patients	269	174	95	251(F166/M85)	18(F8/M10)
Disease duration (mean \pm SD, years)	30.4 \pm 12.0	30.6 \pm 11.9	29.9 \pm 12.2	30.7 \pm 11.7	26.0 \pm 15.2
Age of onset (mean \pm SD, years)	31.5 \pm 9.9	32.6 \pm 10.1	29.3 \pm 9.2	31.0 \pm 9.7	38.2 \pm 11.1
Number of relapses in first two years (mean \pm SD)	2.1 \pm 1.3	2.1 \pm 1.3	2.0 \pm 1.3	2.1 \pm 1.3	1.4 \pm 0.9
>2 relapses in first two years (frequency, %)	76/260 (29.2)	52/169 (30.8)	24/91 (26.4)	74/242 (30.6)	2/18 (11.1)
Age of death (mean \pm SD, years)	61.8 \pm 12.8	63.2 \pm 12.8	59.2 \pm 12.2	61.6 \pm 12.7	64.2 \pm 13.9
Time from onset to progression (mean \pm SD, years)	12.2 \pm 9.4	11.8 \pm 8.4	13.0 \pm 10.9	13.1 \pm 9.1	/
Time from progression to death (mean \pm SD, years)	18.1 \pm 9.2	18.8 \pm 9.0	16.9 \pm 9.4	17.6 \pm 8.3	26 \pm 15.2
Time from progression to wheelchair (mean \pm SD, years)	6.8 \pm 6.0	6.8 \pm 5.7	6.7 \pm 6.4	6.1 \pm 4.9	14 \pm 10.5
MS progressive in last illness (frequency, %)	109/239 (45.6)	67/153 (43.8)	42/86 (48.8)	103/224 (46.0)	6/15 (40.0)

Table 4.1. Demographic and clinical characteristics of MS cases. *SPMS*: Secondary progressive multiple sclerosis; *PPMS*: Primary progressive multiple sclerosis; *F*: Female; *M*: Male.

PVI assessment was a semi-quantitative assessment performed by the neuropathologist independent of this work. Sampling of at least 20 tissue blocks from each of the 269 examined brains within a spectrum of lesions identified macroscopically was carried out, with grading as described by Reynolds et al (2011). PVI assessment (n=265, Figure 4.1) provided a grading (0-5) of the extent of PVI: a grade from 0 to 5 was evaluated according to the extent of cellular infiltration. In particular, a score of 5 corresponded to the highest degree of severity detected; a high degree of inflammation (high PVI) was defined by a grade of 2 or more (Figure 4.1).

For each examined MS cases, the presence of active lesions (AL, n=267), late active/chronic active, inactive, shadow plaques (n=248), as well as the involvement of GM, at the routine analysis (yes/no, n=252) was performed in the same brain tissues examined for the presence/level of PVI.

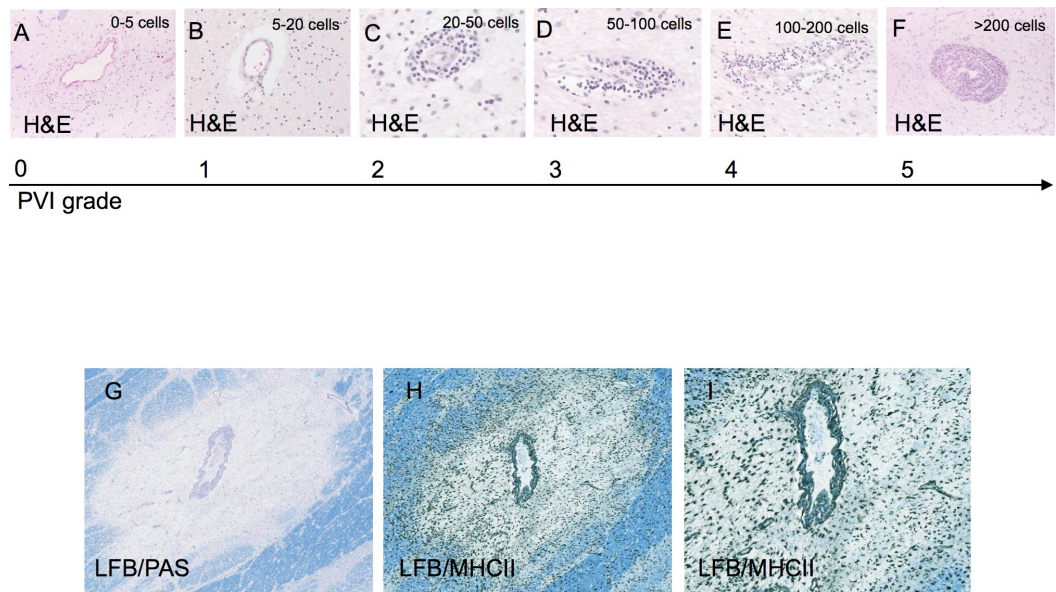


Figure 4.1 Assessment of perivenular inflammation (PVI) and early active lesions (EAL) in progressive MS. Semi-quantitative evaluation of PVI: ranging from 0 to 5 was calculated accordingly to the number of cells stained by haematoxylin-eosin (H&E) detected within the perivenular space (A-F). Active lesions (AL) were defined by LFB/PAS histology (G) and LFB/MHCII immunostaining (H-I), showing membranous debris and the elevated density of MHC-II+ cells around PVI and throughout the lesion core. Original magnification= A-H: 100X, I: 200X.

Perivascular cell count

In order to characterize the inflammatory cell populations present in the perivenular infiltrates associated with on-going demyelination, a quantitative analysis of T and B cells in the perivenular infiltrates associated with ongoing demyelination and in normal-appearing white matter (NAWM), was performed on serial paraffin sections from 22 MS cases (11 with high PVI and 11 with low PVI). Region-matched sections from each case from superior frontal gyrus (sampled 1 cm rostral to the temporal pole), thalamus, primary visual (striate) cortex (sampled 1.5 cm rostral to the occipital pole) and pons (including locus coeruleus) were immunostained with the monoclonal antibodies for myelin oligodendrocyte glycoprotein (MOG) and for CD20 and CD3 as B and T lymphocytes marker respectively following the procedures previously described (Magliozzi et al., 2007; Howell et al., 2011) and digitalized images from entire slices were acquired.

In NAWM, CD3+ and CD20+ cells were quantified from up to four vessels (veins) in cross-section, presenting with a thin tunica media and with a total area (vessel and perivascular space) $>0.002 \text{ mm}^2$. Two randomly non-continuous selected fields per each block (areas of each field of 4 mm^2) have been examined. Fields in proximity of lesions were excluded; if an infiltrate/vessel was on the

edge of the selected area it was included in the analysis; if more than 4 vessels with such characteristics were present in the selected area, only the 4 spaces with more cellularity were counted. The mean number of CD3+ and CD20+ cells was calculated per each field and each case. In the lesions, infiltrates were counted in vessels (veins) in cross-section presenting with a thin tunica media and with a total area (vessel and perivascular space) $>0.003 \text{ mm}^2$. For each examined MS case the number of perivenular CD3+ and CD20+ cells was calculated in 4 vessels with perivascular space $>0.003 \text{ mm}^2$.

Evaluation of meningeal inflammation

Eighty-seven out of 269 evaluated cases had previously been extensively investigated for the presence of meningeal inflammation and lymphoid-like structures (Howell et al., 2011). Briefly, each case was screened on paraffin-embedded sections for the presence of B cell aggregates, assigning an index of inflammation based on the maximum density of meningeal and/or perivascular infiltrates seen. Only tissue blocks containing substantial meningeal infiltrates with lymphoid-like organisation were processed further for anti-CD20 immunohistochemistry and characterized as follicle positive SPMS if at least one aggregate enriched of CD20+ B cells was identified in the meninges together with the presence of CD35+ follicular dendritic cells, proliferating Ki67+ CD20+ cells and IgA, -G, -M+ plasmablasts/plasma cells (Serafini et al., 2004; Howell et al., 2011).

Image acquisition and analysis

Tissue sections were analysed on a Nikon E1000M microscope using brightfield imaging (Nikon Instruments Inc.) with a digital camera (QImaging). Digitized images from entire slices of the 22 cases evaluated in the quantitative analysis (stains for CD3, CD20, MOG, LFB/MHCII, LFB/PAS) were acquired by means of an Aperio AT2 Scan Digital Whole Slide Scanner (20x magnification). Image files were handled using QuPath (Bankhead et al., 2017). All quantifications were manually performed with the observer blinded to case identification of perivascular/meningeal inflammatory status.

Statistical analysis

Demographic, clinical and neuropathological characteristics were described by means and standard deviations in case of continuous variables and by frequencies and percentages in case of categorical variables. Logistic regression models were used with stepwise variable selection to model the probabilities of early active lesions and perivenular inflammation. Factors within the models included: the time interval from birth to onset, onset to progression and progression to death, gender, >2 relapses in the first two years after onset, MS was progressive in last illness, a high grade of perivenular inflammation (none/minimal [0-1] vs. significant presence [2-5]), and the presence of early active plaques found in the standardised assessment. Where appropriate the time interval from progression to use of a wheelchair was used in place of progression to death. To calculate

probabilities groups were generated for the time interval from birth to onset (age of onset ≤ 20 years; $20 < \text{age of onset} \leq 30$ years; $30 < \text{age of onset} \leq 40$ years; $40 < \text{age of onset}$), onset to progression (time to progression ≤ 5 years; $5 < \text{time to progression} \leq 10$ years; $10 < \text{time to progression} \leq 15$ years; $15 < \text{time to progression}$) and progression to death (time from progression to death ≤ 10 years; $10 < \text{time from progression to death} \leq 15$ years; $15 < \text{time from progression to death} \leq 20$ years; $20 < \text{time from progression to death}$). Otherwise, the Chi-square test was used to compare the relationship between perivenular inflammation and early active lesions.

Results of cell count analysis were presented as scatter dot plots with a line at the mean or as box-and-whiskers plots showing min-to-max values, interquartile range and group medians. Two-group comparisons were performed using the Mann-Whitney U test or Wilcoxon matched pairs test, whilst three or more groups were compared by non-parametric one-way ANOVA (Kruskal-Wallis test), using Dunn's multiple comparisons post-test. Correlations were tested by Spearman analysis. Due to the exploratory nature of this study p-values and confidence intervals were not corrected for multiple testing; two-sided p-values smaller than 0.05 were considered statistically significant. All computations were carried out using SAS version 9.4, Stata version 13.0, and GraphPad Prism Software 7.0.

3.3 RESULTS

Demographic and clinical characteristics

In this investigation we selected patients from the MS tissue bank database who had both sufficient information from patient records to determine the key events in the disease course and a neuropathology assessment performed (n=269). Demographic and clinical characteristics of the cohort are described in Table 4.1. All cases had a history of progressive MS, with a mean disease duration of 30.4 ± 12.0 years. 174 (64.7%) were females; no significant differences in clinical milestones were noted according to gender. A progressive disease course from onset (primary progressive multiple sclerosis, PPMS) was found in 18 cases. PPMS cases had a higher age of MS onset (p=0.008), time from progression to wheelchair (p=0.002) and death (p=0.008), and a lower number of relapses (p=0.01) in the first 2 years of MS (Table 1).

Substantial inflammatory activity is present at the time of death in progressive MS

We next quantified the lesion types present in the cases, in each of the 4 blocks examined. 54.8% (136/248) had at least one active lesion (AL, Figure 4.2A, E); 61.3% (152/248) had at least one late active/chronic active lesion (LA/CAL, Figure 4.2B, F), with 91.5% (227/248) and 53.2% (132/248) of cases having inactive (Figure 4.2C, G) or shadow plaques (Figure 4.2D, H), respectively. High PVI was detected in 52% of cases (n=137) and at least one AL (Figure 4.2A) was present in 22% of the cases (n=59, Table 4.2). No significant differences in the incidence of AL and high PVI were detected according to gender (p=0.304

and $p=0.878$, respectively) and MS type ($p=0.378$ and $p=0.470$, respectively, Table 4.2).

Looking at lesion types and their relationship to PVI. ALs were present in 35% (48/136) of high PVI cases but only 10% (11/115) of low PVI cases ($p<0.001$, Figure 4.2E). LA/CAL were present in 84% (112/133) of high PVI cases but only 35% (40/115) of low PVI ($p<0.001$, Figure 4.2F). In contrast there was a higher rate of inactive lesions in the low PVI cases (97% [111/115]) compared to the high PVI cases (87% [116/133], $p=0.01$, Figure 4.2G) and a trend towards higher numbers of shadow plaques in the low PVI cases (58% [67/115]) compared to the high PVI cases (48% [64/133], $p=0.12$, Figure 4.2H).

No substantial differences in parenchymal lymphocyte increase was observed in association with the presence of AL. In addition, the presence of parenchymal lymphocytes was rare, sporadic and heterogeneous, since it was not observed in all the examined MS cases.

	Total MS	Female	Male	SPMS	PPMS
Early Active Lesions (frequency, %)	59/267 (22.1)	39/173 (22.5)	20/94 (21.3)	57/249 (22.9)	2/18 (11.1)
High PVI (frequency, %)	137/265 (51.7)	85/173 (49.1)	52/92 (56.5)	126/247 (51.0)	11/18 (61.1)
Grade of PVI (frequency, %)					
0	30/265 (11.3)	23/173 (13.3)	7/92 (7.6)	29/247 (11.7)	1/18 (5.6)
1	98/265 (37.0)	65/173 (37.6)	33/92 (35.9)	92/247 (37.2)	6/18 (33.3)
2	69/265 (26.0)	41/173 (23.7)	28/92 (30.4)	63/247 (25.5)	6/18 (33.3)
3	47/265 (17.7)	28/173 (16.2)	19/92 (20.7)	43/247 (17.4)	4/18 (22.2)
4	20/265 (7.5)	16/173 (9.2)	4/92 (4.3)	19/247(7.7)	1/18 (5.6)
5	1/265 (0.4)	0/173 (0)	1/92 (1.1)	1/247 (0.4)	0/18 (0)

Table 4.2. Pathological findings at the routine UKMSTB assessment: EALs and PVI grades in the whole population and accordingly to gender and MS type.

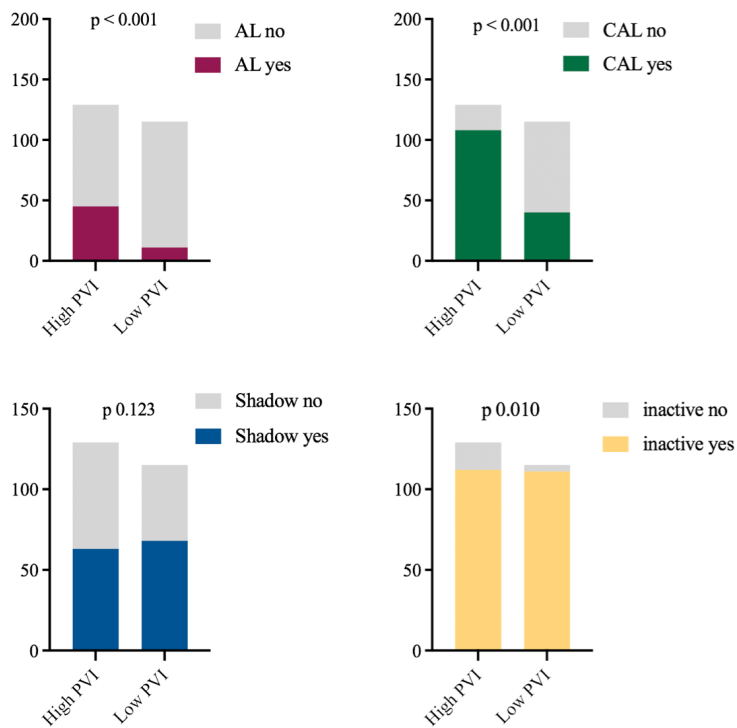
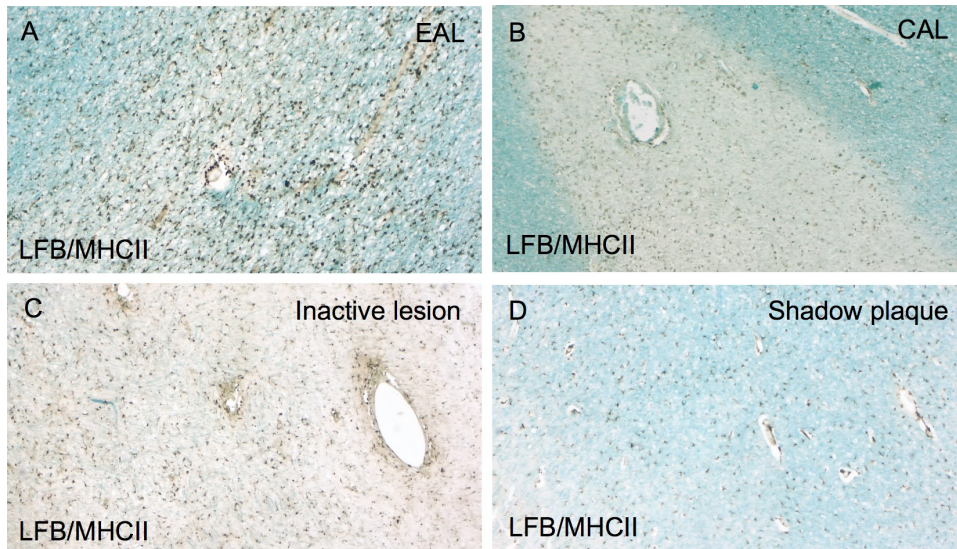


Figure 4.2. Immunostaining for MHCII+ microglia/macrophages combined with LFB myelin staining for the detection of active (A, AL), chronic active (B, CAL), inactive/chronic silent (C, CSL) and remyelinating shadow lesion (D, RML). Cases rated as ‘high’ PVI were more likely to present with at least one AL, or LA/CAL, and less likely to harbour inactive lesions and shadow plaques (E- H). Original magnification= A-D: 100X.

Perivenular inflammation and active lesions are associated with a more severe MS course

A high PVI grade corresponded to a more severe disease course (Table 4.3). Both a significantly earlier age at onset (30.0 ± 10.2 vs 32.9 ± 9.4 years), a shorter time from onset to progression (10.9 ± 8.1 vs 13.6 ± 10.5 years) and a shorter time from progression to death (15.6 ± 8.0 vs 20.8 ± 9.6 years), were seen in cases with high PVI compared to the low PVI group. Likewise, the presence of ALs also associated with a more severe disease course through all the disease phases (Table 4.3). Patients with both ALs and high PVI ($n=48$) had the youngest age of onset (29.1 ± 9.8 years) and of death (50.5 ± 9.6 years), with a mean time from onset to progression of 10 ± 7.1 years and from progression to death 11.5 ± 6.1 years.

Notably, disease activity in the last illness was documented in 45.6% of cases. Among patients with MS progression during their terminal illness, 60% had high PVI, compared to 46% in those not progressing from MS in their terminal illness ($p=0.037$). Similarly, in those with MS progression driving their terminal illness, 30% had ALs compared to 15% where MS was not relevant ($p=0.008$).

Increased probability of perivenular inflammation and active lesions at post-mortem is associated with shorter time from progression to death

After applying the stepwise logistic regression model, the probability for high PVI was most increased in patients with a shorter time from progression to death (OR 0.915, CI 95% [0.884-0.946], $p<0.001$), a shorter time from MS onset to progression (OR 0.922, CI 95% [0.891-0.955], $p<0.001$ and who had a disease onset at a younger age (OR 0.938, CI 95% [0.908-0.968], $p<0.001$; Figure 4.3). A similar association was noticed regarding ALs (age at onset: OR 0.943, CI 95% [0.908-0.980], $p=0.003$; time from MS onset to progression: OR 0.935, CI 95% [0.897-0.975], $p=0.0018$; time from progression to death OR 0.868, CI 95% [0.824-0.913], $p<0.001$; Figure 4.3). After adding Ia/cal to the stepwise logistic regression model AL still associated with time from progression to death ($p<0.001$). The estimated proportion of patients with at least one of each plaque type, including ALs, as a function of time from progression to death (Figure 4.3G) and age of death (Figure 4.3H) is shown in Figure 4.3. Age of onset (OR 0.909, CI 95% [0.877-0.943], $p<0.001$), time from onset to progression (OR 0.930, CI 95% [0.896-0.965], $p<0.001$), and time from progression to death (OR 0.934, CI 95% [0.904-0.966], $p<0.001$) were also identified as predictive factors for MS progression in terminal illness. When MS progression in terminal illness was added to the logistic regression models, the activity of disease was not found to predict independently either high PVI ($p=0.458$) or AL ($p=0.648$). The association between AL and high PVI and MS progression in terminal illness was then explained through age of onset, time from onset to progression and time from progression to death.

Parameter	High PVI	Low PVI	EALs	No EALs
Age of onset (mean \pm SD, years)	30.0 \pm 10.2	32.9 \pm 9.4	29.7 \pm 9.6	31.9 \pm 10
Disease duration (mean \pm SD, years)	26.5 \pm 11.0	34.3 \pm 11.8	22.8 \pm 10.9	32.6 \pm 11.4
Number of relapses in first two years of MS (mean \pm SD)	2.1 \pm 1.4	2.1 \pm 1.2	2.2 \pm 1.4	2.1 \pm 1.3
>2 relapses in first two years of MS (frequency, %)	42/132 (31.8)	33/124 (26.6)	23/58 (39.7)	52/200 (26.0)
Age of death (mean \pm SD, years)	56.4 \pm 11.6	67.2 \pm 11.5	52.5 \pm 10.6	64.5 \pm 12.1
Time from onset to progression (mean \pm SD, years)	10.9 \pm 8.1	13.6 \pm 10.5	10.5 \pm 8.0	12.7 \pm 9.7
Time from progression to death (mean \pm SD, years)	15.6 \pm 8.0	20.8 \pm 9.6	12.4 \pm 6.5	19.8 \pm 9.1
Time from progression to wheelchair (mean \pm SD, years)	5.8 \pm 5.2	8.0 \pm 6.7	5.0 \pm 4.2	7.3 \pm 6.3
MS progressive in last illness (frequency, %)	65/123 (52.8)	44/112 (39.3)	32/52 (61.5)	76/186 (40.9)

Table 4.3. Demographic and clinical characteristics according to degree of PVI (high/low) and presence/absence of EAL.

Perivenular inflammation and active lesions associate with a shorter time from onset of progression to wheelchair

A shorter time from onset of progression to needing a wheelchair was associated with a higher probability of the presence of AL (OR 0.921, 95% CI [0.858, 0.989], $p=0.0230$) as well as a higher level of perivenular inflammation (OR 0.932, 95% CI [0.886, 0.981], $p=0.0071$) at post-mortem, adjusted for age of onset and time from onset to progression which were also found to be statistically significant (Figure 4.3I-L).

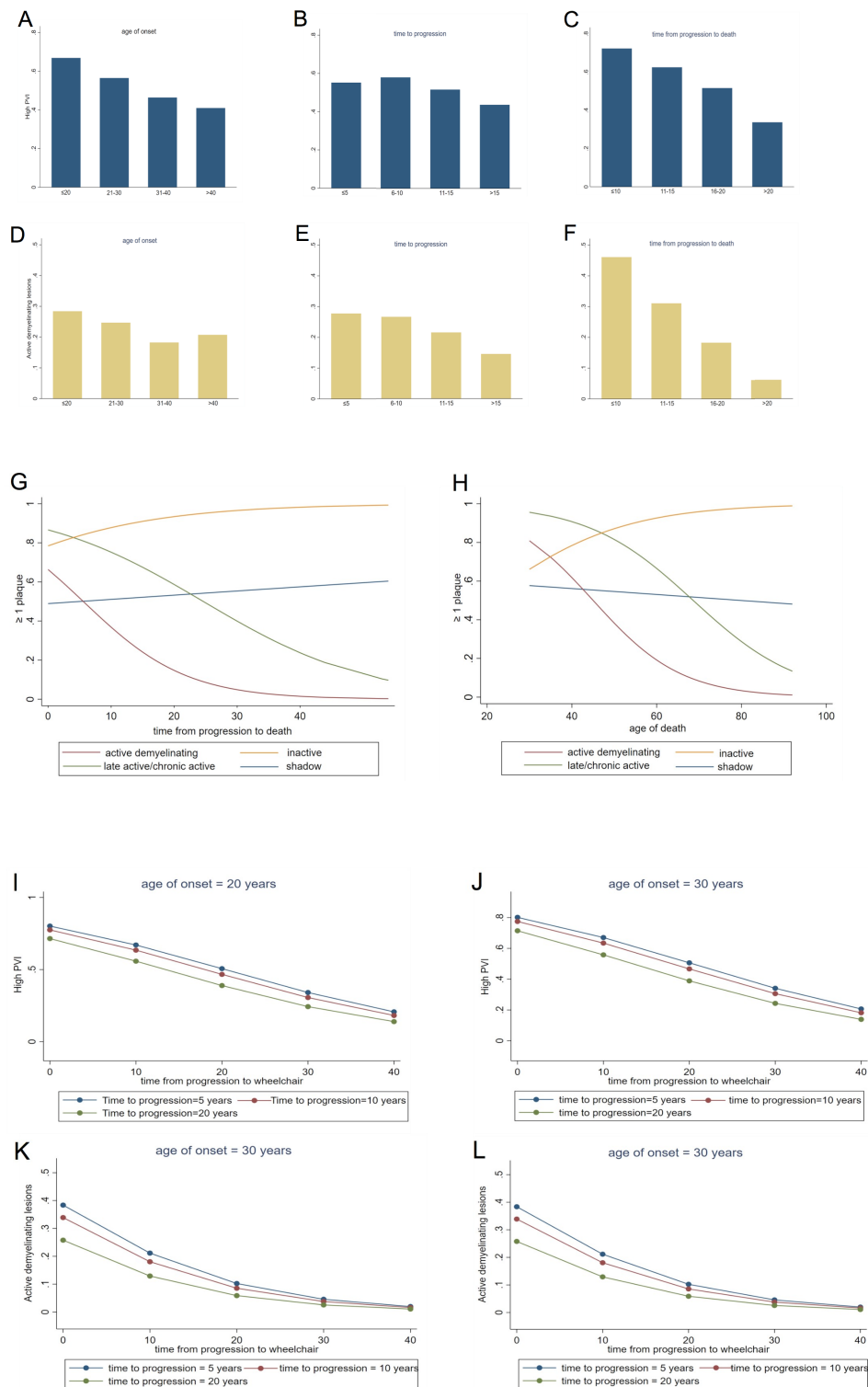


Figure 4.3. Increased probability of perivenular inflammation and active lesions at post-mortem is associated with a younger onset and more rapidly evolving disease course. Probability of high PVI (A-C) and ALs (D-F) depending respectively on age of MS onset (A, D), time from onset to progression (B, E) and time from progression to death (C, F). PVI and ALs were associated with a younger age at onset, shorter time from disease onset to progression and a shorter time from progression to death.

Logistic regression models estimating proportion of patients with at least one of each type of lesion (AI, CA, CI or SP) according to time from progression to death (G) and age of death (H). The probabilities of high PVI (I-J) and ALs (K-L) according to the time from progression to requiring wheelchair (adjusted for age of onset (20 years (I, K) and 30 years (J, L) and time from onset to progression (5, 10 or 20 years). The chance of having high PVI at post-mortem rises to around 80% (I,) in a person with an age of onset at 20 years who reaches the progressive phase in 5 years and who then requires a wheelchair within 5 years of progression onset whereas in this scenario the chance of finding EALs rises to >40%.

Preponderance of B lymphocytes is associated with the extent of demyelination and a more severe disease course

A higher number of perivenular CD3+ T lymphocytes (Figure 4.4A, B) and CD20+ B lymphocytes (Figure 4.4C) was detected in those cases defined as having high PVI in the semi-quantitative analysis (Figure 4.4A), in both white matter lesions and NAWM. Lesions (n=127) from cases with high PVI had increased total lymphocyte number (mean±SD: 40.9±36.7 vs 12.2±13.5, p=0.002), B cells (11.5±18 vs 2±2.1, p=0.002) and T cells (29.4±20.7 vs 10.2±11.5; p=0.002) (Figure 4.4D). Active lesions (n=12, including both AL and late/chronic active ones) were characterized by an increased number of T cells (67.1±76.2 vs 11.5±15.9) and B cells (20.5±35.6 vs 2.6±4.3) in the perivenular infiltrates (p<0.001) compared to inactive ones (n=19). Cases with high PVI were also confirmed to be harbouring higher levels of total (5.4±2.4 vs 3.1±1.6, p=0.013), T (4.4±2.3 vs 2.4±1.2, p=0.032) and B lymphocytes (1±0.4 vs 0.6±0.4, p=0.073) in the perivenular NAWM when compared with the low PVI group (Figure 4.4E). A difference in the total perivenular number of cells was found when comparing thalamus (2.7±2.1) with both prefrontal gyrus (4.9±3.1, p=0.01) and pons (4.7±2.9, p=0.003), but not with visual cortex (4.8±4.5, p=0.285) was detected.

An increased B/T ratio inside the lesions associated with a reduced disease duration (r -0.476, p=0.025, Figure 4.4F). Total number of cells in lesions and in the NAWM perivenular infiltrates did not correlate with the main disease milestones. When evaluating the number of CD20+ cells, a correlation was found with a shorter disease duration (r -0.537, p=0.01) and a younger age at death (r -0.443, p=0.039) (Figure 4.4G).

Perivenular and meningeal inflammation are associated in progressive MS

Among 87 cases previously evaluated for the presence and extent of meningeal inflammation (Magliozzi et al., 2007; Howell et al., 2011), 34 (42.5%) had been defined as having tertiary lymphoid-like structures, also named follicle-like structures. The presence of tertiary lymphoid structures in the meninges was associated with both high PVI (n=29/34, 85.3%, p=0.002) and AL (n=18/34,

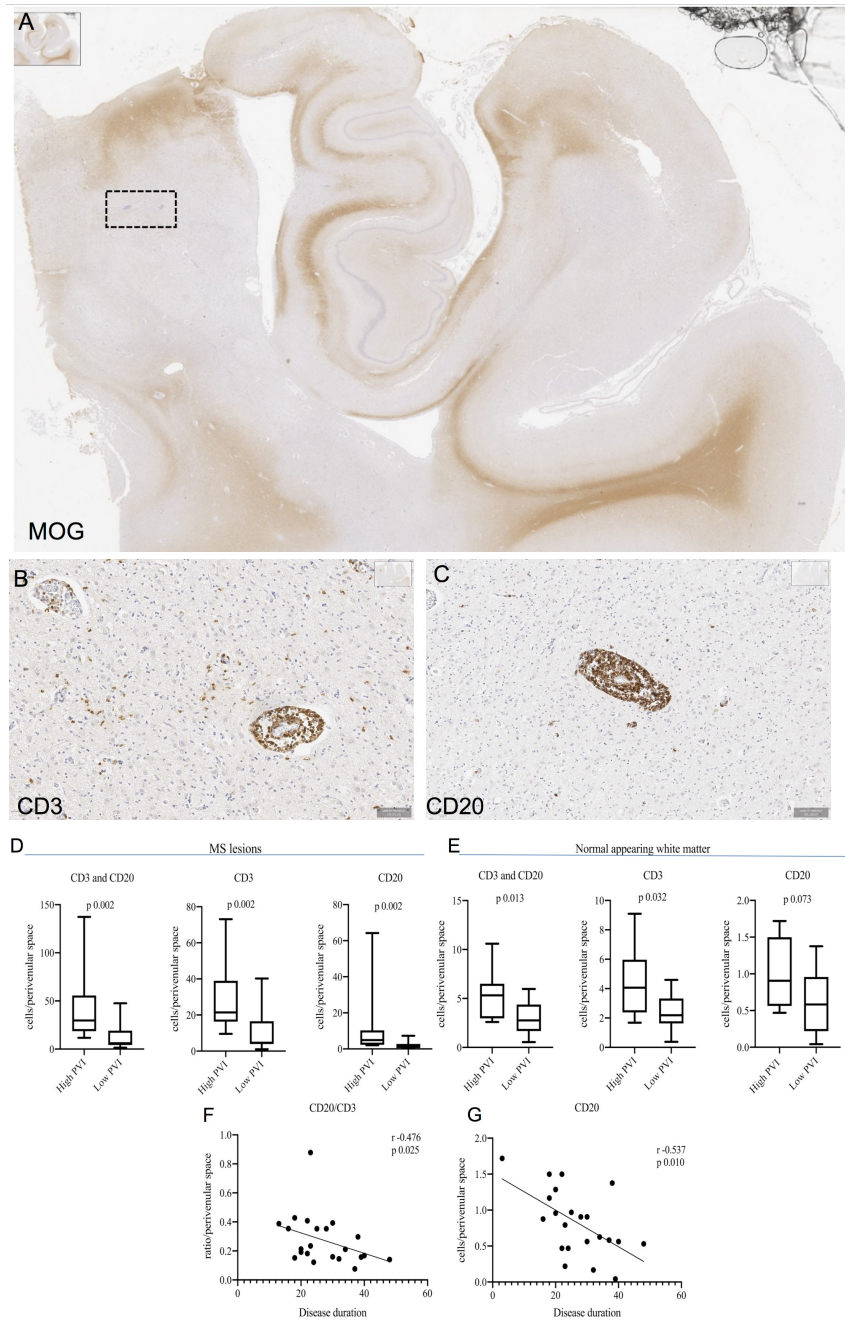


Figure 4.4. Periventricular infiltrates of B lymphocytes are associated with greater demyelination and a more rapidly evolving disease. Substantial demyelination (A) was observed in cases with an elevated density of periventricular CD3+ T lymphocytes (B) and CD20+ B lymphocytes (C) in MS cases defined as having high PVI. Only scattered parenchymal infiltrates of CD3+ T cells (arrowheads in B), but not CD20+ B cells were seen (C). Cell count analysis confirmed the significantly higher number of periventricular lymphocytes in those cases defined as high PVI, in both white matter lesions (D) and NAWM (E), in comparison to low PVI cases. An increased CD20/CD3 ratio (F) and density of CD20+ cells (G) negatively correlated with disease duration. Kruskal Wallis test and Spearman correlation analysis were used. Original magnification= A: 10X; B: 200X.

52.9%, $p=0.006$, Figure 4.5A, C). Seventeen of the 18 subjects with AL also had high PVI.

Furthermore, GM damage ($n=186$) was associated with both a high PVI grade (109/186, 58.6%, $p=0.001$) and presence of AL (53/186, 28.5%, $p<0.001$). Both meningeal inflammation and GM pathology significantly contributed to a severe disease course through all phases (Figure 4.5B, D)

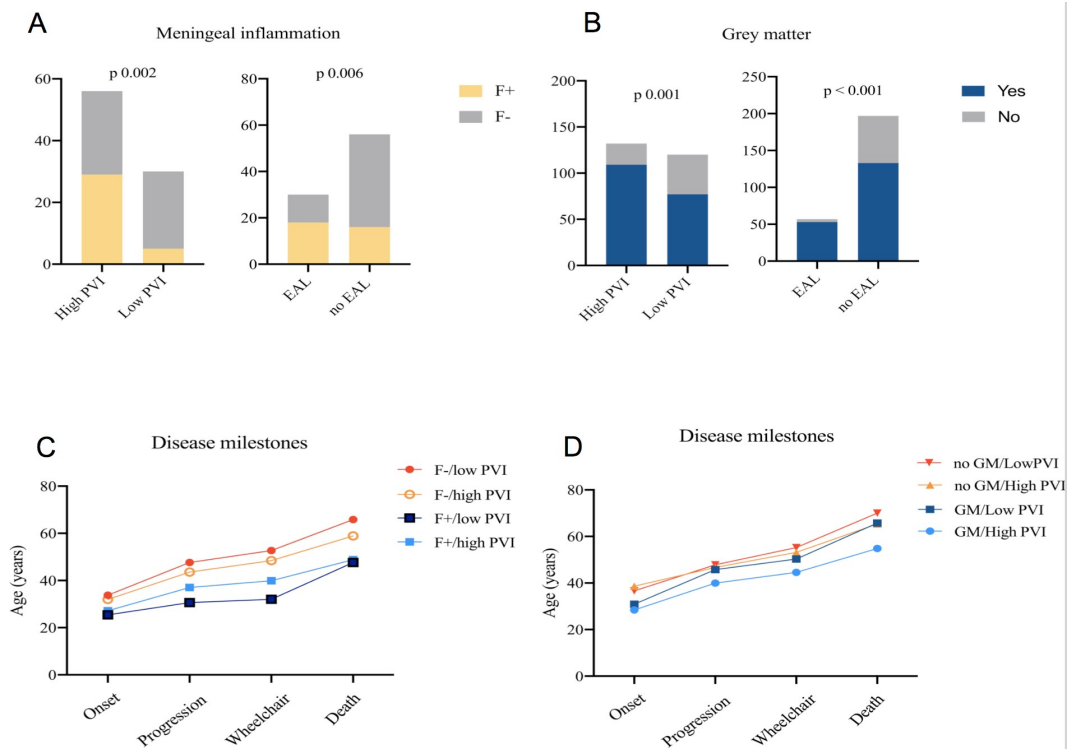


Figure 4.5. Investigating the inter-relationship between perivenular and meningeal inflammation. Association between PVI status and meningeal inflammation (A) and GM pathology (B), revealing that a greater proportion of PVI high cases are also characterised as harbouring ectopic follicle-like structures (F+; A). High PVI cases were also likely to present high cortical grey matter lesion load (B)

Disease course (mean age are plotted) according to PVI status (high/low) and presence/absence of meningeal lymphoid structures (C) and GM pathology (D). C: The study cohort was separated according to the presence (F+) or absence (F-) of meningeal follicle-like structures and PVI status: F- and low PVI ($n=27$), F- and high PVI ($n=25$), F+ and low PVI ($n=5$), F+ and high PVI ($n=29$). Absence of both meningeal and perivenular inflammation is associated with less severe disease outcome, including higher age at progression and at wheelchair use and age at death ($p<0.001$). D: the study cohort was separated according to presence or not of GM pathology and PVI status: no GM and low PVI ($n=46$), no GM and high PVI ($n=23$), GM and low PVI ($n=74$), GM and high PVI ($n=109$). MS cases with both GM damage and high PVI had a lower age at progression and at wheelchair use ($p<0.01$) and age at death ($p<0.001$, for all groups against GM/high PVI group (Kruskal Wallis test and Dunn's multiple comparison post-test were used).

4.4 DISCUSSION

Understanding the role of CNS inflammation in progressive disease is a key issue in MS (Frisher et al., 2009, 2015; Luchetti et al., 2018; Lassmann et al., 2019). Several neuropathological studies have demonstrated ongoing inflammation compartmentalized within the CNS in progressive MS (Frisher et al., 2009, 2015; Howell et al., 2011; Luchetti et al., 2018; Lassmann et al., 2019; Monaco et al., 2020), suggesting its role in driving disease progression (Mahad et al., 2015). However, anti-inflammatory strategies, despite some recent successes, have not yet had a significant impact on slowing disability progression - the dominant clinical manifestation of progressive MS. We approached this problem by examining clinical courses with a variable rate of progression and testing their association with CNS inflammation in post-mortem tissue. The UKMSTB dataset's particular strength is that it has large numbers of subjects with confirmed MS and a wide spectrum of outcomes together with consistent and systematic post-mortem information. A particular issue with histopathological study of brain tissues is the limited sampling. In the UKMSTB, both the brain and spinal cord are available, and information gathered from both areas form part of the comprehensive standardised assessment (<http://www.ICDNS.org>). Though this analysis was extensive, a potential source of bias could be that it was not exhaustive due to the practical constraints in processing a large cohort. The clinical data is subject to ascertainment bias as it was retrospective and based on available clinical records. However, in the UKMSTB 92% of clinical records are of high quality and the database has previously been shown to have characteristics similar to other natural history cohorts (Reynolds et al., 2011).

The strong association found between the presence of early active lesions and substantial perivenular inflammation in the post-mortem brain of SPMS patients with a shorter time from progression to death and a more aggressive disease course implies that inflammatory activity plays a key role in MS pathogenesis not only in the initial relapsing phase, but also during the disease progression, as observed at time of death. Our data, together with studies on independent cohorts (Luchetti et al., 2018), strongly suggest that perivenular inflammatory and demyelinating lesion activity is widely present even in the late stage of the disease, at least in a subgroup of MS cases characterized by rapid disease progression. These findings, together with radiological evidence (Konig et al., 2008; Metz et al., 2021), support the idea that MS heterogeneity is linked to precise patient-dependent immunopathology and may characterize individuals from the beginning of the disease, persisting during the progressive phase, nevertheless with reduced rate of lesion accumulation (Metz et al., 2021; Tobin et al., 2021). In turn, these findings may be helpful to predict the presence of markers of inflammation early in the progressive phase, prior to requiring a

wheelchair, which might extend the timeframe where the inflammatory response could still be a target for therapy (Steinman & Zamvill, 2016).

Despite different terms being used to describe the stages of activity of demyelinated lesions, between authors and studies, there is an agreed sequence of events and pathological changes that evolve over three months as a plaque develops from an early active to an inactive plaque, convergence into a final common pathway that is probably mainly linked to accumulated neuro-axonal degeneration (De Groot et al., 2001; Kuhlman et al., 2017). We herein referred to 'early' demyelination according to the presence of LFB-positive myelin fragments in the cytoplasm of activated macrophages/microglia. The lack of assessment of presence of the minor myelin proteins (i.e. MOG+, CNP+ or MAG+), prevented us to better define (i.e. early vs late and active and demyelinating lesions) the earliest stage of plaque formation (Lucchinetti et al., 2000; Bruck et al., 1995; Kuhkman et al., 2017). According to the idea that plaque composition changes over time, early active plaques, during progressive MS, leave the space to chronic inflammatory process with persistence of microglial activation with demyelination at lesion edge, whose extent associates with disability progression (Luchetti et al., 2018; Zvarwy et al., 2017; Weiner, 2008). A high percentage of our cases showed chronic plaque activity, herein defined as late active/chronic active (Reynolds et al., 2011), somehow corresponding to active and post-demyelinating and mixed active/inactive (Kuhlmann et al., 2017; Frischer et al., 2015).

Nevertheless, the presence of an early active lesion still revealed strictly associated with accumulating disability. Thus, it is remarkable that the probability of their continued presence at post-mortem is increased to nearly 50% if the progressive phase of the clinical disease is less than 10 years and this is not increased further if MS is progressive in the terminal phase, implying a more prolonged period of inflammatory activity.

At the same time, high levels of perivenular inflammation is also associated with a shorter progressive period and the chance of their presence is about 75% in those with a progressive phase of less than 10 years and again this is not increased further if MS is progressive in the terminal phase. All together, these data suggest that when active lesions and high levels of perivenular inflammation coexist they have the greatest impact on the progressive phase, implying they are complementary inflammatory processes contributing to active disease progression.

The finding that focal white matter inflammatory tissue damage contributes to rapid progression in patients who died in early stages after disease onset (Frischer et al., 2009), challenges the idea that slow degenerative axonal loss, that is independent of inflammation, might underlie clinical progression or might act together with ongoing chronic intrathecal inflammation (Monaco et al., 2020).

However, in addition, focal T2 MRI lesions combined with relapses have been shown to possibly explain later EDSS progression (Miller et al., 1988; Sormani et al., 2011). However, it is not known the exact load and effect of underlying neuropathological damage in the disease outcome and whether it is visible using current conventional imaging techniques. The inflammation seen at time of death is almost certainly compartmentalised behind the blood brain barrier and so will not be detectable as acute changes (Meinl et al., 2008; Machado-Santos et al., 2018). Only recent advanced imaging methodologies enabled to detect more precisely the inflammatory lesion stages in in-vivo MS patients (Absinta et al., 2016; Dal Bianco et al., 2021; Metz et al., 2021). In addition, it should be mentioned that the high inflammatory activity might also interfere (delay and/or halt) with remyelinating and repair mechanisms.

Both early active and increased perivenular inflammation were found in a subset of MS patients who also have a high level of meningeal infiltrates corroborating the hypothesis that a generally higher inflammatory activity in the CNS/CSF space characterizes an MS subgroup with more rapid progression (Magliozzi et al., 2007, 2018; Lucchinetti et al., 2011; Howell et al., 2011). The close, anatomical and functional, association between blood brain barrier and the subarachnoid space (Shechter et al., 2013) is further supported by finding that B-cell clonality has been demonstrated between cells present in the meningeal infiltrates and in perivascular cuffs (Lovato et al., 2011). B cells are relatively predominant in the perivascular cuffs of active lesions (Machado-Santos et al., 2018) and meningeal lymphoid-like infiltrates (Magliozzi et al., 2007, 2018; Howell et al., 2011; Haider et al., 2016), suggesting their key inflammatory role in MS progression (Comi et al., 2021; Li et al., 2018). The early active lesions and perivenular infiltrates we have seen are associated in particular with the preponderance of B lymphocytes, characteristically found in meningeal infiltrates (Magliozzi et al., 2007; Howell et al., 2011; Haider et al., 2016). Accordingly, our quantitative analysis, notwithstanding the limited sample size, confirmed a possible correlation between perivascular CD20+ B lymphocytes and more severe disease course. It remains to be better elucidated whether meningeal B cell infiltration in the subarachnoid space preferentially mediates diffuse subpial cortical demyelination. Perivenular B cell infiltration could possibly contribute to the focal white matter pathology, not only through the production of immunoglobulins, but also by producing different pro-inflammatory and regulatory molecules and by their antigen presenting function (Cepok et al., 2001; Duddy et al., 2004; Lisak et al., 2012).

From our results the perivascular compartment emerges as a target for therapies, subject to the ability of the treatment to cross the BBB. Perivenular inflammation could therefore be considered as a potential relevant biomarker of lesion activity

that, whether validated and assessed in early disease stages, might help to discriminate MS patients with higher lesion and disease activity that will benefit of early and more severe anti-inflammatory treatment.

In such a context, an immunosuppressant approach aiming to reduce disease activity in the early stages would make sense (Amato et al., 2020). This however requires an early identification of disability accumulation (Katz Sand et al., 2014; USF MS-EPIC Team 2019) which could be improved with the use of molecular and imaging biomarkers to quantify the intrathecal inflammatory processes underpinning progressive MS (Matthews, 2019; Dal-Bianco et al., 2017; Magliozzi et al., 2018) aiming to capture the window of opportunity for a targeted anti-inflammatory approach (Sorensen et al., 2020; Rotstein and Montalban 2019).

Concluding, high levels of both active lesions and focal perivenular inflammation within the white matter at post-mortem are associated with rapid disease evolution from onset and to the terminal stages. Associated diffuse and/or organized leptomeningeal inflammation, relevant in subpial cortical pathology, contributes to widespread inflammatory damage in a subset of patients. These pathological features are associated with a more rapid worsening after the onset of progression, but before a wheelchair is required, widening the potential use of an anti-inflammatory approach in progressive MS.

5. CORTICAL LESION LOAD AT DIAGNOSIS PREDICTS PROGRESSION INDEPENDENT OF DISEASE ACTIVITY AND LONG TERM DISABILITY ACCUMULATION

Manuscript in preparation

Author contributions: Schiavi GM^{1*}, Marastoni D^{1*}, Ziccardi S¹, Tamanti A¹, Becchi T², Pisani A¹, Guandalini M¹, Magliozzi R¹, Scalfari A³, Romualdi C², De Stefano N⁴, Calabrese M¹

1. Neurology B, Department of Neurosciences, Biomedicine and Movement Sciences, University of Verona, Verona, Italy
2. Department of Biostatistics, University of Padua, Padua, Italy
3. Centre for Neuroscience, Department of Medicine, Charing Cross Hospital, Imperial College London, London, UK.
4. Department of Medicine, Surgery and Neuroscience, University of Siena, Siena, Italy

* equally contributed

5.1 INTRODUCTION

Multiple Sclerosis (MS) is the most common demyelinating disorder of the central nervous system (CNS), characterized by the accumulation of focal and diffuse white matter (WM) and grey matter (GM) damage (Thompson et al., 2018; Kutzelnigg et al., 2005; Calabrese et al., 2015). The disease usually presents with a relapsing-remitting course, defined by the acute occurrence of neurological symptoms followed by a clinical remission with or without subsequent disability accumulation. Later in the disease course, most patients eventually enter the secondary progressive phase (SPMS), characterized by progressive and irreversible disability accumulation, mostly independent of relapses (Lublin et al., 2014).

While this disability accrual may derive from clinical relapses as relapse-associated worsening (RAW), it is now widely recognized that disability progression mostly occurs independent of relapse activity (PIRA), which is characteristic of SPMS, but also of relapsing MS (RMS) (Kappos et al., 2020; Cree et al., 2019). The pathophysiology of PIRA remains to be fully explained, although it is plausible that PIRA is associated with early diffuse neuroaxonal loss and accumulation of cortical atrophy (Cagol et al., 2022).

The high degree of variability of the clinical outcome, with the full spectrum of disease ranging from benign and even asymptomatic course to more aggressive cases, is the hallmark of the disease. Moreover, the recent emergence of PIRA definition further blurred the traditional distinction between an early relapsing phase and a late secondary progressive MS (SPMS). Natural history cohort studies indicate that approximately 50% of patients convert to SPMS and require ambulation aid in less than two decades (Confavreux and Vukusic, 2006; Scalfari et al., 2010). Unfortunately, clinical, and demographic prognostic factors for the

attainment of irreversible disability milestones (Scalfari et al., 2010; Confavreux et al., 2000; Leray et al., 2010) have limited value at individual level. Despite its usefulness as paraclinical tool for the MS diagnosis, the predictive effect of MRI conventional markers of WM damage, such as the number of T2 hyperintense WM lesions or the presence of black holes, remains controversial, supporting the notion of a clinic-radiological paradox (Barkhof, 2002; Chard and Trip, 2017). The presence of lesions in critical anatomical regions, such as the spinal cord or the cerebellum (Scalfari et al., 2014; Gaetani et al., 2017; Tintore et al., 2010), and the occurrence RIM-positive lesions were found to have a more robust association with the disease progression (Absinta et al., 2016,2019). However, the identikit of the patient at high risk of a disability accumulation and disease progression is still incomplete and reliably predicting the long-term outcome since the early disease stage remains a crucial unmet need and would be paramount for an effective therapeutic management (Derfuss et al., 2020; He et al., 2020; Amato et al., 2020).

The GM damage is known to be a strong predictor of the long-term disability accumulation (Filippi et al., 2013; Fisniku et al., 2008; Haider et al., 2021). Its crucial role in determining the disease progression is corroborated by post-mortem observations showing that extensive GM demyelination and neuronal damage are the hallmarks of progression, often exceeding the extent of WM damage (Howell et al., 2011; Calabrese et al., 2011). The focal and global cortical damage can be radiologically detected very early in the disease course, it progresses sub-clinically for years and, with the gradual exhaustion of the CNS compensatory mechanisms, it becomes the main driver of the clinical course (Calabrese et al., 2011; Lucchinetti et al., 2011; Calabrese et al., 2012). Indeed, the cortical lesions (CLs) have been recently included in the MS diagnostic criteria (Thompson et al., 2018) and their occurrence is routinely evaluated as part of patients' prognostic workup by an increasing number of clinicians.

We previously showed that CLs volume and number are significantly associated with the accumulation of physical and cognitive disability (Calabrese et al., 2012) in the short-term and are a good predictor of the disease evolution towards the SP phase (Calabrese et al., 2013; Scalfari et al., 2018). This was further confirmed by a recent independent study demonstrating that the accumulation of CLs can explain about 40% of the variance of disability progression after 30 years of disease course (Haider et al., 2021).

However, the predictive role of early appearance of CLs remains to be fully elucidated, as MRI studies with a follow-up long enough to observe a sufficient number of patients transitioning to the progressive phase, which is the key event of the long-term prognosis, are scarce. A clear relationship between early CL load and PIRA is also yet to be established. Here we present the data of our cohort of

patients followed up for a mean of 18.0 years; our aim was (i) to draft the identikit of the patient at high risk of progression independent of relapse activity (PIRA) and accumulating severe disability and eventually progression to SPMS phase; (ii) to evaluate the prognostic impact of CLs detected at the time of diagnosis and accumulated in the first 2 years.

5.2 METHODS

Study population

We performed a retrospective evaluation of 199 RRMS patients longitudinally followed up at the MS tertiary centre of Verona University Hospital. The study Inclusion criteria were: I) diagnosis of RRMS that, at the retrospective evaluation, satisfies the most recent revision of the McDonald criteria; II) the availability of a 1.5T MRI examination, including the double inversion recovery (DIR) sequence performed at the time of diagnosis; III) a clinical and radiological follow-up, that included a 1.5T MRI Scan with DIR sequences at least two years after the first assessment; IV) at least 15 years of clinical follow-up.

All patients underwent regular clinical evaluations every six months, with additional visits in case of relapses. The disability was assessed by consensus of two MS neurologists trained in EDSS rating (MC, DM, www.neurostatus.net) using the Expanded Disability Status Scale (EDSS) score. A relapse was defined as acute development of new symptoms or worsening existing symptoms lasting >24 hours. All patients were started on a first line disease modifying treatment (DMT) after the diagnosis, and time to switch to 2nd line therapies were recorded. None of the enrolled patients was administered a 2nd line treatment as the first therapeutic option.

Confirmed disability accumulation was defined by an increase in EDSS by 1.5 points if the last EDSS before conversion to SPMS was 0, an increase by 1 point if the EDSS was lower than 5.5, or an increase by 0.5 points if the EDSS was above 5.5 confirmed by an assessment 12 months later. Progression independent of relapse activity was defined using a sustained PIRA definition (Lublin et al., 2022) and for the purpose of this study we considered disability worsening that occurred in the absence of both clinical relapse and specific changes on conventional MRI imaging (new or enlarged T2 lesions or gadolinium enhancing lesions), where all following assessment confirmed the disability accumulation.

SPMS was defined by:

1. the occurrence of 12-months confirmed disability accumulation within the leading Functional System, in the absence of relapse within 30 days before the clinical assessment.
2. A minimum EDSS of 4.0 (Lorscheider et al., 2016).

Image acquisition protocol

Each patient was relapse- and steroid-free for at least one month before each MRI examination. All images were acquired with the same 1.5T scanner (Achieva, Philips Medical Systems, Best, the Netherlands), with a 33-mT/m power gradient

and a 16-channel head coil. No major hardware upgrades of the scanner occurred during the study period, and bimonthly quality assurance sessions took place to guarantee measurement stability. At follow-up, participants were carefully repositioned according to published guidelines for serial MRI studies of MS (Miller et al., 1991). The following images were acquired from each participant: (1) 3-dimensional (3D) DIR (3D sequence without any interpolation techniques; repetition time [TR] 6.500 milliseconds, inversion time 2.800 milliseconds, delay 500 milliseconds, echo time [TE] 265 milliseconds, slice thickness 1.5 mm, number of averages 2, matrix 256 x 256; (2) 3D fluid-attenuated inversion recovery (FLAIR, TR 10,000 milliseconds, TE 120 milliseconds, inversion time 2,500 milliseconds, echo train length 23, slice thickness 1.5 mm, matrix 172 x 288, and field of view 250 x 200 mm²), and (3) 3D fast-field echo (FFE): 120 contiguous axial slices with the off-centre positioned on zero, TR = 25 msec, TE = 4.6 msec, flip angle = 30°, slice thickness = 1.2 mm, matrix size = 256 x 256, and a FOV = 250 x 250 mm; (4) Post-contrast T1-weighted spin echo: TR = 618 msec, TE = 10 msec, 20 slices with a thickness = 5.5 mm, flip angle 90 a matrix size = 224 x 256, and a FOV = 230 x 230 mm, resolution = 1.03x0.89mm. This sequence was acquired 5 minutes after gadolinium-EDTA (0.1 mmol/kg) intravenous administration

MRI analysis

MRI data were evaluated at diagnosis (T0) and after two years (T2). Each MRI image has been assessed by consensus of two physicians (GMS and MC), blinded to patients' clinical details. The following MRI parameters were analyzed: the number of white matter lesions (WML) and white matter lesions volume (WMLv), the number of CLs and cortical lesion volume (CLv). The presence/absence of spinal cord lesions was recorded using MRI reports.

The number of new and pre-existing CLs lesions with clear morphological evidence of cortical involvement was assessed on DIR images according to the recommendations for CL scoring in patients with MS (Geurts et al., 2011). Owing to the suboptimal performance of the image-acquisition sequences on MRI in visualizing subpial lesions (Seawann et al., 2012), the present analysis has taken into account mainly the intracortical and leukocortical lesions. Cortical lesion volume (CLv) was calculated using a semi-automatic thresholding technique based on a fuzzy C-mean algorithm⁴⁰ included in software developed at the National Institutes of Health, Medical Images Processing, Analysis and Visualization (<http://mipav.cit.nih.gov>). WM lesion number was examined on FLAIR images. Four classes of WMLs based on their number were identified: 0 lesions, 1-3 lesions, 4-10 lesions, >10 lesions. WML volume (WMLV) was assessed through the same software adopted for CLv (Pham et al., 1999).

Statistical analysis

Data are provided as means with standard deviations (SD) or medians (range), as appropriate. We used the Fisher's exact test to compare categorical data and the

Mann-Whitney test to compare means across patient groups for nonnormal variables. The Shapiro-Wilks test was applied to test normality.

Random survival forest analysis and Cox regression analysis were performed to calculate the risk of attaining a PIRA event, entering the SP phase and the risk of attaining EDSS = 4.0 and = 6.0 based on demographic variables (age and sex), CLn was classified into two classes (according to quartile distribution values: patients with CLn equal or greater and lower than the 3rd quartile, that was 3 CLs) and CLv, WMLv and WMLn (classified in 4 classes: 0 lesions, 1-3 lesions, 4-10 lesions and more than ten lesions), and the presence of the spinal cord lesions and Gd+ lesions, at the time of diagnosis. The location of WM lesions (brainstem and/or cerebellar lesions) was also included in an explorative analysis.

The number of new WML, new CLs, new relapses and EDSS change at T2 were also included in separate models. Proportional hazard assumption was checked by visual inspection of Schoenfeld residual plots and corresponding statistical tests.

The receiver operating characteristic (ROC) analysis (Youden index method) was used to identify a cortical lesion number cut-off that maximizes specificity and sensitivity in identifying patients who attained SPMS status at the end of the study. Sensitivity, Specificity, Accuracy and Area Under Curve (AUC) with 95% Confidence Interval (CI) were reported. The Kaplan-Meier analysis estimated the time to SPMS conversion and the attainment of EDSS 4 and 6 among patients grouped by baseline CLs number optimal cut-off, identified by ROC analysis. Finally, the Kaplan-Meier analysis was used to estimate the time to the conversion to SPMS based on the presence of spinal cord lesions at diagnosis and the CLs number cut-off identified by ROC analysis. Statistical estimates are reported with a 95% CI and the corresponding P-value. The statistical analysis was performed with STATA and R-studio. P-values < 0.05 were considered statistically significant.

5.3 RESULTS

Study cohort

Among the 199 patients included in the study, after a mean follow-up of 18.0 ± 3.2 years (range 15-22 yrs), eighty-three patients (41.7%) experienced PIRA, with a mean time to reach PIRA of $7.6y \pm 3.6$ years. At the end of the follow-up period 39 (19.6%) had converted to SPMS after a mean of 10.6 ± 3.4 years. Notably, 44 PIRA patients were classified as SPMS at the end of the follow-up period. Compared to patients who had no progression independent of disease activity, those who entered the PIRA phase had higher baseline EDSS ($p < 0.001$) and experienced more severe EDSS change in the first two years ($p = 0.014$). No significant differences in age and sex were noted between the two groups (see Table 5.1 for the whole demographic and clinical data, and Table 5.2 for radiological data).

	All patients (n = 199)	PIRA (n = 83)	No-PIRA patients (n = 116)	p-value
<i>At baseline</i>				
Female sex (%)	135 (67.8)	50 (60.2)	85 (73.2)	0.067
Age (yrs, mean ± SD)	32.7 ± 9.6	33.3 ± 9.4	32.2 ± 9.8	0.420
Median EDSS at baseline (range)	1.0 (0 - 4.0)	1.5 (0 - 4.0)	1.0 (0 - 3.0)	<0.001
Relapses T0-T2 – (mean ± SD)	0.6 ± 0.9	0.8 ± 1.0	0.5 ± 0.8	0.133
Mean EDSS change T0-T2	0.3±0.9	0.7±1.1	0.2±0.8	0.014
Pts with relapses T0-T2 (%)	79	38	41	0.144
<i>End of follow-up</i>				
Time to PIRA (yrs, mean ± SD)	/	7.6±3.6	/	/
EDSS ≥ 4 - n (%)	54 (27.1)	51	3	< 0.001
Time to EDSS ≥ 4 (yrs, mean ± SD)	9.6 ± 4.6	9.67 ± 4.6	9.0	-
EDSS ≥ 6 - n (%)	28 (14.0)	27	2	< 0.001
Time to EDSS ≥ 6 (yrs, mean ± SD)	11.5 ± 3.5	11.56 ± 3.6	11.0	-
Median EDSS (range)	2.0 (0-8.0)	5.0 (1.0-8.0)	2.0 (0.0-6.0)	< 0.001
Switch 2 nd Line Therapy- n (%)	92 (46.2)	55 (66.2)	37 (31.9)	< 0.001
Time to switch to 2 nd line (yrs, mean ±SD)	9.1±4.6	9.5±4.6	8.7±4.7	0.712
Mean disease duration (yrs)	18.0 ± 3.2	18.0 ± 3.2	18.3 ± 3.3	0.865

Table 5.1. Patients with SPMS were characterized by baseline higher EDSS and, at the end of follow-up, showed significant disability accumulation and a shorter time to reach disability milestones. Abbreviations: EDSS = Expanded Disability Status Score; MS = multiple sclerosis; RR = relapse remitting; SPMS = secondary progressive multiple sclerosis. The p values were obtained by comparing the RR and the SP groups with a binomial test for proportions (*n* [%] variables) and a nonparametric Mann-Whitney test for nonnormal variables.

	All patients (n = 199)	PIRA (n = 83)	NON-PIRA Patients (n = 116)	p
<i>At baseline</i>				
CLn (<i>mean ± SD</i>)	2.3 ± 3.3	4.7 ± 3.7	0.4 ± 0.95	< 0.001
0 CLs (<i>n, %</i>)	102 (51.3)	13 (61.9)	89 (76.7)	< 0.001
1-2 CLs (<i>n, %</i>)	36 (18.1)	12 (21.9)	24 (20.7)	< 0.001
≥ 3 CLs (<i>n, %</i>)	61 (30.6)	58 (69.9)	3 (2.6)	< 0.001
≥ 1 Spinal cord lesion (<i>n, %</i>)	106 (53.2)	49 (59.0)	57 (49.1)	0.195
≥ 1 Brainstem lesions (<i>n, %</i>)	30 (15.0)	15 (18.0)	15 (12.9)	0.327
≥ 1 Cerebellar lesion (<i>n, %</i>)	20 (10.0)	12 (14.5)	8 (6.9)	0.089
0 WMLs (<i>n, %</i>)	9 (4.5%)	2 (2.5)	7 (6.0)	0.309
1-3 WMLs (<i>n, %</i>)	30 (15.1%)	9 (10.8)	21 (18.1)	0.227
4-10 WMLs (<i>n, %</i>)	84 (42.2%)	29 (34.9)	55 (47.4)	0.083
>10 WMLs (<i>n, %</i>)	76 (38.2%)	43 (51.8)	33 (28.4)	0.001
CLv (<i>mm3</i>) <i>mean ± SD</i>	110.6 ± 347.6	482.3 ± 406.2	34.3 ± 77.6	<0.001
WMLv (<i>mm3</i>) <i>mean ± SD</i>	2191.6 ± 1834.1	2778.1 ± 1986.2	1771.9 ± 1597.8	0.137
<i>At T2</i>				
New CLs at T2 - <i>mean ± SD</i>	0.6 ± 1.3	1.3 ± 1.7	0.06 ± 0.3	< 0.001
Patients with ≥ 1 New CLs at T2 - <i>n (%)</i>	44 (22.1)	39 (47.0)	5 (4.3)	< 0.001
New WMLs at T2 <i>mean ± SD</i>	0.8 ± 1.2	0.9 ± 1.3	0.7 ± 1.0	0.133
Patients with New WMLs at T2 - <i>n (%)</i>	87 (43.7%)	39 (47.0)	48 (41.3%)	0.470

Table 5.2. Patients with progressive MS showed increased baseline both white and grey matter damage. Notably, in the first two years of the disease, radiological activity with increased CLs, but not WMLs, was noticed in patients that eventually developed SPMS. Abbreviations: RRMS = relapsing-remitting multiple sclerosis; SPMS = secondary progressive multiple sclerosis; CLN = cortical lesion number; CLs = cortical lesions; Gd+ lesions = Gadolinium enhancing lesions; WMLs = white matter lesions; CLV = cortical lesion volume; WMLV = T2-weighted white matter lesion volume. The p values were

obtained by comparing the RR and the SP groups with a binomial test for proportions (n [%] variables) and a nonparametric Mann-Whitney test for nonnormal variables.

During the observation period, 54 (27.1%) patients reached an EDSS ≥ 4 (mean time 9.6 ± 4.6 yrs), and 28 (14.1%) reached EDSS ≥ 6 (mean time 11.5 ± 3.5 yrs). A significant difference was observed between the PIRA and non-PIRA group in the number of patients who reached the EDSS score of 4 (51 vs 3) and 6 (27 vs 2). Most of patients with PIRA were eventually switched to a second line DMT ($n = 55$, 66.2%), but notably the mean time to therapy switch was longer than time to PIRA (Table 5.1).

The early appearance of CLs characterizes patients who will attain progressive MS

More severe focal cortical pathology at diagnosis distinguished patients who eventually had progression independent of disease activity. At baseline, these patients had a higher number (mean 4.7 ± 3.7 vs 0.3 ± 0.9 , $p < 0.001$) and volume (mean 482.2 ± 406.2 mm³ vs 34.4 ± 77.6 mm³, $p < 0.001$) of CLs, compared to the non-PIRA group. Similarly, a higher amount of CLs characterized the patient with a diagnosis of SPMS at the end of the follow-up (mean CLs, 6.3 ± 3.5 vs 1.2 ± 2.3 , $p < 0.001$; mean CLv 657.7 ± 404.2 mm³ vs 114.7 ± 236.5 mm³, $p < 0.001$).

Cortical lesions at diagnosis predict the onset of PIRA

The random survival forest analysis selected CLs, CLv and EDSS as the most important variables predictive of PIRA.

The Cox regression analysis confirmed the results: CLs (HR 1.15 [1.02-1.30], $p = 0.018$), CLv (HR 1 [1-1], $p = 0.003$), and EDSS (HR 1.8 [1.41-2.31], $p < 0.001$) were the variables predictive of occurrence of disability progression independent of relapses (Figure 5.1).

Cortical lesions at diagnosis predict the diagnosis of secondary progressive MS and achievement of disability milestones

When evaluating disability milestones, CLs volume, number of CLs, and baseline EDSS, combined with the presence of spinal cord lesions were as well the best associated/predictors of reaching a diagnosis of SPMS and an EDSS ≥ 4 and ≥ 6 over the follow-up.

In figure 5.2 A-B-C results from both random survival forest and Cox regression models are summarized and graphically shown according to the above-mentioned clinical outcomes.

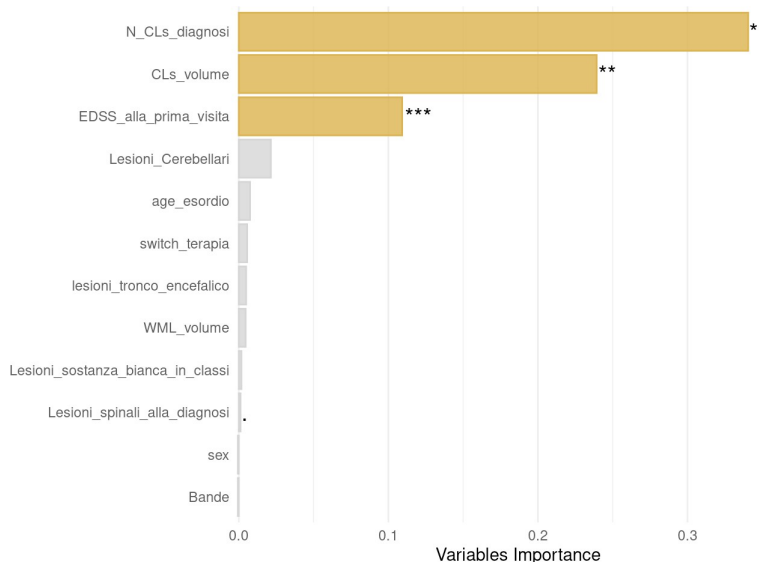
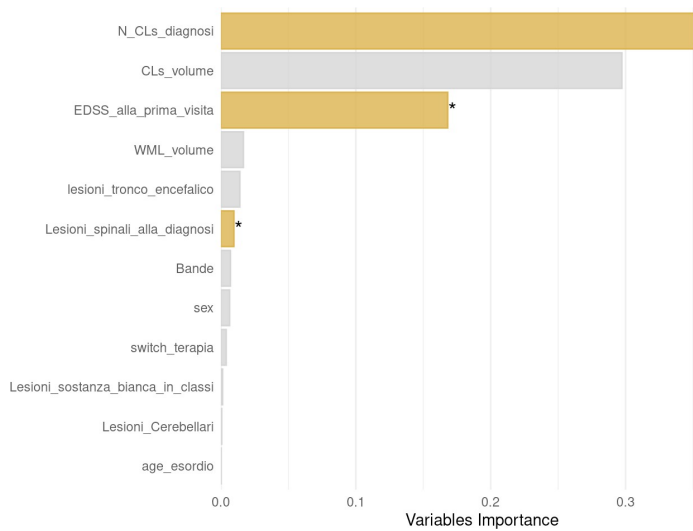


Figure 5.1 Cortical damage at diagnosis predicts the risk of PIRA. The graph allows to visualize both Cox and Random.Forest.Survival results. The length of the bar represents the importance of that variable obtained with Random.Forest.Survival model, yellow bars are the ones that results as significant ($p < 0.05$) with Cox model. The number of stars indicates the significativity for Cox model



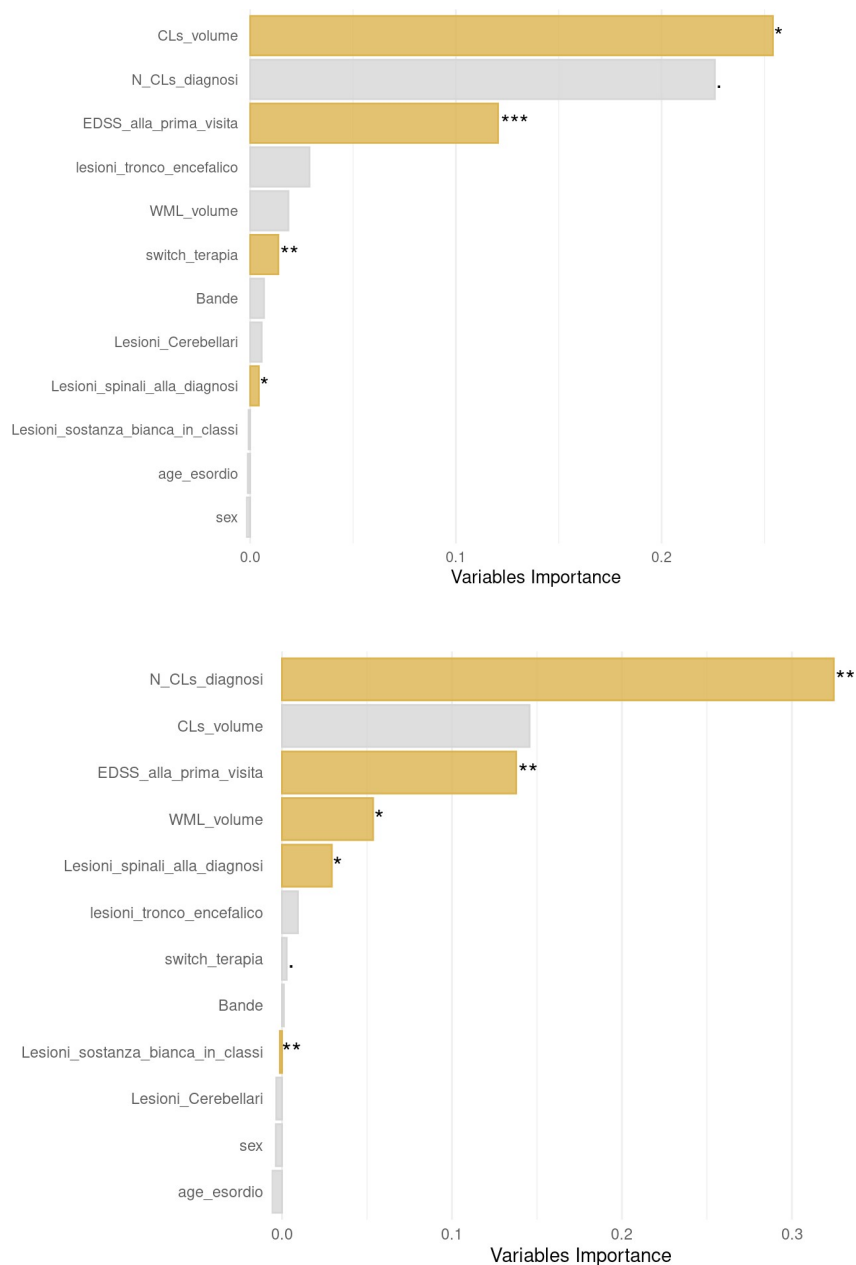


Figure 5.2A-B-C Cortical damage at diagnosis predicts the risk of SPMS (first graph) and attainment of EDSS 4 (second graph) and 6 (third graph).

An optimal cut-off to predict disability progression

Among the 102 patients without CLs at diagnosis, 12 patients (11.7%) eventually entered PIRA phase, and only 3 patients progressed to SPMS despite the long follow-up. The lack of CLs was also associated with a lower disability burden: 7 patients (6.8%) reached EDSS = 4 (mean time 11y, range 7-20), and 2 reached an EDSS = 6 (11y, [11-11]).

By applying ROC curve analysis (Figure 5.3) we estimated an optimal cut-off value of 3 CLs at diagnosis to identify patients at high risk of developing SPMS

($AUC = 0.90$ [0.83-0.96], $Sensitivity = 90\%$ [80-97%, 95%CI], $Specificity = 84\%$ [78-90%, 95%CI], $Accuracy = 85\%$ [80-89%, 95%CI]).

Accordingly, when comparing the group with at least three CLs (61 patients) with the group with less than three CLs (138), a significant difference ($p < 0.001$) in the number of patients entering SPMS was observed (57.3% vs 2.9%) with a significant shorter time to reach SPMS status and also to eventually attain the disability milestones of EDSS 4 and EDSS 6 at the end of the follow-up (Figure 5.4).

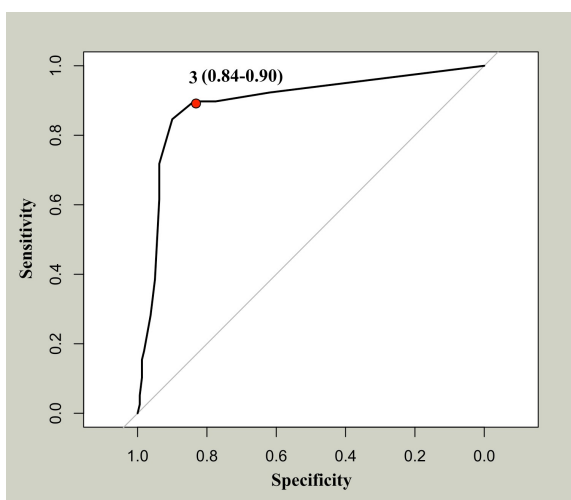


Figure 5.3. ROC Analysis. ROC curve highlighting the best cut-off for discriminating between SPMS converting and RRMS was reported. Specificity and Sensitivity measures in brackets. The optimal threshold for each protein was 3 (red dot) Abbreviations: ROC = receiver operating characteristic.

Accumulation of Cortical Lesions in the two years after diagnosis is a predictor of progression

We also assessed the probability of MS progression in a multivariate analysis, including the clinical and radiological variables after two years. The accumulation of new CLs in the first two years, but not of new WMLs, predicted the subsequent onset of SPMS (HR 1.3 [CI 1.1-1.5], $p < 0.001$). When assessing the risk of attaining EDSS milestones, including variables at T2 in the analysis, the accumulation of new CLs was also found to be a good predictor of reaching EDSS = 4 (HR 1.28 [CI 1.09-1.51], $p = 0.002$) and EDSS = 6 (HR 1.39 [CI 1.12-1.73], $p = 0.003$).

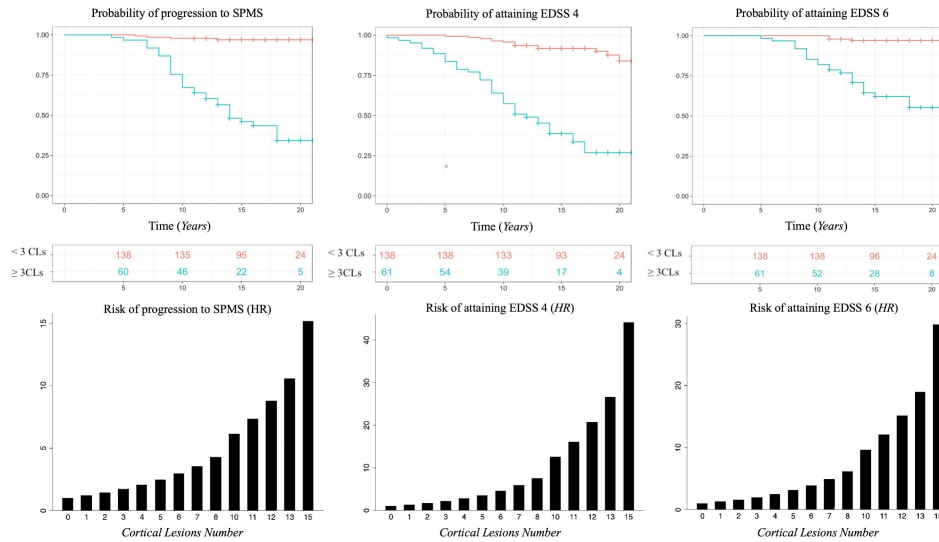


Figure 5.4. Probability of conversion to SPMS, Attaining EDSS 4 and EDSS 6 according to CL number at the time of diagnosis. Panel A. Patients with 3 or more CLs at the time of diagnosis had a significantly increased risk of entering in MS progressive phase and developing significant disability ($p < 0.001$). **Panel B.** Hazard Ratios (y-axis) of entering MS progressive phase and developing significant disability according to the number of cortical lesions (x-axis) are shown. Abbreviations: CLs= cortical lesions, EDSS=expanded disability status scale.

Combined spinal cord and cortical involvement and risk of disability progression

The spinal cord involvement at the diagnosis was not significantly associated with CL load (not shown). However, when evaluating patients with combined cortical and spinal involvement, the probability of developing MS progression significantly increased compared to the groups of patients with either isolated cortical or isolated spinal cord involvement (Figure 5.5). Nevertheless, having at least three CLs without spinal cord lesions still provided a significantly higher probability of disease progression than having spinal cord lesions alone ($p = 0.03$, Figure 5.5).

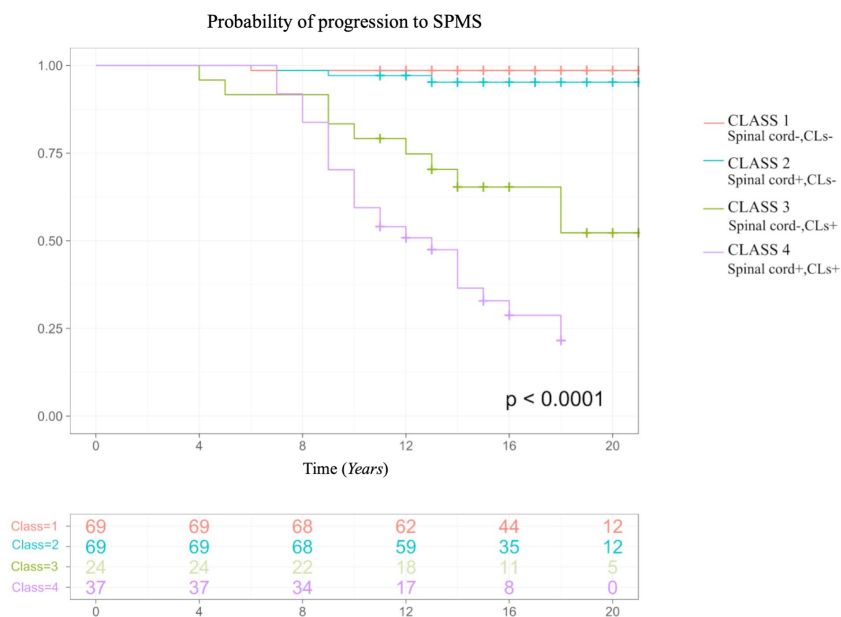


Figure 5.5. Kaplan-Meier survival curve according to cortical and spinal cord involvement at the time of diagnosis and the risk of conversion to SPMS.

All patients were divided into classes: 1: < 3 CLs and no spinal cord involvement; 2: < 3 CLs, spinal cord involvement; 3: ≥ 3 CLs, no spinal cord involvement; 4: ≥ 3 CLs and spinal cord involvement. Patients with cortical pathology and spinal cord involvement were characterized by a higher risk of disability progression ($p < 0.0001$).

5.4 DISCUSSION

In this large cohort of MS patients observed for almost 20 years, we provided evidence that the presence of CLs, especially more than three, at diagnosis and the occurrence of new CLs within the first two years are associated with an increased risk of progression independent of disease activity and also a shorter time to disability milestones (EDSS 4 and 6). In addition, we highlighted that patients without CLs at diagnosis exhibited a rather mild disease course, with a minor risk of accrual of disability independent of relapse and only rarely developed a progressive accumulation of disability in the first 20 years of disease.

GM damage: disease progression, and disability accumulation

The pathological basis of the disability progression in MS is still under investigation: seminal long-term cohort studies highlighted the prognostic role on MS-related disability, of several demographic and clinical variables (Chung et al., 2020; Rudick et al., 2006) as male gender, the age and type of onset, the WM lesion load especially when it involves the spinal cord (Brownlee et al., 2019); nevertheless, despite the undoubted improvements that have occurred in the last

decade, our ability to identify at the time of diagnosis those patients at risk of experiencing an early disease progression remains, so far, inadequate.

The crucial role of the focal and diffuse GM damage among patients with a more severe MS course and a more rapid disease progression has been deeply investigated in post-mortem and in vivo studies (Calabrese et al., 2010, 2015): the GM damage, especially when it occurs in critical deep GM structures (Rocca et al., 2010; Eshaghi et al., 2018) has been consistently identified as a key factor, strongly associated with disability accumulation and progressive MS. (Fisniku et al., 2008; Calabrese et al., 2007; Mahad et al., 2015).

Although the relationship between CLs and cortical atrophy remains debated (Treaba et al., 2021), several studies also highlighted the contribution of CLs to the disease progression (Beck et al., 2022; Calabrese et al., 2013). This concept has been recently confirmed in an elegant study showing a strong correlation between the disability accumulation and the extent of focal cortical damage after 30 years of disease duration (Haider et al., 2021). However, data on the predictive value of the early appearance of CLs and the long-term MS evolution are still limited (Pisani et al., 2021). Starting from the results of our previous study (Scalfari et al., 2018), we here confirmed in a long-term clinical setting that the presence of CLs at the time of diagnosis is a reliable marker of both the subsequent accumulation of irreversible disability, even independent from relapse and disease activity, and the conversion to the progressive phase. We identified a significantly higher risk of converting to PIRA and later SPMS among patients with a higher number of CLs at diagnosis, which in the RSF model was found to be the best predictor of progression, among the clinical and paraclinical variables. Importantly, only few patients without CLs at the time of diagnosis eventually became SPMS, while the large majority remained free of progression despite being observed for 18 mean years. This confirms our previous data: low degree of early cortical pathology characterizes MS patients with a benign course. Those patients, even with short follow-up periods when compared to our current study, subsequently accrued less CLs, experienced lower disability over time, and entered the progressive phase less frequently and less rapidly (Calabrese et al., 2009; Calabrese et al., 2016).

Cortical lesions compared to other radiological and clinical parameters at diagnosis and after two years

In line with previous studies (Arrambide et al., 2018), we also confirmed the prognostic relevance of the spinal cord damage, as early predictor of the disease evolution. Interestingly, we did not find any correlation between the extent of spinal cord lesions and CLs, which are presumably driven by independent pathological processes, indicating that the combined cortical and spinal

involvement since the early stage exert a detrimental effect on the long-term disability accumulation.

In the random forest analysis, despite the significant difference in the number of WM lesions at baseline between patients who experienced PIRA and the non-PIRA patients, the WM lesion burden was found to have limited impact on the risk of both progression and disability accumulation when compared to previous literature data (Tintore et al., 2015); this is probably explained by the dominant predictive effect exerted by the presence of CLs and spinal cord lesions. Even the inclusion in the regression analysis of the presence of lesions in critical areas (Giorgio et al., 2013), such as the cerebellum or brainstem, did not show a significant change in the risk of both attaining PIRA status or reaching higher EDSS scores (not shown). This could be due to the low number of patients showing cerebellar or brainstem lesions.

When considering the other tested variables after two years from diagnosis, the occurrence of new CLs also represented the best surrogate marker for predicting subsequent disability accumulation compared to other clinical and radiological variables at T2. Among others, the accumulation of new T2 WM lesions did not provide predictive value, thus also suggesting the central contribution of routinely assessing the number of new CLs in follow-up clinical studies (Sormani et al., 2011) and routinely in clinical practice.

Correlation to neuropathological basis of cortical damage

The lack of sensitivity of focal GM damage assessed by MRI compared with the underlying subpial pathology raises an issue (Geurts et al., 2005,2012). In particular, subpial demyelination, associated with the persistent inflammatory milieu in the adjacent meningeal sulci and a severe MS course (Reynolds et al., 2011), remains undetectable with current MRI techniques adopted in clinical practice. DIR sequences have been recognized to mainly address the presence of leukocortical and, partly, intracortical lesions. Nevertheless, it has been demonstrated that the number of radiologically detectable CLs, even at 1.5 Tesla MRI, might represent just the tip of the iceberg which correlates with the total amount of focal cortical damage (Seawann et al, 2011).

Recently several new MRI sequences, such as Phase Sensitive Inversion Recovery (PSIR), magnetization-prepared rapid acquisition with gradient echo (MPRAGE) and T2*-weighted images have been introduced to detect cortical lesions. However, despite the advances in MRI techniques, histological studies evidenced extensive GM demyelination and neuronal damage that were undetectable by MRI (Vercellino et al., 2005). This is due to the small size of CLs (Seawann et al., 2011) and to their low contrast-to-noise ratio (Tardif et al., 2012) as well as the

partial volume effects and the susceptibility and flow artifacts at the cortex/CSF interface (Kidd et al., 1999; Peterson et al., 2001; Schmierer et al., 2010).

Nevertheless, we believe that the point is not to identify all lesions. In the last decade, several studies have demonstrated a strict association between CLs and meningeal inflammation, diffuse or aggregated in ectopic B cell follicle-like structures, either in post-mortem MS cohorts or in MS biopsies (Haider et al., 2016; Pikor et al., 2016; Griffiths et al., 2020; Church et al., 2021). It was hypothesized that GM active demyelination and neurodegeneration might be driven by soluble factor(s) produced in the meningeal inflammatory infiltrates, through either directly or indirectly microglia activation (Magliozzi et al., 2018; James et al., 2020; Picon et al., 2021, van Olst et al., 2021).

We suggest that CLs, as visualized by MRI, should be considered as a possible surrogate marker of meningeal inflammation, which is linked with disease progression (Choi et al., 2021) rather than a precise estimation of the total number of CLs. This association was confirmed in cross-sectional and longitudinal studies with focal and diffuse GM damage being associated with a specific intrathecal inflammatory profile confirming the correlation between meningeal inflammation, cortical demyelination and diffuse neurodegeneration, which is the base of the “silent” disease progression since the time of diagnosis in both RRMS and primary progressive MS (Magliozzi et al., 2020; Marastoni et al., 2021). On the other hand, diffuse GM damage has been also observed in PIRA patients (Cagol et al., 2022), moreover chronic inflammatory tissue injury is also considered to be a significant contributor to PIRA and believed to be driven by meningeal inflammatory aggregates (Ransohoff, 2023).

It could then be considered that even the presence of CLs on 1.5T MRI could indicate those patients with a profile susceptible to meningeal inflammation and, therefore, disease progression even independently from relapses. We highlighted in our results the relatively low number of three CLs at diagnosis: this data in line with our previous one (Scalfari et al., 2018) showing that a number of 7 CLs characterized patients at high risk of developing SPMS. Despite the difference in the number of CLs that could be explained by the different follow-up and endpoints, the hypothesis remains the same: having MRI visible CLs at disease onset could be a sign of the presence of meningeal B cell follicles whose activity is strongly related to the disability progression.

The long follow-up of our study compared to the strong predictive factors of CLs early in the disease is a strong suggestion that prognosis in MS could be determined early stage. This possible association between CLs and resident meningeal follicles is a further indication in the same direction: the compartmentalization of B-cell population organized in lymphoid like structures

early in the disease can go on to develop neurodegenerative processes that could eventually determine the disease progression years later, independently of active lesions (Serafini et al., 2004; Bevan et al., 2018).

Therapeutic implications and other considerations

The presence and number of CLs at diagnosis should be considered in the patient's treatment choice, and those with a higher load of CLs should be selected for a high-efficacy therapy. On this latest hypothesis, an early introduction of therapy could matter, and has been suggested as a recommended approach for patients with active relapsing-remitting multiple sclerosis (He et al., 2020). A lot of attention is now surrounding early induction treatment versus escalation therapy even on the matter of progression, where induction treatment has been found to have greater beneficial effect on preventing long term disability accumulation and disease progression (Iaffaldano et al., 2021; Brown et al., 2019) and our results and hypothesis certainly do not seem to contradict these data. It can be proposed that therapies able to reduce intrathecal inflammation, in particular B-cell compartmentalization and/or the associated glia activation, may represent potential practical approaches to block/delay the disease progression. This hypothesis is supported by the fact that anti-B cell therapies represent one of the partially effective treatments in progressive MS (Stathopoulos et al., 2022). Moreover, we also observed that the new accumulated CLs after two years were the major predictor of disability even among T2 variables and this fuels the suggestion that patients with more severe focal cortical damage early in the disease course should be managed with an early aggressive therapeutic approach in the first years since diagnosis.

Notably, DMT was found to prevent the development of new CLs and reduce the progression of cortical atrophy in patients aged 18 to 55 with RRMS (Calabrese et al., 2012; Crescenzo et al., 2019; Bajrami et al., 2018). Regarding the current study, it has to be noted that the majority (78%) of the secondary progressive patients were eventually switched to second-line therapy. However, the time of exposition to second-line therapy did not alter the prediction model and wasn't considered as a variable in the regression models.

Study limitations

This study is not without limitations: it was designed to evaluate the role of CLs and not to fully assess the role of all possible variables including WM lesions on disability progression, therefore, many MRI variables, including WM lesion type, size, and location, have not been fully assessed. Furthermore, we classified the WM lesions' number in four classes to maintain homogenous data among patients with vastly different imaging presentations and lesion burdens, some of them with

large confluent lesions. Still, we also accounted for WM lesions volume to minimize statistical errors. This can explain why the accumulation of WM lesions did not provide predictive value and could limit our results' interpretation. Moreover, the cognitive evaluation was not included in the clinical evaluation. Our analysis was also limited by the absence of fully quantitative data on spinal cord total lesion number and area.

Finally, the number of patients who enter the SP phase is relatively low; therefore, other studies with a larger sample size but a similar follow up, although very difficult to be carried out, should be designed to confirm our results.

In conclusion, we provided evidence that, among the different MRI markers of disability progression, the presence of cortical lesion early in the disease course strongly predicts MS progression, even independent of disease activity and accumulation of disability. Further effort is needed to include the assessment of cortical damage in the clinical routine to optimize patient stratification towards a personalized approach based on the risk of subsequent early disability accumulation.

6. CSF LEVELS OF CXCL12 AND OSTEOPONTIN AS EARLY MARKERS OF PRIMARY PROGRESSIVE MULTIPLE SCLEROSIS

Published in: *Neurol Neuroimmunol Neuroinflamm* 2021;8:e1083.
doi:10.1212/NXI.0000000000001083.

Authors: Damiano Marastoni, MD^{1,*}, Roberta Magliozzi, PhD^{1,*}, Anna Bolzan, MD¹, Anna Isabella Pisani, PhD¹, Stefania Rossi, PhD¹, Francesco Crescenzo, MD¹, Stefania Montemezzi, MD², Francesca Benedetta Pizzini, PhD², and Massimiliano Calabrese, MD¹

- 1 Neurology B, Department of Neurosciences, Biomedicine and Movement Sciences, University of Verona, Verona, Italy
- 2 Neuroradiology and Radiology Unit, Azienda Ospedaliera Universitaria Integrata, Verona, Italy

6.1 INTRODUCTION

Multiple sclerosis (MS) is the most common immune-mediated disorder of the CNS. The disease course is usually characterized by an initial relapsing-remitting MS (RRMS) phase, defined by the occurrence of new neurologic symptoms and subsequent disability. Later in the disease course, most patients enter a secondary progressive MS (SPMS) phase defined by progressive accumulation of disability, mostly independent of relapses (Thompson et al., 2018; Lublin et al., 2014). About 10%–15% of patients exhibit a progressive disease course from the onset (primary progressive MS [PPMS]), with superimposed relapses in few cases (Miller and Leary, 2007). Both focal and diffuse white matter (WM) and gray matter (GM) damage characterize MS pathology (Kutzelnigg et al., 2005; Calabrese et al., 2015). GM damage occurs since earlier disease stages (Lucchinetti et al., 2011; Calabrese et al., 2015) and is a negative prognostic factor for MS-related disability (Calabrese et al., 2012). Inflammation is a major driving force in progressive MS: inflammatory infiltrates, particularly compartmentalized in the meningeal spaces, persist in both SPMS and PPMS associating with GM subpial demyelination and a severe disease course (Lassmann, 2019; Magliozzi et al., 2007; Howell et al., 2011; Choi et al., 2012). In a combined ex vivo and in vivo study, CSF analysis revealed an inflammatory profile that associates with GM pathology (Magliozzi et al., 2018) and predicts MS disease activity in the first years after diagnosis (Magliozzi et al., 2020). Here, we evaluated the presence and levels of inflammatory markers in the CSF of patients with PPMS at the time of diagnosis, with the aim to identify molecules capable of distinguishing PPMS from RRMS. This will shed some light on the pathogenesis of progressive MS and, at the same time, will define in vivo the extent of intrathecal inflammation in PPMS and its association with disease severity.

6.2 METHODS

Patient Cohort

Sixteen consecutive treatment-naive patients with PPMS and 80 with RRMS from the MS Center of Verona University Hospital (Italy) were evaluated at diagnosis between September 2014 and February 2017. Age and disability were different between the 2 groups, whereas the disease duration was similar. Detailed demographic, clinical, and MRI characteristics of patients with MS are shown in Table 6.1. All patients had a confirmed MS diagnosis according to the most recent diagnostic criteria (Polman et al., 2011). They underwent a neurologic evaluation, including the Expanded Disability Status Scale (EDSS) assessment (Kurtzke,1983), a brain 3T MRI, and CSF examination. A group of 13 age- and sex-matched (with patients with PPMS) controls with noninflammatory neurologic disorders (2 myopathy, 2 ischemic stroke, 2 peripheral neuropathy, 1 idiopathic tremor, 1 migraine, 1 fibromyalgia, 1 spondylotic myelopathy, 1 amyotrophic lateral sclerosis, 1 idiopathic spastic paraparesis, and 1 endocranial hypertension) that underwent neurologic evaluation and lumbar puncture was also included in the study.

	Total MS	PPMS	RRMS	<i>p</i>
N	96	16	80	
Age (years; mean±SD)	39.7±13.2	54.2±9.4	36.8±11.9	<0.001
Gender (f:m)	68:28	6:10	62:18	0.003
Disease duration (years;mean±SD)	6.2±5.3	6.2±8.5	6.2±4.4	0.075
Median EDSS (range)	2 (0-5)	3.25 (0-5)	2 (0-5)	<0.001
OCB (positive/negative/n.a)	78/17/1	11/4/1	67/13	0.461
IgG Index	0.8±0.4	0.7±0.2	0.8±0.4	0.177
WMLN (mean±SD)	8.9±4.1	10.1±5.4	8.6±3.8	0.323
WMLV (mm ³ ; mean±SD)	1167.9±1268.8	2738.7±2404.8	853.8±487.9	0.002
CLN (mean±SD)	4.3±5.2	5.7±5.5	4.1±5.1	0.194
CLV (mm ³ ; mean±SD)	431.4±561.5	646.7±688.8	387.3±526.1	0.109
CTh (mm; mean±SD)	2.5±0.4	2.4±0.5	2.5±0.3	0.496

Table 6.1. Demographic, clinical and MRI characteristics of MS patients. Abbreviations: EDSS: Expanded Disability Status Scale; OCB: oligoclonal bands; n.a.: not available; IgG index: Immunoglobulin-G index; WMLN: T2 white matter lesion number; WMLV: T2 white matter lesion volume; CLN: cortical lesion number; CLV: cortical lesion volume; CTh: global cortical thickness. P values for each comparison between PPMS and RRMS groups are reported.

CSF Analysis

CSF samples were obtained at least 1 month after the last relapse and within 1 week of the MRI, according to the Consensus Guidelines for CSF and Blood Biobanking (Teunissen et al., 2009). After centrifugation, the supernatant and the cell pellet were stored separately at -80°C until use. Immunoglobulin G index and presence/absence of oligoclonal bands for each patient with MS were evaluated. Analysis of CSF levels of 34 inflammatory mediators was performed using a combination of immune assay multiplex techniques based on the Luminex technology (37- and 40-plex customized panel, Bio-Plex X200 System equipped with a magnetic workstation; BioRad, Hercules, CA) using Bio-Plex Software Manager 6.1 as previously described.¹² All samples were analyzed in duplicate in 2 independent experiments to verify the results' reproducibility and consistency. The CSF level of each protein detected during the analysis was normalized to the total protein concentration of each CSF sample (measured by the Bradford protocol)(Magliozzi et al., 2018).

MRI Protocol and Analysis

Three-Tesla MRI equipped with a 8-channel head coil was performed at the Radiology Unit of the University Hospital of Verona using a Philips Achieva 3T MRI Scanner, on each patient at least 1 month from the last relapse. MRI sequences were acquired as previously described (Magliozzi et al., 2018). The following sequences were acquired: (a) 3D T1-weighted turbo field echo (repetition time (TR)/echo time (TE) = 8.4/3.7 ms, voxel size of $1 \times 1 \times 1$ mm), total acquisition time of 5:51 minutes; (b) 3D double inversion recovery (DIR) (TR/TE = 5,500/292 ms, inversion times (TI) TI1/TI2 = 525 ms/2530 ms voxel size of $1 \times 1 \times 1$ mm), turbo spin echo (TSE) readout with an optimal variable flip angle scheme, number of excitations 3, the total acquisition time of 10: 49 minutes; and (c) 3D fluid attenuated inversion recovery (FLAIR) (TR/TE = 5,500/292 ms, TI = 1650 ms voxel size of $1 \times 1 \times 1$ mm), same TSE readout as the DIR sequence, number of excitations 1, the total acquisition time of 5:44 minutes

WM Lesion Detection and Lesion Load Assessment

To identify and segment WM lesions, thus obtaining a T2 hyperintense WM lesion volume (WMLV) at baseline, a semiautomatic lesion segmentation technique, included in Medical Image Processing and Visualization (MIPAV, mipav. cit.nih.gov) software, was applied to FLAIR images.

Cortical Lesion Number and Volume

The number of cortical lesions (CLs) was assessed on DIR images following the recent recommendations for CLs scoring in patients with MS (Geurts et al., 2011). Such number included both intracortical and mixed (WM/GM) lesions, whereas subpial were not counted due to technical difficulties. A semiautomatic thresholding technique based on a Fuzzy C-mean algorithm (Pham et al., 1999) included in MIPAV software was adopted to calculate the total CL volume.

Cortical Thickness Evaluation

FreeSurfer (release v5.3.0), semiautomatic software based on a T1- weighted structural volumetric image (surfer.nmr.mgh.harvard.edu/) was adopted to obtain global and regional measurements of the cortical thickness (CTh) and a semiautomatic procedure with lesion filling, was used to correct topological defects in the cortical surface due to intracortical lesions. Regions included in the correlation analysis were cingulate, cuneus, insula, precentral gyrus, precuneus, superior frontal gyrus, and hippocampus. The mean of the left and right hemispheres for each region of interest of the FreeSurfer parcellation was considered for the analysis (Crescenzo et al., 2019).

Statistical Analysis

Differences among PP and RR patients' groups were initially assessed with the Mann-Whitney test and Fisher exact test. Inflammatory molecules were divided into subgroups according to their main immunologic function. For each pathway identified, the associations between CSF protein levels at diagnosis and the disease course (PPMS and RRMS) were assessed with logistic regression, adjusted for age at onset. CSF levels were log transformed to obtain reliable odds ratio (OR). The log base 2 allowed a more intuitive interpretation of ORs, as each unit in log base 2 (protein level) corresponds to a doubling in protein level. Before performing the logistic regression models, the multicollinearity among independent variables was checked using the variance inflation factor (VIF). No multicollinearity was detected ($VIF < 10$) (Vittinghoff et al., 2011). The receiver operating characteristic (ROC) analysis (Youden index method) was used to identify both CXCL12 and osteopontin cutoff that maximize specificity and sensitivity of identifying patients with PPMS from RRMS. Sensitivity, specificity, accuracy, and area under curve with 95% CI were reported. Logistic regression analysis was used to evaluate the association of CXCL12 and Osteopontin levels with a PPMS disease course and noninflammatory controls. A pairwise univariate Spearman rank index was used to evaluate the correlation between EDSS, MRI parameters, and inflammatory molecules in PP patients' group. A false discovery rate correction with significance level of 0.05 was applied. Pathway analysis,

including gene ontology analysis, was performed by using Enrichr (maayanlab.cloud/ Enrichr/) analysis. p Value <0.05 was considered statistically significant. Statistical analysis was performed with Prism 7.0 and R studio 3.5.3 version.

6.3 RESULTS

Differences in the CSF Profile Between PPMS and RRMS

Increased levels of the lymphoid chemokine CXCL12 (fold change 1.42) and of molecules related to monocyte/ macrophage recruitment and innate immunity activity as chemokine (C-C motif) ligand (CCL2) and osteopontin (1.47 and 1.74, respectively) were detected in patients with PPMS compared with RRMS. Patients with PPMS had increased levels of many other cytokines, in particular tumor necrosis factor (TNF) (fold change 1.51), its soluble TNF receptors (sTNFRs) sTNFR1 and sTNFR2 (fold change 1.29 and 1.68, respectively) and the TNF superfamily member TNF ligand superfamily member 14 (fold change 2.21). Among other molecules, levels of IFN λ and IL4 were increased in patients with PPMS with a fold change of 1.46 and 1.35, respectively. Conversely, patients with RRMS showed higher levels of matrix metalloproteinase (MMP) 2 (fold change 2.72), IL12 (1.91), IL10 (1.73), CCL19 (1.61), CXCL11 (7.1), and CXCL13 (2.34). Levels of all the examined molecules in each MS group are reported in Table 6.2.

Logistic Regression and ROC Analysis

The multivariate logistic regression analysis showed that the CSF level at diagnosis of CXCL12 (OR = 3.97, 95% CI [1.34–11.7]) and osteopontin (OR = 2.24, 95% CI [1.01–4.99]) independently predicted a higher probability of a primary progressive course of the disease. Conversely, elevated IL10 levels were significantly associated with the diagnosis of RRMS (OR = 0.28, 95% CI [0.09–0.96]). ROC curve analysis estimated the optimal cutoff values of 2063.58 and 184,736.4 pg/mL for CXCL12 and osteopontin, respectively (Figure 6.1). Both CXCL12 and osteopontin levels were found increased compared with control group patients with noninflammatory neurologic disorders (OR = 1.10, 95% CI [1.05–3.15], and OR = 1.38, 95% CI [1.08–5.23], respectively).

	Total MS	PPMS	RRMS	PPMS/RRMS
<i>T cells pathway</i>				
IFN gamma	14.7±24.0	10.7±14.1	15.5±25.6	0.69
IFN alfa2	14.2±18.7	16.2±15.1	13.8±19.4	1.18
IFN lambda2	191.3±470.1	259.7±544.8	177.7±456.4	1.46
IL12(p40)	13.1±21.8	7.4±13.4	14.2±23.0	0.52
CXCL8	61.7±79.3	56.3±69.0	62.8±81.6	0.90
IL 22	33.5±30.8	32.4±21.6	33.8±32.5	0.96
CCL19	96.4±93.2	64.0±59.2	102.9±97.6	0.62
CCL20	1.0±1.6	1.0±1.2	1.0±1.6	1.02
CCL21	1599.9±1000.5	1300.3±968.5	1659.9±1001.9	0.78
CCL25	123.3±81.6	141.0±115.7	119.8±73.4	1.18
IL4	19.9±18.1	25.4±19.6	18.7±17.7	1.35
<i>B cells pathway</i>				
CXCL12	2087.1±1924.6	2765.7±2173.0	1951.4±1856.3	1.42
CXCL13	11.2±25.4	5.3±9.3	12.4±27.4	0.43
BAFF	9894.8±6333.8	11387.0±10110.0	9596.3±5319.2	1.19
IL10	19.5±18.6	12.0±8.8	21.1±19.6	0.57
IL35	286.4±204.8	270.1±198.5	289.7±207.1	0.93
GMCSF	87.4±99.8	76.7±90.0	89.6±102.0	0.86
<i>Monocyte/macrophage pathway</i>				
IL1beta	2.5±3.5	2.0±2.7	2.5±3.6	0.80
IL6	26.5±49.2	23.5±39.0	27.1±51.1	0.87
CCL2	526.2±598.0	717.4±674.2	488.0±578.6	1.47
CCL8	183.5±587.0	157.3±430.7	188.7±615.6	0.83
CX3CL1	348.4±248.4	325.6±260.4	353.0±247.4	0.92
CXCL10	431.6±507.3	421.4±425.8	433.6±524.4	0.97
CXCL11	64.6±499.6	10.6±26.9	75.4±547.1	0.14
sCD163	49534.7±33284.3	51226.7±23913.1	49196.3±34970.7	1.04
MMP1	708.2±927.3	739.4±616.9	702.0±980.6	1.05
MMP2	1165.5±3189.4	478.3±556.0	1302.9±3472.7	0.37
Osteopontin	84163.9±95433.9	130158.0±139428.3	74965.1±82139.4	1.74
<i>TNF pathway</i>				
TNF	39.7±38.4	55.2±43.1	36.6±36.9	1.51
sTNFR1	4300.7±2653.3	5294.0±3304.1	4102.0±2480.6	1.29
sTNFR2	1062.4±886.4	1604.3±1227.6	954.1±766.4	1.68
APRIL	54318.8±61277.7	63853.0±62885.8	52411.9±61175.9	1.22
LIGHT	318.2±434.0	585.6±511.1	264.72±399.5	2.21
TWEAK	2060.4±1979.0	2337.3±2014.9	2005.0±1979.9	1.17

Table 6.2. Levels of the cytokines and chemokines detected in the CSF of MS patients. Values are expressed as pg/ml; mean±SD are reported. In the PPMS/RRMS column values are reported as fold change between the two groups. Abbreviations: IFN-G, interferon gamma; IFN-alfa2, interferon alfa2; IFN-lambda2, interferon lambda2; IL-12(p40), interleukin-12 subunit p40; CXCL8, interleukin-8 or (C-X-C motif) chemokine ligand 8; IL-22, interleukin 22; CCL19, Chemokine (C-C motif) ligand 19; CCL20, Chemokine (C-C motif) ligand 20; CCL21, Chemokine (C-C motif) ligand 21; CCL25, Chemokine (C-C motif) ligand 25; IL-4, interleukin 4; CXCL12, stromal cell-derived factor or C-X-C motif chemokine 12; CXCL13, chemokine (C-X-C motif) ligand 13 or B lymphocyte chemoattractant; BAFF, B cell activating factor or tumour necrosis factor ligand superfamily member 13B; IL-10, interleukin 10; IL-35: interleukin35; GM-CSF, Granulocyte-macrophage colony-stimulating factor; IL-1beta, interleukin 1 beta; IL-6, interleukin 6; CCL2, Chemokine (C-C motif) ligand 2; CCL8, Chemokine (C-C motif) ligand 8; CX3CL1: chemokine (C-X3-C motif) ligand 1;

CXCL10, C-X-C motif chemokine 10 or interferon gamma-induced protein 10; CXCL11: C-X-C motif chemokine 11; sCD163, soluble-CD163 (cluster of differentiation 163); MMP1, matrix metalloproteinase 1; MMP2, matrix metalloproteinase 2; TNF, tumor necrosis factor; sTNF- R1, soluble tumour necrosis factor-receptor 1; sTNF-R2, soluble tumour necrosis factor-receptor 2; APRIL, A proliferation-inducing ligand, or tumour necrosis factor ligand superfamily member 13; LIGHT, tumor necrosis factor ligand superfamily member 14 or tumour necrosis factor superfamily member 14; TWEAK, TNF-related weak inducer of apoptosis or tumour necrosis factor ligand superfamily member 12.

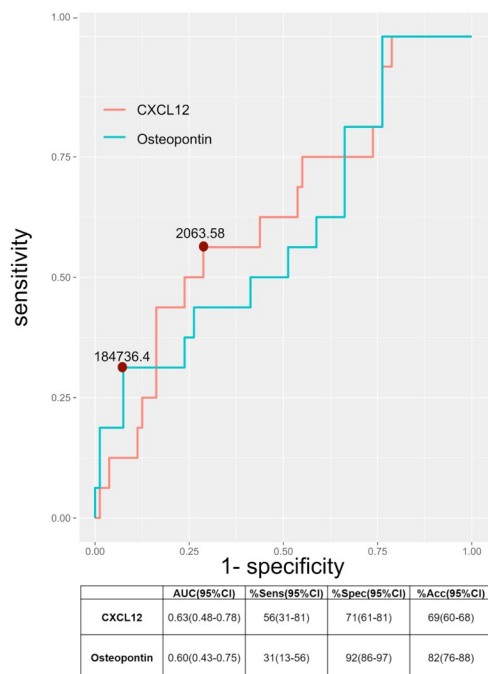


Figure 6.1. Results of ROC Curve Analysis. For each protein, AUC, Sensitivity, Specificity and Accuracy in discriminating between PPMS and RRMS are reported. The optimal threshold for each protein is reported in the curve and in the text. ROC: receiver operating characteristic; AUC: area under curve; CI: confidence interval; Sens: Sensitivity; Spec: Specificity; Acc: Accuracy.

Correlations and Pathway Analysis in PPMS

Patients with increased CSF CXCL12 showed a concurrent increment of the monocyte chemoattractant protein CCL2 levels ($r = 0.647$, $p = 0.040$; Figure 6.2A). Despite a not significant correlation after adjusting for multiple comparisons, the same patients displayed high levels of B-cell activating factor (BAFF) ($r = 0.597$, $p = 0.064$; Figure 6.2A), IL4 ($r = 0.653$, $p = 0.106$), the lymphoid chemokine CCL19 ($r = 0.603$, $p = 0.129$), and both the TNF receptors, sTNFR1 ($r = 0.515$, $p = 0.186$) and sTNFR2 ($r = 0.559$, $p = 0.147$). Pathway analysis revealed these molecules as mainly involved in regulation of dendritic cell (DC) processes, calcium ion import, leukocyte apoptotic processes, immunologic synapse formation, regulation of endothelial cell development and extravasation, and regulation of glial cell apoptotic process (Table 6.3). Increased osteopontin levels were detected in PPMS patients with higher expression of MMP2 ($r = 0.747$, $p = 0.013$), sTNFR1 ($r = 0.829$, $p = 0.002$; Figure 6.2B), and CXCL10 ($r = 0.674$, $p = 0.040$), molecules mainly involved in

regulation of endothelial cell development and endothelial barrier, regulation of sphingolipid and ceramide biosynthesis, cell death regulation, regulation of cyclic adenosine monophosphate-mediated signaling, regulation of epithelium morphogenesis, and T-cell chemotaxis (Table 6.3).

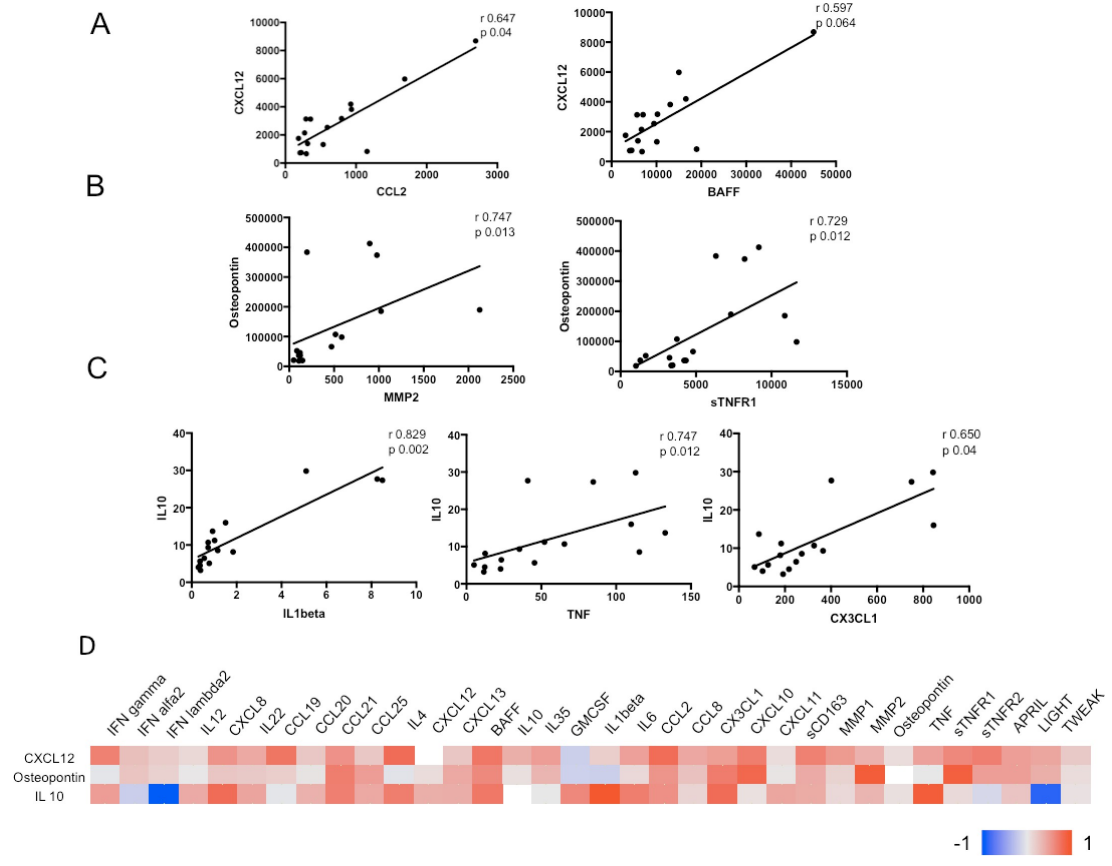


Figure 6.2. PPMS inflammatory profile
 (A) Increased levels of CXCL12 correlate with CCL2 and, almost significantly, BAFF. (B) Significant correlations between Osteopontin and MMP2 and sTNFR1 levels. (C) IL10 levels significantly correlated with IL1beta, TNF and CX3CL1. (D) panel showing the entire correlation matrix. See Table 2 for the list of all abbreviations.

Finally, patients with high IL10 levels were also characterized by increased TNF ($r = 0.747$, $p = 0.012$), IL1beta ($r = 0.829$, $p = 0.002$), and chemokine (C-X3-C motif) ligand 1 ($r = 0.650$, $p = 0.040$) CSF levels (Figure 6.2C). The pathway analysis revealed that these molecules are linked with cell adhesion, regulation of fever generation, regulation of endothelial cell development, cytokine secretion, regulation of membrane protein, response to corticosteroids, and regulation of acute inflammatory response (Table 6.3). The entire correlation panel is graphically shown in Figure 6.2D.

Name	P-value	Odds Ratio	Combined score
CXCL12 and related molecules			
(1) negative regulation of dendritic cell apoptotic process (GO:2000669)	0.000001574	952.38	12725.67
(2) regulation of dendritic cell apoptotic process (GO:2000668)	0.000003371	666.67	8400.14
(3) positive regulation of calcium ion import (GO:0090280)	0.000003371	666.67	8400.14
(4) negative regulation of leukocyte apoptotic process (GO:2000107)	0.000004943	555.56	6787.49
(5) positive regulation of dendritic cell antigen processing and presentation (GO:0002606)	0.001799	555.56	3511.45
(6) immunological synapse formation (GO:0001771)	0.001799	555.56	3511.45
(7) regulation of endothelial cell development (GO:1901550)	0.001799	555.56	3511.45
(8) negative regulation of cellular extravasation (GO:0002692)	0.001799	555.56	3511.45
(9) positive regulation of antigen processing and presentation (GO:0002579)	0.001799	555.56	3511.45
(10) regulation of glial cell apoptotic process (GO:0034350)	0.001799	555.56	3511.45
Osteopontin and related molecules			
(1) regulation of endothelial cell development (GO:1901550)	0.001799	555.56	3511.45
(2) positive regulation of sphingolipid biosynthetic process (GO:0090154)	0.002098	476.19	2936.47
(3) death-inducing signaling complex assembly (GO:0071550)	0.002098	476.19	2936.47
(4) positive regulation of ceramide biosynthetic process (GO:2000304)	0.002098	476.19	2936.47
(5) positive regulation of cAMP-mediated signaling (GO:0043950)	0.002398	416.67	2513.82
(6) regulation of morphogenesis of an epithelium (GO:1905330)	0.002697	370.37	2190.93
(7) T cell chemotaxis (GO:0010818)	0.002997	333.33	1936.76
(8) regulation of T cell chemotaxis (GO:0010819)	0.002997	333.33	1936.76
(9) regulation of ceramide biosynthetic process (GO:2000303)	0.003296	303.03	1731.85
(10) regulation of establishment of endothelial barrier (GO:1903140)	0.003595	277.78	1563.39
IL10 and related molecules			
(1) positive regulation of heterotypic cell-cell adhesion (GO:0034116)	4.948e-10	1363.64	29218.41
(2) positive regulation of fever generation (GO:0031622)	4.499e-7	1666.67	24357.23
(3) regulation of endothelial cell development (GO:1901550)	4.499e-7	1666.67	24357.23
(4) positive regulation of cell-cell adhesion (GO:0022409)	6.138e-12	606.06	15646.39
(5) regulation of heterotypic cell-cell adhesion (GO:0034114)	2.905e-9	789.47	15518.51
(6) regulation of cytokine secretion involved in immune response (GO:0002739)	0.000001079	1111.11	15265.62
(7) regulation of membrane protein ectodomain proteolysis (GO:0051043)	4.617e-9	681.82	13086.55
(8) response to corticosteroid (GO:0031960)	0.000001649	909.09	12104.88

(9) regulation of establishment of endothelial barrier (GO:1903140)	0.000001979	833.33	10944.26
(10) positive regulation of acute inflammatory response (GO:0002675)	0.000003147	666.67	8446.00

Table 6.3. Gene ontology analysis: pathways associated with CXCL12, Osteopontin, IL10 and their related chemokines in PPMS CSF

Correlations Between CSF Inflammation and Disease Severity in PPMS

No correlations were found between the selected inflammatory molecules and EDSS (not shown). Both cortical lesion number ($r = 0.832$, $p = 0.001$) and cortical lesion volume ($r = 0.821$, $p = 0.001$) were increased in patients harboring higher intrathecal CXCL12, whereas a similar trend was not observed regarding osteopontin and IL10. No significant associations were observed between CXCL12 and osteopontin levels and WM lesion number or WMLV. CXCL13 levels were particularly increased in those patients with lower CTh of cuneus ($r = -0.762$, $p = 0.024$), hippocampus ($r = -0.678$, $p = 0.063$), cingulate gyrus ($r = -0.652$, $p = 0.063$), and insula ($r = -0.633$, $p = 0.063$). All correlations are graphically shown in Figure 6.3.

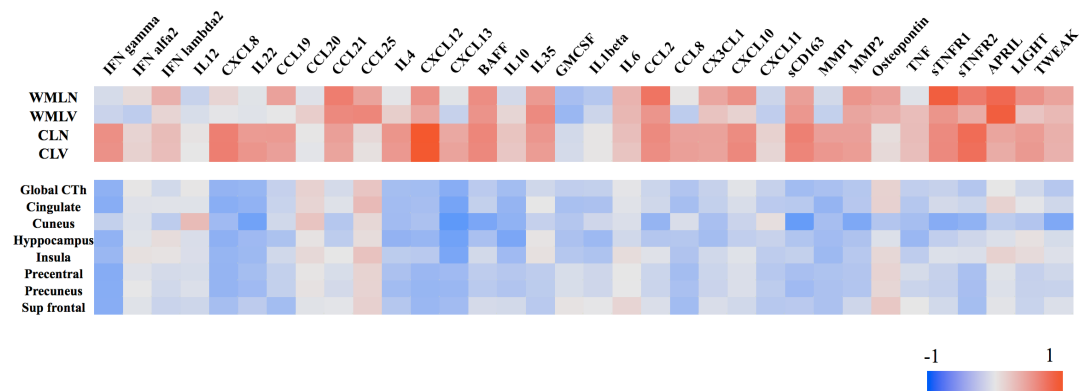


Figure 6.3. Panels showing the correlations between molecules and MRI measures. CXCL12 showed a significant correlation with CLN and CLV. IFNgamma and CXCL13 best correlated with a reduced global and regional CTh. See text and Supplementary Table 3 for further details. WMLN: white matter lesion number; WMLV: white matter lesion volume; CLN: cortical lesion number; CLV: cortical lesion volume; CTh: cortical thickness. See Table 2 for the list of all molecules abbreviations.

6.4 DISCUSSION

The analysis of the CSF profile in PPMS revealed that higher CXCL12 and osteopontin are associated with a progressive disease course and suggest that a chronic intrathecal inflammatory process, although partly different from RRMS, also occurs in patients with progressive MS, since the time of diagnosis and independently of relapses.

Such findings are in line with the idea that inflammation exerts a major role in progressive MS, including PPMS. Whether PPMS and RRMS/SPMS represent similar physiopathologic entities has been debated; differences between SPMS and PPMS seem to be quantitative rather than qualitative (Lassmann et al., 2019; Antel et al., 2011). Furthermore, the similar age at onset and rates of disability progression indicate that a similar process underlies the 2 entities (Confavreux and Vukusic, 2006; Scalfari et al., 2016). Although based on a small cohort, our preliminary results highlighted 2 molecules as associated with the primary progressive disease course: the CXCL12 and the osteopontin.

Besides modulating neuronal activity through multiple regulatory pathways, CXCL12 is a potent chemoattractant molecule for different immune cells, including monocytes, T cells, B cells, and plasma cells (Guyon et al., 2014). Elevated levels of CXCL12 have been detected both in active and inactive lesions and have been suggested as contributors to the maintenance of immune cells within the CNS (Krumbholz et al., 2006). Along with CXCL13, it mediates germinal center organization in lymphoid tissue, and possibly, a similar process could occur in the CNS of patients with MS, thus contributing to the persistence of B cells and plasma cells in inflamed meninges and perivascular spaces. In line with previous findings, we have found CXCL12 strictly associated with the local production by astrocytes of the B-cell survival factor BAFF (Krumbholz et al., 2006) and with CLs, thus confirming the link between B cell-associated CSF inflammation and the adjacent cortical pathology (Magliozzi et al., 2018,2020). Probably due to the low sample size, a significant correlation between the CXCL12 and the CTh was not observed. On the contrary, after correction for multiple comparisons, CXCL13 levels correlated with the CTh of many brain regions that are early involved in PPMS pathology (Eshaghi et al., 2014,2018). Such observations could have clinical prognostic value, as cortical pathology has been recognized as a crucial substrate for the progression and irreversible clinical and cognitive disability in MS (Fisniku et al., 2008; Calabrese et al., 2012).

Osteopontin, which in the brain is mainly released by endothelial cells, microglia, macrophages, and DCs, has a role in mediating MS severity and progression (Niino et al., 2003; Chiochetti et al., 2005; Caillier et al., 2003; Hensiek et al., 2003). CSF levels of osteopontin are higher than in plasma, further suggesting a contribution from CNS resident or infiltrating cells as intrathecal sources of the molecule (Braith et al., 2008). It is increased in lesional brain tissue from patients with progressive MS (Chabas et al., 2001) and in the CSF of patients with MS (Braith et al., 2008; Bornsen et al., 2011) and decreases after treatments (Khademi et al., 2009). Of interest, patients with SPMS showed stable and continuously increased osteopontin levels (Romme Christensen et al., 2013). Osteopontin mainly reflect activation of innate immune system and exerts an

essential role in inflammation and immune response, influencing T helper differentiation 1-type and 2-type responses, as well as regulating DC migration at multiple levels (Denhardt et al., 2001; Del Prete et al., 2019). Among others, it enhances interferon and IL12 proinflammatory activity and reduces IL10-mediated responses, all cytokines involved in MS and other inflammatory diseases (Denhardt et al., 2001). Osteopontin increases myelin-reactive T-cell survival and induces relapses and progression in experimental autoimmune encephalomyelitis (Hur et al., 2007); accordingly, osteopontin-deficient mice show a greater number of remissions, less progression, and higher IL10 levels in a preclinical MS model (Chabas et al., 2001). All these shreds of evidence further point to a detrimental role of osteopontin in MS progression since the early stages. As suggested by pathway analysis, the molecules identified as associated with PPMS in this study are mainly related to several inflammatory processes of both innate and adaptive immune responses that occur in the CNS. Indeed, as MS progresses, inflammation becomes increasingly compartmentalized within the CNS beyond a relatively intact blood-brain barrier (Machado-Santos et al., 2018; Magliozzi et al., 2010; Reynolds et al., 2011), with lesions showing less prominent focal inflammation but persisting microglia activity at the edge of chronic active demyelinating plaques (Frischer et al., 2009). A major contribution to MS progression is given by meningeal inflammation: diffuse and clustered meningeal and perivascular infiltrates, enriched in B cells, associated with subpial GM pathology, have been detected in both SPMS and PPMS postmortem brains, although, in the case of PPMS, they appeared less extensive and not clustered in tertiary lymphoid follicles (Magliozzi et al., 2007, 2010; Howell et al., 2011; Choi et al., 2012).

The current study is mainly limited by the low number of PPMS cases evaluated, whose follow-up is still ongoing. This implies that our observations are preliminary and that further validation in a larger cohort is needed. The analysis of CSF intrathecal profile in a larger cohort could confirm the markers capability to early identify patients with severe progressive MS course that could benefit from an immunosuppressant approach. In summary, our work showed that (1) intrathecal inflammation is significant in the CSF of patients with PPMS at the time of diagnosis; (2) the CSF profile of patients with PPMS is characterized explicitly by higher levels of CXCL12 and osteopontin when compared with patients with RRMS and associate with a specific proinflammatory innate immune profile; (3) as observed in RRMS, also in PPMS, the lymphoid chemokines CXCL12 and CXCL13 are associated with an increased level of GM pathology already at the time of diagnosis. Our observations highlight the potential differential signature of intrathecal inflammation in PPMS, suggesting possible clinical implications for the diagnosis and treatment of PPMS that warrant further investigations.

7. CSF OSTEOPONTIN IS ASSOCIATED WITH CORTICAL DAMAGE AND DISABILITY ACCUMULATION IN EARLY MULTIPLE SCLEROSIS.

Article in preparation.

Authors: Marastoni D¹, Tamanti A¹, Turano E¹, Colato E¹, Pisani AI¹, Scartezzini A¹, Carotenuto S¹, Camera V¹, Ziccardi S¹, Guandalini M¹, Pizzini FB², Virla F¹, Mariotti R¹, Magliozzi R¹, Bonetti B³, Steinman L⁴, Calabrese M^{1*}

1 Neurology B, Department of Neurosciences, Biomedicine and Movement Sciences, University of Verona, Verona, Italy

2 Neuroradiology and Radiology Unit, Azienda Ospedaliera Universitaria Integrata, Verona, Italy

3 Neurology A, Azienda Ospedaliera Universitaria Integrata, Verona, Italy

4 Department of Neurology and Neurological Sciences, Stanford University

7.1 INTRODUCTION

Multiple sclerosis (MS) is the most common immune-mediated disorder of the Central Nervous System (CNS). The disease course is usually characterized by an initial relapsing-remitting phase (RRMS), defined by the occurrence of new neurological symptoms and subsequent disability (Thompson et al., 2018). Later in the disease course, most patients develop a progressive accumulation of disability, mostly independent of relapses (Secondary Progressive MS, SPMS, Thompson et al., 2018; Lublin et al., 2014).

Both focal and diffuse white matter (WM) and grey matter (GM) damage characterize MS pathology. GM damage occurs from earlier disease stages and represent a negative prognostic factor for MS-related disability, being associated with compartmentalized meningeal and perivascular inflammation (Magliozzi et al., 2018; Filippi et al., 2013) that persist in both RRMS and SPMS associating a severe disease course (Howell et al., 2011).

Nevertheless, even if focal GM damage represents a surrogate marker of long-term disability, its pathogenesis continues to be debated. Contemporary ideas on pathogenesis include analysis, not limited to, but focusing: 1) on persistent inflammation in the adjacent meningeal sulci and subsequent subpial demyelination; 2) on focal and diffuse intracortical demyelination; 3) finally on neuroaxonal degeneration associated with persistent WM inflammatory activity (Calabrese et al., 2015; Treaba et al., 2021).

Notably, in the clinical context, disease activity in the first years after a diagnosis of MS and early cortical atrophy accumulation actively influence long-term prognosis (Rotstein et al., 2022; Scalfari et al., 2018). These observations catalyzed a search for inflammatory markers that might associate with an early severe course, allowing for the development of a tailored and personalized therapeutic approach (Rotstein and Montalban, 2019). Such research might

illuminate new aspects of MS pathophysiology, including how GM damage accumulates.

In line with this aim, cerebrospinal fluid (CSF) remains an easily accessible and a reasonable surrogate of intrathecal inflammatory processes (Heming et al., 2022). CSF inflammatory markers, particularly related to B-cell recruitment, have been previously associated with focal and diffuse GM damage and disease activity and accumulation of cortical atrophy in early MS (Magliozzi et al., 2020). Similarly, molecules implicated in chronic microglial activation as CHIT-1L3 and sCD163 have been suggested as good surrogate markers of chronic microglial activity at the edge of demyelinating lesions (Pinteak et al., 2020; Magliozzi et al., 2019; Stilund et al., 2014).

Notably, Osteopontin (OPN) emerged as one major driver of lymphocyte recruitment and activation in the CNS, being also related to monocyte/microglia activation (Steinman, 2009). We therefore aimed to evaluate in a cohort of patients with RRMS at the time of diagnosis an extensive panel of inflammatory molecules, including OPN with the aim to explore their association with both early GM damage accumulation and disease activity. We explored their potential value in predicting MRI and clinical outcomes. This would help to provide surrogate markers of compartmentalized inflammatory processes in early MS.

7.2 METHODS

Patients cohort

One-hundred seven consecutive treatment-naive patients with RRMS were enrolled from January 2018 at the time of diagnosis at the MS Center of Verona University Hospital (Italy), and followed-up for at least 2 years. A subgroup of 39 patients completed a 4-year follow-up. All patients had a confirmed MS diagnosis according to the most recent diagnostic criteria (Thompson et al., 2018). They underwent regular neurological evaluation every three months in the first year and then every sixth months, including EDSS (Expanded Disability Status Scale) assessment (Kurtzke 1984), with additional visits in case of relapses. A relapse was defined as a worsening of a neurological impairment or appearance of a new symptom or abnormality attributable to MS, lasting at least 24 hours and preceded by the stability of at least 1 month (Poser, 1983).

All patients were started a first line disease modifying therapy (dimethyl fumarate or teriflunomide) and were scheduled to undergo a brain 3T-MRI after 3 (re-baseline), 12, 24 and, when possible, 48 months after diagnosis and treatment initiation. A lumbar puncture with CSF collection and analysis was performed at the time of diagnosis.

The combined three-domain status of ‘No evidence of disease activity’ (NEDA-3) was defined by no evidence of relapses, MRI activity (new or enlarged white matter, WM, T2 lesions, Gadolinium enhancing lesions, Gd+) and 6-months confirmed disability worsening (CDW), defined as an increase of ≥ 1 point in

EDSS (Giovannoni et al., 2017). The appearance of cortical lesions (CLs) was included in the definition of NEDA-3 that we adopted in the current study. Occurrence of progression independent from relapsing activity (PIRA events) was recorded; PIRA event was defined as a 6-month CDW event, without prior relapses or an onset more than 90 days after the start date of the last relapse without occurrence of relapse within 30 days before or after the EDSS confirmation (Lublin et al., 2022).

CSF analysis

CSF samples were obtained at the time of diagnosis, at least one month after the last relapse and within one week of the MRI, according to Consensus Guidelines for CSF and Blood Biobanking (Teunissen et al., 2012). After centrifugation, the supernatant was stored separately at -80°C until use. Analysis of CSF levels of 67 inflammatory mediators was performed using a combination of immune-assay multiplex techniques based on the Luminex technology (40- and 37-Plex, Bio-Plex X200 System equipped with a magnetic workstation; BioRad, Hercules, CA) as previously described (Magliozzi et al., 2018). All samples were duplicated in the same experiment and in 2 consecutive experiments to verify the results' reproducibility and consistency. The CSF level of each protein detected during the analysis was normalized to the total protein concentration of each CSF sample (measured by Bradford protocol). CSF/serum albumin ratio, ImmunoglobulinG Index, and presence/absence of oligoclonal bands were evaluated.

MRI Protocol and Analysis

Three Tesla MRI was performed on each patient at least one month from the last relapse at the using a Philips Achieva 3T MRI Scanner at the Neuroradiology Unit of the University Hospital of Verona. The following image sets were acquired:

- a) 3D-T1 weighted Turbo Field Echo (TFE) (Repetition Time (TR)/Echo Time (TE) = 8.4/3.7 ms, voxel size of 1x1x1 mm), the acquisition time of 5:51 minutes;
- b) 3D-Double Inversion Recovery (DIR, TR/TE = 5,500/275 ms, Inversion Times (TI) TI1/TI2 = 450ms/2,550 ms voxel size of 1 x 1 x 1 mm), Turbo Spin Echo (TSE) readout with an optimal variable flip angle scheme, number of excitations 3, acquisition time of 10:49 minutes;
- c) 3D-Fluid Attenuated Inversion Recovery (FLAIR) (TR/TE = 8,000/288 ms, TI = 2,356 ms voxel size of 1 x 1 x 1 mm), same TSE readout as the DIR sequence, number of excitations 1, the acquisition time of 4:48 minutes;
- d) 3D-T1 weighted TFE post-contrast with the same parameters of the pre-contrast sequence (TR/TE = 8.4/3.7 ms, voxel size of 1 x 1 x 1 mm, the acquisition time of 5:51 minutes).

White matter lesion detection and lesion load assessment.

A semi-automatic lesion segmentation technique, included in MIPAV (Medical Image Processing and Visualization, <http://mipav.cit.nih.gov>) software, was applied to FLAIR images to identify and segment WM lesions, thus obtaining a T2 hyperintense WM lesion volume (WMLv) at baseline.

Cortical lesion number and volume

The number of cortical lesions (CLs) was assessed on DIR images following the recent recommendations for CLs scoring in patients with MS (Geurts et al., 2012). Such number included both intracortical and mixed (WM/GM) lesions, while subpial were not counted due to technical difficulties. The total CL volume (CLv) was calculated using a semi-automatic thresholding technique based on a Fuzzy C-mean algorithm included in MIPAV software.

Cortical Thickness Evaluation

Global measurements of the cortical thickness (CTh) have been obtained by applying Freesurfer (Fischl, 2012, release v7.1.0), a semi-automatic software based on a T1-weighted structural volumetric image (<http://surfer.nmr.mgh.harvard.edu/>) and using a semi-automatic procedure with lesions filling to correct topological defects in the cortical surface due to intracortical lesions. The mean of the left and right hemispheres for each ROI of the Freesurfer parcellation was considered for the analysis.

Statistical analysis

Differences among groups (patients with and without disease activity) were initially assessed with Mann-Whitney test and Chi-Square/Fisher exact test when appropriate. Rho correlation values between protein values and atrophy rates were initially calculated with Spearman rank test.

Random Forest (RF) approach was used to obtain CSF markers associated with CTh change and NEDA-3 outcome using the Minimal Depth (MD) and the total number of trees (times a root).

Minimal depth variable in a tree equals the depth of the node which splits on that variable and is the closest to the root of the tree; lower MD, higher the variable predictive accuracy. Times a root measure corresponds to the total number of trees in which the variable is used for splitting the root node; higher times a root measure reflects higher prediction power of the variables.

In order to better investigate the CSF proteins significantly associated with the sample traits in the previous analyses we used STRING (<https://string-db.org/>) to i) quantify module connectivity and ii) enriched biological function. Module connectivity was evaluated by the Protein-Protein Interaction (PPI) enrichment p-value. Low PPI p-value indicates that the nodes (proteins) are not random and that the observed number of edges (the interaction between proteins) is significant. While strength and False Discovery Rate (FDR) measures were used to evaluate,

respectively, how large and significant the enrichment effect is for each biological process detected by the pathway analysis.

Multivariable linear regression models were applied in order to assess the value of clinical, demographical, MRI and CSF markers collected at the time of diagnosis in predicting CTh changes after 2 and 4 years. Likelihood ratio tests (LRT) were used to compare the goodness of fit hierarchically models showing whether adding the CSF variables makes the model significantly more accurate. Multivariable logistic regression models were applied to assess the value of clinical, demographical, MRI and CSF markers in predicting disease activity (including CDW, new relapses and new lesions) after two years. A p-value <0.05 was considered statistically significant. Statistical analysis was performed by means of R studio 3.5.3 version and GraphPad Prism 9.

7.3 RESULTS

Study cohort

Detailed demographic, clinical and MRI characteristics of MS patients at the diagnosis and after two years of follow-up are shown in Table 7.1. After two years 48% (51/107) of patients remained free from disease activity (Table 7.1). Twenty-nine patients experienced a relapse, while the occurrence of new or enlarging T2 lesions, new CLs, or Gd enhancing lesions was evident in 49 patients and CDW occurred in 32, while PIRA was evident in 5 patients. No severe adverse drug reactions leading to therapy discontinuation were reported during the two-years of follow-up.

Patients with disease activity were characterized by a higher EDSS at the time of diagnosis ($p = 0.002$), increased cortical lesion load (CLn, $p = 0.001$; CLv, $p = 0.002$; Table 7.1).

Osteopontin and CXCL13 best associated with accumulating cortical atrophy

Patients with higher cortical atrophy rates in the first two years of follow-up showed, among others, increased levels of both Osteopontin ($r = -0.452$, $p < 0.001$) and CXCL13 ($r = -0.374$, $p < 0.001$) at the time of diagnosis.

The random forest selected OPN, CXCL13, TWEAK, TNF, IL19, sCD30, sTNFR1, IL35, IL16, sCD163 as the most important variables associated to accumulating brain atrophy. Osteopontin and CXCL13 provided the best performance (Figure 7.1A). Notably, CXCL13 was strictly linked with focal cortical damage, associating with both CLs at the diagnosis ($r = 0.716$, $p < 0.001$) and new CLs ($r = 0.611$; $p < 0.001$), while OPN revealed only slightly increased in those patients with higher number CLs at the time of diagnosis ($r = 0.191$, $p = 0.049$).

	Total MS (n = 107)	2y EDA (n = 56)	2y NEDA (n = 51)	p value
Age - yr	35.7 ± 11.8	35.5 ± 11.7	38.4 ± 11.7	0.021
Female sex – no. (%)	82 (76.6)	45 (80.4)	37 (72.6)	0.369
EDSS score - median (range)	2 (0-5)	2 (0-5)	1.5 (0-4)	0.168
WMLN - mean ± SD	9 ± 5.1	9.4 ± 4.5	8.5 ± 3.9	0.347
WMLV - mean ± SD	1015.8 ± 957.1	1217.6 ± 1199.1	794.2 ± 514.5	0.121
Spinal Cord lesion number	0.6 ± 1.1	0.7 ± 1.2	0.5 ± 1.1	0.418
Gd+ lesions - mean ± SD	0.2 ± 0.5	0.2 ± 0.6	0.1 ± 0.5	0.459
CLn - mean ± SD	4 ± 4.6	5.6 ± 5.1	2.3 ± 3.3	0.001
CLv - mean ± SD	353.4 ± 437.0	483.6 ± 492.5	207.5 ± 309.6	0.002
Global CTh – mm ³	2.5 ± 0.3	2.4 ± 0.3	2.5 ± 0.2	0.757
Annual CTh change (%) - mean ± SD	- 0.58 ± 0.38	- 0.71 ± 0.46	- 0.44 ± 0.19	0.194
Albumin CSF/serum	5.2 ± 1.8	5.2 ± 1.7	5.2 ± 1.8	0.920
IgG Index	0.63 ± 0.27	0.59 ± 0.14	0.69 ± 0.40	0.566
CSF OCBs (yes/not)	81/26	43/13	38/13	0.824

Table 7.1. Baseline demographic, clinical and MRI characteristics of the whole population and accordingly to disease activity at the two-years follow-up. Patients with disease activity after two-years were characterized by older age and higher gray matter damage, reflected by increased cortical lesion number and volume.

Abbreviations: EDA = evidence of disease activity; NEDA = no evidence of disease activity; EDSS = Expanded Disability Status Scale; WMLn = White Matter Lesion Number; Gd+ lesions = Gadolinium enhancing lesions; CLn = Cortical lesion number; CLv = Cortical lesion volume; CTh = Cortical Thickness, CSF = cerebrospinal fluid; IgG = Immunoglobulin G; OCBs = Oligoclonal bands. P values for each comparison between EDA and NEDA groups after two years are reported. A *p* value < 0.05 was considered significant.

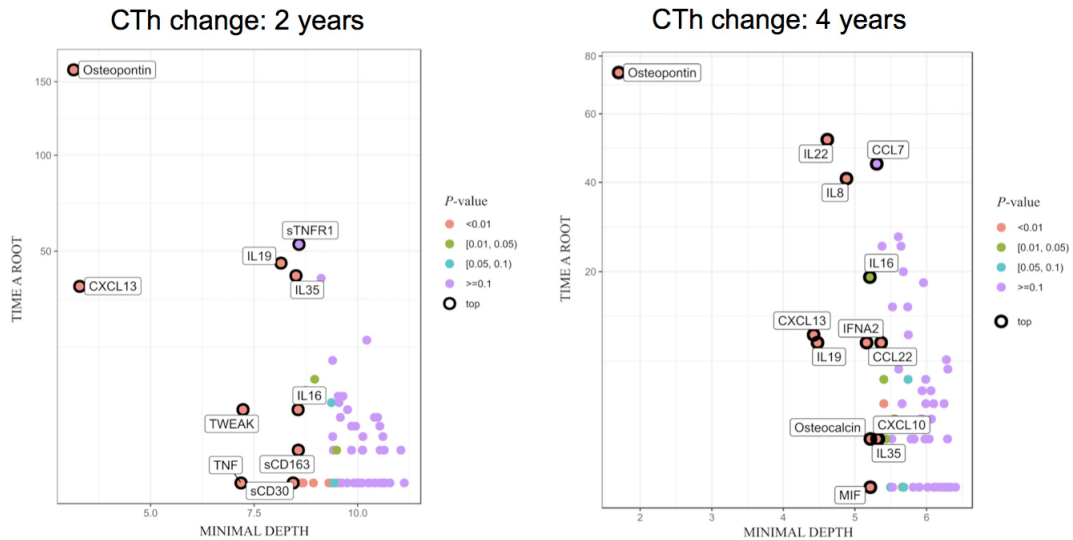


Figure 7.1. Random forest approach: OPN and CXCL13 best associate with cortical thickness change after 2 and 4 years' follow-up.

Multiway importance plot: OPN and CXCL13 were selected as the most important variables associated with the cortical thickness change after two-years of follow-up (panel on the left, A), while OPN was selected as the most important variable after 4 years (B). Abbreviations: CXCL13, chemokine (C-X-C motif) ligand 13 or B lymphocyte chemoattractant; OPN, Osteopontin; TNF, tumor necrosis factor; TWEAK, TNFSF12 or TNF Superfamily Member; IL19, interleukin-19; IL-35, interleukin-35; IL16, interleukin-16; sCD163, soluble Cluster of Differentiation 163; sCD30, soluble Cluster of Differentiation 30; sTNFR1, soluble TNFRSF1A or TNF receptor superfamily member 1A; IL22, interleukin-22; IL8, interleukin-8; CCL7, chemokine (C-C motif) ligand 7; IFNA2, interferon alfa2; CCL22, chemokine (C-C motif) ligand 22; CXCL10, chemokine (C-X-C motif) ligand 10; MIF, macrophage migration inhibitory factor.

No correlation between CXCL13 and OPN levels occurred ($r = 0.163$, $p = 0.136$). Patients with both high levels of OPN and CXCL13 had significantly higher atrophy rates, suggesting different, complementary, effects on cortical damage accumulation (Figure 7.2).

OPN was selected as the best marker of cortical atrophy accumulation ($r = -0.691$, $p < 0.001$) also in the subgroup of patients who underwent a 4 years follow-up with yearly MRI scans. The other markers significantly increased in those patients with higher atrophy rates after 4-years were CXCL13, IL22, IL19, IL8, IFNalpha2, CCL22, Osteocalcin, IL35 and MIF (Figure 7.1B).

Pathway analysis

Pathway analysis confirmed a non-random interaction among CSF candidate markers (protein-protein interaction p -value < 0.001 , Figure 7.3). Biological processes that particularly emerged associated with the selected cytokines profile were the regulation and establishment of endothelial barrier, a positive regulation of a chronic inflammatory response, and the activation of the TNF-mediated signaling pathway (Table 7.2).

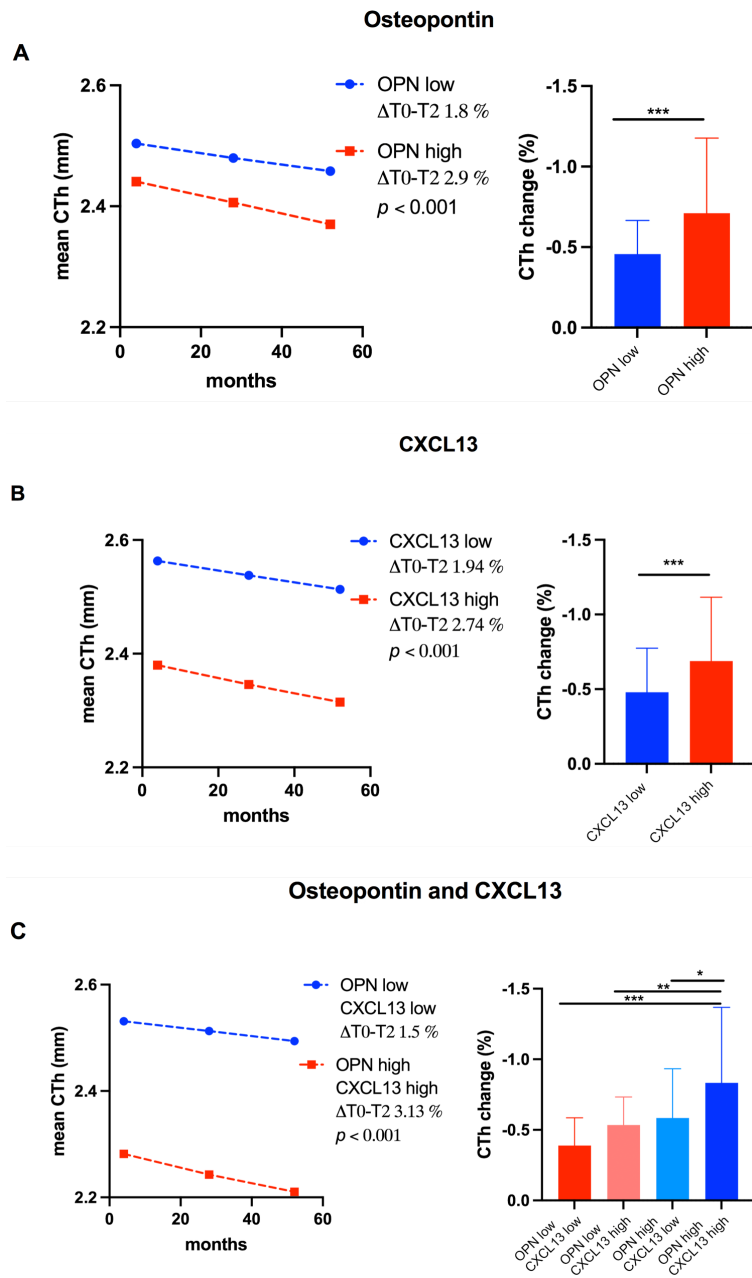


Figure 7.2. Cortical atrophy rates according to Osteopontin and CXCL13 levels. A-B. Osteopontin and CXCL13 were significantly increased in those patients developing more cortical thinning both after 2 and 4 years. C. Having high levels of both molecules led to higher atrophy rates. High/Low were defined according to median values. Abbreviations: CTh: cortical thickness. ΔT0-T2: cortical thickness change between baseline and the end of 4 years follow-up (T2).

Biological process	Strength	False discovery rate
Cytokine-mediated signaling pathway	1.35	2.71e-05
Tumor necrosis factor-mediated signaling pathway	1.84	0.00071
Cellular response to organic substance	0.87	0.00097
Inflammatory response	1.32	0.0032
Death-inducing signaling complex assembly	2.74	0.0099
Extrinsic apoptotic signaling pathway	1.81	0.0115
Negative regulation of response to external stimulus	1.37	0.0136
Chronic inflammatory response	2.56	0.0146
Positive regulation of ceramide biosynthetic process	2.56	0.0146
Regulation of establishment of endothelial barrier	2.46	0.0182
Positive regulation of inflammatory response	1.66	0.0217
Regulation of response to external stimulus	1.03	0.0229
Positive regulation of response to external stimulus	1.23	0.0265
Regulation of anatomical structure morphogenesis	1.0	0.0275
Regulation of multicellular organismal process	0.67	0.0404
Signal transduction	0.55	0.0464
Molecular function	Strength	False discovery rate
Cytokine activity	1.75	8.21e-07
Cellular component	Strength	False discovery rate
Extracellular region	0.67	0.0015
Extracellular space	0.74	0.0033

Table 7.2: Pathway analysis. Biological processes that particularly emerged associated with the selected cytokines profile were the regulation and establishment of endothelial barrier, a positive regulation of a chronic inflammatory response, and the activation of the TNF-mediated signaling pathway.

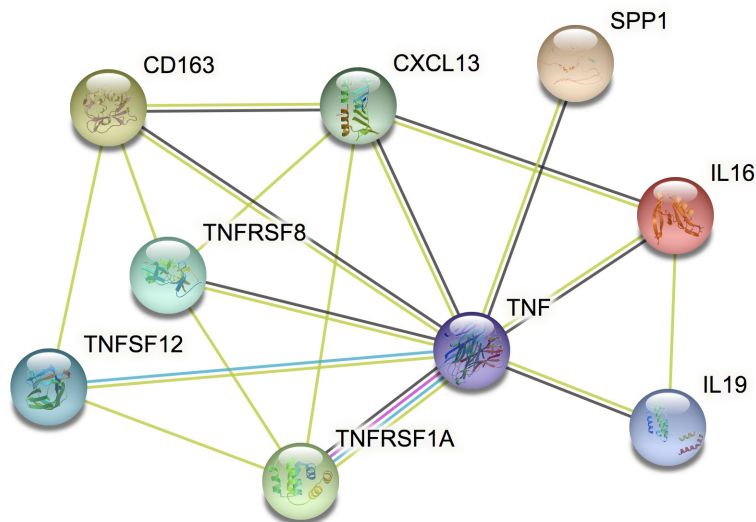


Figure 7.3. Pathway analysis of CSF markers identified as associated with accumulating cortical atrophy. Protein-protein associations between molecules detected at the RF approach (protein-protein enrichment p value = $7.93e-13$). See Table II for the specific functions related with the pathway. Abbreviations: SPP1, Secreted Phosphoprotein 1 or Osteopontin; CXCL13, chemokine (C-X-C motif) ligand 13 or B lymphocyte chemoattractant; TNF, tumour necrosis factor; IL-19, interleukin-19; IL-16, interleukin-16; IL-35, interleukin-35; CD163, Cluster of Differentiation 163; TNFRSF8 TNF Receptor Superfamily Member 8 or Cluster of Differentiation 30; TNFSF12, TNF Superfamily Member 12 or TWEAK; TNFRSF1A, TNF receptor superfamily member 1A or TNFR1.

Predicting cortical atrophy

i) When including the molecules that emerged from the random forest approach in a multivariate linear regression model, OPN ($p < 0.001$), CXCL13 ($p = 0.001$), and sTNFR1 ($p = 0.024$) confirmed to be independent predictors of accumulating atrophy (adjusted R-squared 0.615).

ii) The multiple regression analysis including age, sex, EDSS, WMLN, number of spinal cord lesions and Gadolinium enhancing lesions but also CLn and CLv provided evidence of a correlation between WMLn ($p = 0.015$), WMLv ($p = 0.011$) and CLs ($p = 0.086$) with accumulating cortical atrophy (adjusted R-squared 0.19). Notable, after exclusion of CLn and CLv from the model, the adjusted R square was 0.07, with WMLn ($p = 0.033$), WMLv ($p = 0.006$) and presence of spinal cord lesions ($p = 0.046$) best associated with accumulating atrophy.

iii) The ten selected CSF markers were then added in a single model that included all the above mentioned clinical, demographical and MRI variables. OPN ($p = 0.002$) and IL19 ($p = 0.022$) levels were confirmed significantly increased in patients with more CTh change over the follow-up (adjusted R-

squared 0.619). Notably, after exclusion of measures of cortical damage (CLn and CLv), along with OPN ($p < 0.001$), molecules associated with focal cortical damage as CXCL13 ($p = 0.001$) and sTNFR1 ($p = 0.022$) confirmed to provide additional value when compared with the model based on demographical, clinical and radiological measures most adopted in clinical practice (adjusted R-squared 0.600).

The LRT approach confirmed that these (iii) latter models were significantly more accurate than the one with only clinical, demographic, and MRI variables at baseline ($p < 0.001$), suggesting an additional prognostic value when testing CSF markers.

Predicting cortical atrophy after 4 years

A similar regression approach was adopted to further evaluate and confirm the association between molecules selected by the random forest logarithm (OPN, CXCL13, IL22, IL19, IL8, IFN α 2, CCL22, Osteocalcin, IL35 and MIF), clinical, demographical and MRI variables and 4-years cortical thinning:

i) a multivariate linear regression model confirmed, among the ten cytokines, OPN ($p < 0.001$), CXCL13 ($p < 0.001$), as well as IL35 ($p = 0.030$) as highly expressed in patients with accumulating atrophy (adjusted R-squared 0.773)

ii) a model with clinical, demographical and MRI variables, selected WMLv ($p = 0.018$) and WMLn ($p = 0.027$) as the best associated with annual atrophy rates (adjusted R-squared 0.348)

iii) a comprehensive model that included all CSF variables had improved accuracy (adjusted R-squared 0.818), with OPN being the most significant variable ($p < 0.001$), further suggesting the additional value of testing CSF variables. The LTR approach confirmed the higher accuracy of the latter model ($p < 0.001$).

Predicting disease activity and disability accumulation

Patients with disease activity had higher atrophy accumulation rates (mean annual reduction of -0.424 ± 0.190 vs 0.682 ± 0.436 mm³) and increased levels of many proinflammatory molecules.

The random forest approach was applied to evaluate molecules best associated with disease activity. When considering minimal depth and time a root measures, CXCL13 and OPN revealed the best associated, along with TNF, IFN gamma, IL8, CXCL5, CCL1, IL4 and IL6 (Figure 7.4). A logistic regression model confirmed CXCL13 levels as significantly increased in those patients with MS activity.

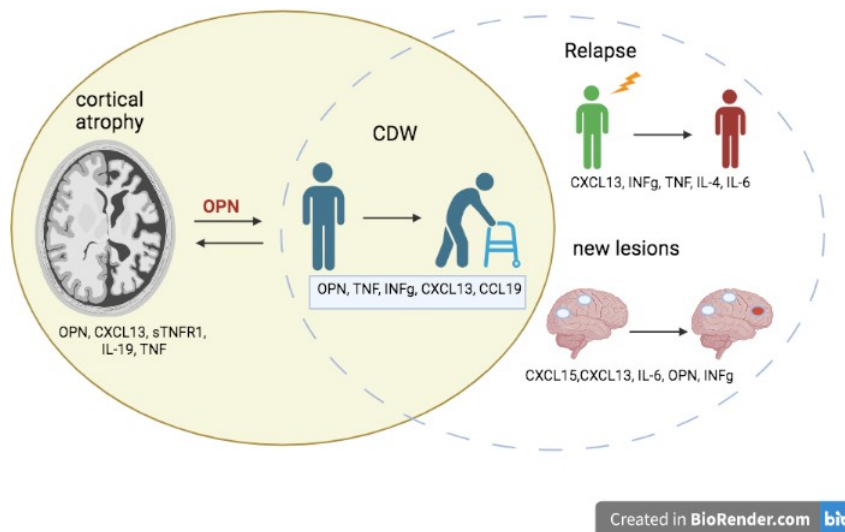


Figure 7.4. Cytokines and Chemokines best associated with cortical atrophy and disease activity. The molecules best associated with each outcome are shown. OPN emerged as the best associated with accumulating cortical atrophy and confirmed disability worsening. Abbreviations: OPN, Osteopontin; CDW, Confirmed Disability Worsening; CXCL13, chemokine (C-X-C motif) ligand 13 or B lymphocyte chemoattractant; sTNFR1, soluble TNFRSF1A or TNF receptor superfamily member 1A; IL-19: interleukin 19; TNF, tumour necrosis factor; IFNg, interferon gamma; CCL19, chemokine (C-C motif) ligand 19; IL-4, interleukin 4; IL-6, interleukin 6; CXCL15, chemokine (C-X-C motif) ligand 15.

Confirmed disability worsening

Notably, among markers of disease activity, OPN revealed the one best associated with CDW over the follow-up (OR 1.85 [1.11-3.39], $p = 0.028$ figure 3, Supplementary table).

Accordingly with the hypothesis that higher atrophy accumulation associated with disability accumulation in early MS, patients with CDW developed more cortical thinning (mean annual percentage change of -0.845 ± 0.010 vs -0.465 ± 0.208 , $p < 0.001$).

A logistic regression model with baseline demographical, clinical and MRI variables, confirmed OPN (OR 2.468 [1.46-5.034] $p = 0.004$), along with EDSS (OR 2.747 [1.379-6.186] $p = 0.007$), as significantly increased in those patients accumulating more disability.

Results were overall confirmed after 4 years, when CDW was evident in 22 out of 39 patients, of which 10 showed PIRA events. In particular, CDW after 4 years was associated with accumulating atrophy (mean percentage annual decrease of

0.814 ± 0.005 vs $0.458 \pm 0.183 \text{ mm}^3$, $p < 0.001$) and higher baseline OPN levels (114174.48 ± 60991.97 vs 53338.52 ± 76842.52 , $p < 0.001$).

Occurrence of new relapses and radiological activity

Among inflammatory markers, CXCL13 (OR 1.329 [1.082-1.705], $p = 0.013$) and IFN γ (OR 1.913 [1.132-3.499], $p = 0.023$) were best associated with relapses (Figure 4), while decreased CXCL5 levels (OR 0.743 [0.560-0.948], $p = 0.038$) and increased CXCL13 (OR 1.197 [1.01-1.453], $p = 0.047$) were confirmed in the logistic regression model in those patients experiencing new radiological activity (Figure 7.4).

7.4 DISCUSSION

In the current work we observed that OPN, even more than other inflammatory markers as CXCL13 and even more than other molecules related to the TNF superfamily, associated with accumulating GM damage, as well as with disease activity and disability accumulation, beginning with the early stages or RRMS. Accumulating GM damage has been recognized as a major factor in driving MS associated disability (Kutzlenigg et al., 2005; Fisniku et al., 2008; Calabrese et al., 2015; Howell et al., 2011), with extensive GM demyelination characterizing progressive MS but also being suggested as a reliable marker of disability progression occurring independently from disability in the first years of the disease course (Cagol et al., 2022).

In a previous study we showed how inflammatory markers of focal GM damage, including the lymphoid chemokines CXCL12 and CXCL13 and TNF, assessed at the time of diagnosis, associated with both disease activity and accumulating cortical atrophy (Magliozzi 2020). This in line with the notion that meningeal inflammatory aggregates are strictly linked with the underlying subpial demyelination (Howell et al., 2011; Magliozzi et al., 2018). Nevertheless, the complex physiopathology of diffuse GM damage, its relationship with meningeal inflammation, with focal GM demyelination, and persisting WM smouldering lesions with subsequent retrograde degeneration, suggested us to better investigate candidate markers that apparently not closely reflect the focal GM damage as detected by DIR sequences.

Among all markers, OPN clearly emerged as the most prominent associated with accumulating GM atrophy, notably providing additional value when included in a regression model with demographical and radiological variables.

OPN represents a member of SIBLING (small integrin-binding ligand, N-linked glycoproteins) family of proteins. OPN is a binding partner of $\alpha 4\beta 1$ integrin, the main homing molecule for lymphocyte entry to the brain in MS, as well as several

extracellular matrix proteins, including fibronectin and vitronectin (Chabas et al., 2001; Steinman, 2009). OPN, by interacting with many binding partners, influences various biological processes including cell adhesion, coagulation, up-regulation of pro-inflammatory cytokines from both the TH1 and TH17 pathways in mice and in man (Chabas et al., 2001; Jansson et al., 2002; Murugaiyan et al., 2008). OPN influences the downregulation of IL10 levels through CD44 ligand (Brocke et al., 1999). OPN is involved in the induction of autoreactive T cells that persistently produce inflammation in the central nervous system by protecting from apoptotic death (Brocke et al., 1999; Hur et al., 2007; Chabas et al., 2001). Accordingly, OPN is expressed by the inflamed endothelium in the brains of patients with MS within active plaques, but also in the white matter adjacent to plaques, reactive astrocytes and microglial cells (Sinclair et al., 2005, Chabas et al., 2001). Notably, neurons have been suggested as capable of secreting OPN, a process that could lead to the inhibition of cell lysis thus protecting the axon from degeneration during autoimmune demyelination (Chabas et al., 2001; Steinman 2009).

Our results are in line with an initial *in vivo* report of OPN associated with long term atrophy in patients with MS (Orsi et al., 2021). Whether these results reflect chronic inflammatory processes occurring in active plaques in both WM and GM or microstructural changes in NAWM (Orsi et al., 2021), remains to be elucidated. Of note, these findings, suggest a potential role of OPN in mediating progressive chronic inflammation that underlies the course of progressive MS. Accordingly, progressive EAE course is rare in osteopontin-deficient mice after immunization with MOG₃₅₋₅₅, being OPN^{-/-} mice totally protected from EAE-related death (Chabas et al., 2001). Furthermore, in relapsing EAE induced by the PLP₁₃₉₋₁₅₁ in SJL/j mice, recombinant OPN injection, after remission from a relapse, led to a more progressive disease without return to a state of remission (Hur et al., 2007). In line with experimental evidence, we similarly found increased CSF levels of OPN in patients with primary progressive MS at the time of diagnosis (Marastoni et al., 2021), further suggesting a role of OPN, not only in relapse-associated inflammatory bouts, but also in the occurrence, of disability progression independent of relapses.

Along with OPN, we confirmed the role of the lymphoid chemokine CXCL13 as a marker of focal grey matter damage and accumulating GM atrophy (Magliozzi et al., 2020), possibly associated with B and T cell recruitment and organization of meningeal tertiary lymphoid structures in the sulci adjacent to the demyelinated GM (Krumbholz et al., 2006; Howell et al., 2011). Notably, the additive effect of OPN and CXCL13, with the latter clearly associated with focal cortical damage, as also emerged from the regression models, suggest the involvement of the molecules in different mechanisms of cortical damage, and put them as good, complementary, candidate markers of grey matter damage accrual.

Globally, our study expands the field of possible markers of cortical atrophy and disability accumulation, remarking the importance of cerebrospinal fluid assessment at the time of diagnosis and its potential in providing reliable predictors of disability accumulation as well as treatment response (Marastoni et al., 2022).

Along with molecules associated with focal cortical damage that clearly emerged as reflecting chronic meningeal inflammation, we suggest OPN as a reliable and new marker that needs further validation in a larger and separate cohort, particularly in line with the preclinical and in vivo accumulating evidence of its role in chronic compartmentalized inflammation. OPN may have varying roles whether in smouldering chronic WM lesions, in WM or in GM, or in normal appearing or demyelinated tissue. Clearly OPN deserves increased attention for its role in the pathogenesis of different forms of MS.

8. INTRATHECAL INFLAMMATORY PROFILE PREDICT DISABILITY PROGRESSION INDEPENDENT OF RELAPSE ACTIVITY IN EARLY MS

Manuscript in preparation.

Author contributions: Marastoni D¹, Colato E¹, Tamanti A¹, Ziccardi S¹, Eccher C¹, Crescenzo F¹, Bajrami A¹, Schiavi GM¹, Camera V¹, Virla F¹, Guandalini M¹, Turano E¹, Pizzini FB², Montemezzi S², Bonetti B³, Magliozzi R¹, Calabrese M¹

1 Neurology B, Department of Neurosciences, Biomedicine and Movement Sciences, University of Verona, Verona, Italy

2 Neuroradiology and Radiology Unit, Azienda Ospedaliera Universitaria Integrata, Verona, Italy

3 Neurology A, Azienda Ospedaliera Universitaria Integrata, Verona, Italy

8.1 INTRODUCTION

Multiple sclerosis (MS) is an autoimmune demyelinating disease of the central nervous system (CNS) affecting primarily young adults and leading to significant neurological disability.

Initial observations from natural history large-cohort studies supported a two-staged disease model, in which most patients initially experience a relapsing-remitting course (RRMS) with prominent inflammatory activity, expressed as acute neurological relapses, subsequently followed-by a progressive and irreversible disability accumulation (secondary progressive MS, SPMS, Scalfari et al., 2010, Confavreux et al., 2006). This two stage theory has changed (Steinman and Zamvill, 2015, Lassmann, 2019), with inflammation being suggested as a major cause of disability accumulation in progressive MS (Lassmann, 2019). Furthermore, mounting evidence indicates that, even in young adults with RRMS, a steady and ‘silent’ progression of disability despite the lack of new inflammatory attacks is the major determinant of confirmed disability accumulation over time (Kappos et al., 2020; Cree et al., 2019; Lublin et al., 2022).

Such progression independent of relapse activity (PIRA) represents an unmet therapeutic and clinical need, as its measure is often beyond the sensitivity of many commonly MRI measures adopted in clinical practice (Filippi et al., 2019).

Preliminary observations suggest that the intrathecal meningeal and perivascular inflammation associated with grey matter (GM) damage and ongoing tissue damage (Lucchinetti et al., 2011; Howell et al., 2011; Calabrese et al., 2015) are likely to play a key role in determining the gradual disability accumulation since the early stage of the disease. This is in line with the recent notion that such independent progression parallels changes in brain and cortical atrophy,

highlighting a key pathological role of cortical GM damage (Cree et al., 2019; Cagol et al., 2022).

By combining molecular neuropathology on progressive MS cases at post-mortem analysis and both imaging and cerebrospinal fluid (CSF) analysis on MS patients at the time of diagnosis, we demonstrated that a common intrathecal (meninges and CSF) inflammatory profile, including IFN γ , TNF, LIGHT, TWEAK, and molecules associated with sustained B-cell activity and lymphoid-neogenesis, such as CXCL13, CXCL12, is linked to increased cortical pathology and predictive of subsequent disease activity and cortical atrophy accumulation in early RRMS (Magliozzi et al., 2018; 2020).

In this retrospective study, we aimed to determine i) a specific CSF profile of intrathecal compartmentalized inflammation that associates and possibly predict progression independent of relapses; ii) brain MRI measures best associated and candidate predictors of PIRA.

8.2 METHODS

Study design

This was a longitudinal, retrospective study including clinical, CSF, and MRI data from 80 patients diagnosed with RRMS and followed prospectively at the MS Center of Verona, University Hospital, Verona, Italy for five years. We included in this study baseline clinical, CSF, and MRI data acquired between December 2014 and December 2017 from patients fulfilling the following eligibility criteria: the availability of i) CSF obtained at the time of diagnosis; ii) a clinical follow-up of at least 5 years; iii) a 3T brain MRI acquired within one week from the lumbar puncture; iv) a diagnosis of MS according to the most recent criteria.

Patients were therapy free at the time of the lumbar puncture and underwent a first-line disease modifying therapy. Concurrent infections were excluded by clinical and laboratory analysis. The study was approved by the Ethics Committee of the University of Verona and informed consent was collected from all participants.

Clinical data

Participants underwent a complete neurological evaluation using the Expanded Disability Status Scale (EDSS) performed by two certified raters (MC, DM) at the time of the diagnosis and every 6 months for 5 years, with additional visits in case of relapses. The occurrence of relapses or new or enlarging lesions was recorded at each visit.

Confirmed disability progression (CDP) was defined as an increase of 1.5 points from a baseline EDSS score of 0; 1 point from an EDSS score equal or below 5.5; and 0.5 points from an EDSS score greater than 6, confirmed at least at 6 months. We classified patients as either PIRA or stable patients. Patients with PIRA were defined as having a CDP episode with no relapses during the entire follow-up period. Stable patients were defined by the absence of any clinical relapse or PIRA event for the entire duration of the study (Cagol et al., 2022). Stable patients were further divided according to the occurrence or not of new radiological activity at the MRI follow-up.

CSF analysis

We collected CSF samples at the time of the diagnosis, at least one month after the last relapse, and within one week from the MRI, according to the Consensus Guidelines for CSF and Blood Biobanking. After centrifugation, we stored the supernatant at -80°C. We analysed the CSF levels of inflammatory mediators using a combination of immune-assay multiplex techniques based on the Luminex technology (40- and 37-Plex, Bio-Plex X200 System equipped with a magnetic workstation; BioRad, Hercules, CA) as previously described. All samples were duplicated in the same experiment and in 2 consecutive experiments to verify the reproducibility and consistency of results. The CSF concentration of each protein detected during the analysis was normalized to the total protein concentration of each CSF sample (measured by Bradford assay). The levels of neurofilament protein light chain (Nf-L) in the CSF samples were measured using Human Nf-L ELISA kit (MyBioSource, San Diego, CA, USA) according to previously optimized procedures. The quantification of Nf-L was detected by a multiwell plate reader at a wavelength of 450nm (Biorad, Italy).

MRI analysis

MRI protocol

Participants underwent a 3T Philips Achieva MRI acquisition at the Radiology Unit of the University Hospital of Verona every six months, with additional evaluations in case of relapses. The MRI protocol included 3D T1-weighted, 3D Double Inversion Recovery (DIR), 3D Fluid Attenuated Inversion Recovery (FLAIR), and 3D T1-weighted post-contrast images. See Supplementary materials for further details on the image acquisition protocol.

We quality-checked images for scanner inhomogeneities and artifacts.

MRI acquisition protocol

Patients underwent an MRI protocol acquired using a 3T Philips Achieva MRI scanner. The following image sets were acquired:

- a) 3D T1weighted magnetization prepared rapid gradient echo (MPRAGE) with Repetition Time (TR) = 8.4ms, Echo Time (TE) = 3.7 ms, voxel size = 1x1x1 mm³, field of view (FOV) = 240x240x180, number of excitations (NEX) = 1;
- b) 3D Fluid Attenuated Inversion Recovery (FLAIR) with TR/TE = 8000/292 ms, TI = 2350 ms, voxel size = 1x1x1 mm³, field of view (FOV) = 240x240x180, NEX = 1;
- c) 3D Double Inversion Recovery (DIR) with TR/TE = 5500/292 ms, Inversion Times (TI) TI = 2550 ms, delay 450ms, voxel size = 1x1x1 mm³, field of view (FOV) = 240x240x180, NEX = 3;
- d) 3D-T1 weighted TFE post-contrast with the same parameters of the pre-contrast sequence (TR/TE = 8.4/3.7ms, voxel size of 1x1x1 mm, the acquisition time of 5:51 min).

Image processing

We automatically segmented WM lesions on FLAIR images using Lesion Segmentation Tool (LST) implemented in the Statistical Parameter Mapping (SPM) software on Matlab 2020b and obtained T2 hyperintense WM lesion masks, volume (WMLV) and number (WMLN). We used lesion masks to fill hyperintensities on 3D T1-weighted images. We automatically segmented and parcellated the brain using MALF.

We manually segmented and assessed the number of cortical lesions (CLs) on DIR images following the recommendations for cortical lesions scoring in patients with MS (Geurts et al., 2011). Such numbers included both intracortical and mixed (WM/GM) lesions, while subpial were not counted due to technical difficulties. We used FSL to estimate the CL volume using the CL masks.

Statistical analysis

We used R (version 4.1) for statistical analysis.

Clinical and Demographics

We used Mann-Whitney, Chi-Square, and Fisher exact test where appropriate to assess differences between PIRA and non-PIRA patients.

We repeated the analysis on a subsample of participants without radiological activity.

CSF and MRI markers associated with PIRA

CSF feature selection and association with PIRA

We used Random Forest (RF) analysis, a feature selection technique, to identify the baseline CSF molecules most associated with and that best discriminate

between stable participants and those that developed PIRA by the end of the follow-up. Lower Minimal Depth (MD) values reported by a variable indicates higher predictive accuracy, while higher times a root measure indicates a higher predictive power. We split the cohort into training (80%) and testing (20%) sets. We fit the RF (1000 trees, 8 variables tried at each split) on the training set and used the testing set to evaluate its performance. We used univariate logistic regressions to determine the association between the baseline, statistically significant CSF variables and PIRA events at 5 years, when correcting for age and sex. We used univariate Cox Proportional regression models to predict the time to PIRA, having as predictors the CSF variables identified using the RF analysis, and correcting for age and sex.

CSF markers associated with PIRA without radiological activity

We repeated the abovementioned statistical analysis on a subsample of participants without radiological activity.

Pathway analysis

To better investigate the CSF proteins significantly associated with the sample traits in the previous analyses we used STRING (<https://string-db.org/>) to quantify module connectivity and enriched biological function. Module connectivity was evaluated by the Protein-Protein Interaction (PPI) enrichment p-value. Low PPI p-value indicates that the nodes (proteins) are not random and that the observed number of edges (the interaction between proteins) is significant. While strength and False Discovery Rate (FDR) measures were used to evaluate, respectively, how large and significant the enrichment effect is for each biological process detected by the pathway analysis. The analysis was performed on both the groups of molecules selected by RF as associated with PIRA and PIRA without radiological activity.

MRI feature selection and association with PIRA

As for the CSF, we applied a RF analysis on GM regional volumes extracted from MALF, WM lesion volume, cortical lesion volume, and mean thickness measures to identify the baseline MRI measures that best discriminate between stable participants and those developing PIRA. We split the cohort into training (80%) and testing (20%) sets. We fit the RF (1000 trees, 5 variables tried at each split) on the training set and used the testing set to evaluate its performance. We used univariate logistic regressions to determine the association between the baseline, statistically significant MRI variables and PIRA events at 5 years, when correcting for age and sex. We corrected for multiple comparisons using Benjamini-Hochberg technique.

We repeated the abovementioned statistical analysis on the subsample of participants without radiological activity.

8.3 RESULTS

Study cohort

We included in this study 80 patients with RRMS (mean age 39.3 ± 12.3 years, 16 males, 64 females) (Table 8.1). During the follow-up period, 23 (28.8%) patients experienced confirmed disability accumulation independent of relapses (mean time 2.7 ± 1.1 years) with a mean increase of EDSS of 1.5 ± 0.6 . Of these, 8 developed new or enlarged, asymptomatic, brain lesions.

At baseline, participants with PIRA had increased baseline age (44 ± 10.7 vs 37.4 ± 12.4 , $p = 0.017$) and EDSS (median EDSS [IQR] of 3[2-4] for PIRA group and 1.5[1-2] for stable participants, $P < 0.001$).

Patients with PIRA had higher T2 WM lesion load (7.54 ± 5.77 vs. 2.33 ± 3.79 , $P < 0.001$), higher T2 WM lesion number (27.1 ± 13.1 vs. 17.5 ± 16.2 , $P < 0.01$), higher CLn (6.1 ± 6.1 vs 2.9 ± 3.6 , $p = 0.032$) and CLv (571.87 ± 719.86 vs 260.32 ± 340.10 , $p = 0.039$). On the contrary, they showed lower whole brain GM volume (748688.21 ± 60539.53 vs. 802183.4 ± 61299.59 , $P < 0.01$), and lower mean cortical thickness (2.37 ± 0.11 vs. 2.43 ± 0.08 , $p < 0.05$) when compared with the stable group (Table 8.1). Clinical, demographical and radiological characteristics of the subgroup of patients without radiological activity are shown in Table 8.2.

	RRMS at diagnosis	End of follow-up		<i>p</i>
		PIRA	No PIRA	
<i>N</i> (%)	80	23 (29)	57 (71)	
Age (years; mean [SD])	39.3 [12.3]	44 [10.7]	37.4 [12.4]	<0.05
Gender (M/F)	16/64	5/18	11/46	0.768
Median EDSS [25 th -75 th interquartile range]	2[1-3]	3[2-4]	1.5[1-2]	<0.001
OCB (positive/negative)	60/20	17/6	43/14	0.99
CSF/serum albumin ratio	5.02[1.61]	5.02[1.66]	5.02[1.61]	0.99
Whole brain WM volume (mm ³ ; mean [SD])	696300.02[48622.97]	675945.35[56075.45]	704033.1 [43574.61]	0.059
Whole brain GM volume (mm ³ ; mean [SD])	787767 [65277.39]	748688.21 [60539.53]	802183.4 [61299.59]	<0.01
Mean cortical thickness (mm ³ ; mean [SD])	2.42[0.09]	2.37[0.11]	2.43[0.08]	<0.05
WMLN (mean [SD])	20.3[15.8]	27.1[13.1]	17.5[16.2]	<0.01
WMLV (mm ³ ; mean [SD])	3.8[5]	7.54[5.77]	2.33[3.79]	<0.001
Spinal cord lesions (mean [SD])	0.49[0.95]	0.70[1.18]	0.40[0.84]	0.311
Gd+ lesions (mean [SD])	0.16[0.54]	0.08 [0.29]	0.19[0.61]	0.751
CLn (mean [SD])	4.72[7.67]	6.13[6.07]	2.91 [3.59]	0.032
CLv (mm ³ ; mean [SD])	219.8[399.73]	571.87[619.3]	260.32[340.1]	0.039

Table 8.1. Demographic, clinical and MRI characteristics at baseline in all study cohort and according to occurrence or not of PIRA

	RRMS at diagnosis	End of follow-up		<i>p</i>
		PIRA without radiological activity	Stable Without radiological activity	
<i>N</i> (%)	41	15 (37)	26 (63)	
Age (years; mean [SD])	43.6 [12.0]	46.1 [11.9]	42.2 [11.1]	0.250
Gender (M/F)	12/29	4/11	8/18	0.999
Median EDSS [25 th -75 th interquartile range]	2[1-4]	3.5[2-4]	2[1-2]	0.010
OCB (positive/negative)	60/20	12/3	20/6	0.999
Whole brain WM volume (mm ³ ; mean [SD])	696300.02 [48622.97]	675945.35 [56075.45]	703933.02 [43656.98]	p<0.05
Whole brain GM volume (mm ³ ; mean [SD])	787767[6527 7.39]	748688.21[6 0539.53]	802421.55 [61266.81]	p<0.005
Mean cortical thickness (mm ³ ; mean [SD])	2.42[0.09]	2.37[0.11]	2.43[0.09]	p<0.05
WMLN (mean [SD])	20.3[15.8]	27.1[13.1]	17.7[16.1]	p<0.01
WMLV (mm ³ ; mean [SD])	3.8[5]	7.5[5.8]	2.3[3.8]	p<0.001
Spinal cord lesions (mean [SD])	0.49[0.95]	0.3[0.56]	0.56[1.07]	0.17
Gd+ lesions (mean [SD])	0.16[0.54]	0.17[0.49]	0.16[0.56]	0.90
CLn (mean [SD])	4.8[5.2]	6.7[6.1]	3.7[4.4]	0.116
CLv (mm ³ ; mean [SD])	466.22 [543.71]	697.8 [680.49]	332.62 [403.64]	0.08

Table 8.2. Demographic, clinical and MRI characteristics of a subsample of participants without radiological activity. Abbreviations: SD: standard deviations; M: males; F: females; EDSS: Expanded Disability Status Scale; OCB: oligoclonal bands; IgG index: Immunoglobulin-G index; CSF: cerebrospinal fluid; GM: grey matter; WM: white matter; WMLN: T2 white matter lesion number; WMLV: T2 white matter lesion volume; Gd+ lesions: Gadolinium enhancing lesions; CLn: cortical lesion number; CLv: cortical lesion volume.

CSF markers of PIRA

Patients with PIRA had increased values of many proinflammatory cytokines/chemokines (Figure 8.1).

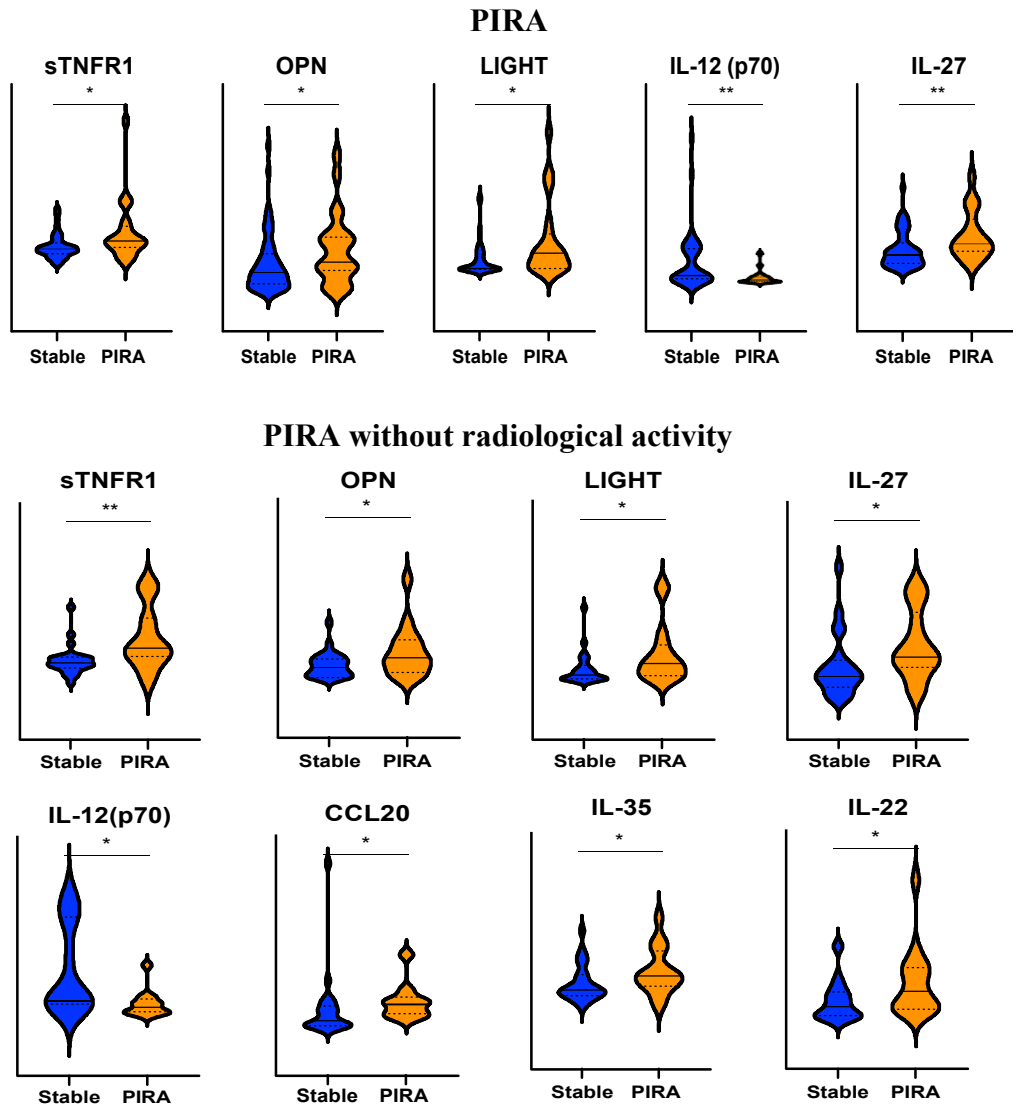


Figure 8.1. Increased markers in patients with PIRA (panel above) and in patients with PIRA without radiological activity.

The RF performed on CSF markers showed that the most important features capable to discriminate between stable and participants with PIRA were LIGHT, CXCL13, sTNFR1, Chitinase3like1, IL27, INFgamma, Osteopontin, CCL2, CCL7, and APRIL (Figure 8.1). The model had an OOB on the training set of 34.4% and achieved an accuracy of 0.69 when applied to the testing set.

Logistic regression analysis on the statistically significant molecules selected by RF, showed that sTNFR1 (β 1.05, se: 0.39, $p = 0.007$), LIGHT (β : 0.27, se:0.10, $p = 0.005$), and IFN gamma (β : 0.42, se:0.17, $p= 0.013$) were associated with PIRA events when correcting for multiple comparisons and adjusting for age and sex.

Similar results were noticed at the Cox regression analysis, with LIGHT ($p=0.009$), CXCL13 ($p=0.018$) and sTNFR1 ($p=0.009$) as significant predictor of an earlier accumulation of disability without relapses. Notably, LIGHT ($r = 0.392$, $p= 0.003$), CXCL13 ($r= 0.407$, $p= 0.004$) and sTNFR1 ($r=0.281$, $p = 0.036$) levels significantly correlated with neuro-axonal damage measured with Nf-L.

CSF markers of PIRA without radiological activity

When repeating the analysis on the subsample of participants without radiological activity (Figure 8.1B), the RF model showed that the most important features to discriminate between stable and participants with PIRA without radiological activity were sTNFR1, Osteopontin, IL35, IL20, IL19, sCD163, CCL21, sTNFR2, CXCL13. The model had an OOB on the training set of 44 and achieved an accuracy of 0.78 on the testing set. Logistic regression on the statistically significant features, adjusted for sex and age, identified by the RF showed that sTNFR1, sTNFR2, IL20, IL19 were associated with PIRA during the 5 years follow-up. Cox regression analysis confirmed sTNFR1 ($p<0.001$), sTNFR2 ($p=0.011$), IL19 ($p=0.006$) as predicted of shorter time to PIRA events. sTNFR1 and sTNFR2 correlated with Nf-L levels ($r = 0.311$, $p=0.039$ and $r = 0.432$, $p =0.012$ respectively).

A CSF immune profile related with TNF superfamily and progression of disability

At the STRING pathway analysis all the selected molecules (from the PIRA group) were confirmed to be involved in chronic inflammatory processes, including in particular recruitment of adaptive and innate immune cells through cytokine and chemokines activity and the cellular signaling in the response to tumor necrosis factor and tumor necrosis factor superfamily molecules (Figure 8.2A).

Similarly, we performed a STRING pathway analysis on the molecules selected in the group of patients with disability progression without relapses and new radiological activity. This confirmed the involvement, regarding molecular function, of TNF superfamily binding and activity and, among inflammatory processes that emerged, the importance of negative regulation of extracellular

matrix protein secretion and dendritic and T cells chemotaxis (PPI p-value < 0.0001).

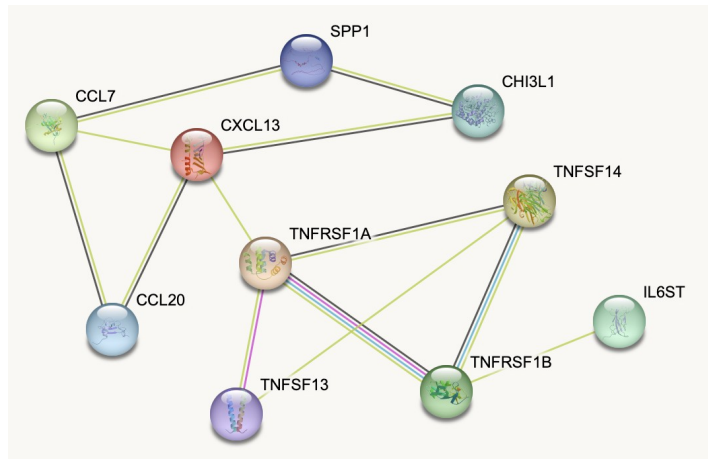


Figure 8.2. STRING pathway analysis on CSF markers associated with disability progression. Molecules detected at the RF approach were associated with many proinflammatory intrathecal processes including in particular recruitment of adaptive and innate immune cells and the cellular signaling in the response to tumor necrosis factor and tumor necrosis factor superfamily molecules (see Supplementary Table 3 for the full processes list). PPI p-value < 0.001.

Abbreviations: CSF: cerebrospinal fluid; IFNG: interferon gamma; CXCL8: interleukin-8 or (C-X-C motif) chemokine ligand 8; CCL3 = Chemokine (C-C motif) ligand 3; CCL19 = Chemokine (C-C motif) ligand 19; CCL25, Chemokine (C-C motif) ligand 25; CXCL13, chemokine (C-X-C motif) ligand 13 or B lymphocyte chemoattractant; TNFSF13B: BAFF, B cell activating factor or tumour necrosis factor ligand superfamily member 13B; TNFRSF1A: sTNF-R1, soluble tumour necrosis factor-receptor 1; TNFRSF1A: sTNF-R2, soluble tumour necrosis factor-receptor 2; TNFSF14: LIGHT, tumour necrosis factor superfamily member 14.

MRI markers associated with PIRA

The RF was then applied on MRI measure. The model had an OOB on the training set of 33% and achieved a prediction accuracy of 0.87 on the testing set. The baseline most important features to discriminate between stable patients and participants with PIRA were the volume of the T2 WM lesions, the cortical thickness of the frontal pole, medial frontal cortex, temporal pole, planum polare, middle temporal gyrus, inferior frontal gyrus, volume of the cerebellum and whole brain GM volume. Univariate logistic regression analysis on the statistically significant identified MRI variables showed that none of the MRI measures were associated with PIRA events at 5 years.

When repeating the analysis on MRI measures in the subgroup of patients without radiological activity, the RF had an OOB on the training set of 43, and achieved a

prediction accuracy of 0.8 on the testing set. The model showed that the most important features to discriminate between stable and participants with PIRA without radiological activity were the middle temporal gyrus, parahippocampal gyrus, inferior temporal gyrus, middle cingulate gyrus, middle frontal gyrus thickness, and the hippocampus volume. Univariate logistic regression on the statistically significant features identified by the RF showed that none of the identified MRI features were associated with PIRA at 5 years when correcting for multiple comparisons.

8.4 DISCUSSION

Defining candidate markers of early disability progression, including that occurring independently of relapses (PIRA), as well defining its pathological determinants, represents an unmet need, in line with the need of a personalized approach since the time of diagnosis (Scalfari et al., 2022; Amato et al., 2020).

We previously identified a specific inflammatory CSF profile at diagnosis, associated with early cortical damage and disease activity (Magliozzi et al., 2018, 2020). In the current study we evaluated at the time of diagnosis, the CSF and MRI profile of patients who would have shown a PIRA in the following 5 years compared to clinically stable patients. A specific profile that included molecules of the TNF superfamily was noticed as the best surrogate marker of PIRA.

Many pathological processes probably concur to PIRA, including the presence of demyelinating activity in chronic lesions (Martire et al., 2022), the early accumulation of focal and diffuse grey matter demyelination (Calabrese et al., 2015; Lucchinetti et al., 2011; Bevan et al., 2019), all leading to premature and irreversible neuro-axonal damage. Certainly compartmentalized CNS inflammation, linked to persistence of adaptive and innate immune infiltrates in niches as perivascular and meningeal spaces represent a key driver (Magliozzi et al., 2018). Particularly subpial cortical demyelination has been associated with large B and T cell infiltrates in the adjacent meningeal sulci (Magliozzi et al., 2007, Howell et al., 2011), in line with the hypothesis that inflammatory factors could diffuse into the underlying tissues either influencing activation status of CNS parenchymal cells and providing a cytotoxic effect (Lisak et al., 2017, Gardner et al., 2013). Accordingly, an outside gradient moving away from the subarachnoid and ventricular CSF filled compartments (Magliozzi et al., 2010; 2022; Fadda et al., 2018) has been described. On the other side, CLs accumulation has been described early in disease course (Scalfari et al., 2018) and associated with subsequent disability (Calabrese et al., 2011; Haider et al., 2021) confirming these processes among best surrogates of PIRA.

Among markers that emerged, LIGHT was the most important variable associated with PIRA. LIGHT is a protein that coexists in both a membrane-bound and a

soluble form. Notably the membrane bound form could exert proinflammatory activity, including survival of CD4+ memory T-cell (Soroosh et al., 2011) as well as the co-stimulation of T-cells (Tamada et al., 2000), while, after shedding, it decreases stimulatory signals and acts as a T-cell inhibitor by stabilizing the *cis* HVEM:BTLA complex (Cheung et al., 2009). Accordingly, the LIGHT gene polymorphism was shown to increase the MS risk in a genome-wide association study (Sawcer) with lower serum levels in patients at higher risk, and in those treated with natalizumab (Malmstrom et al., 2013). Patients with active MS displayed increased serum levels of the molecule, somehow explained by a peripheral protective and compensatory reaction to disease activity (Malmstrom 2013). Nevertheless, soluble LIGHT through the interaction with the lymphotoxin-beta receptor (LTbetaR) seems to exert a proinflammatory role in an experimental hepatitis model (Anand et al., 2006) and has also been reported to contribute to the maintenance of lymphoid microenvironment including B-cell follicles (Wang et al., 2002). However, the functional role of LIGHT in CNS inflammatory response, still remains partially explored. Further studies could evaluate such intriguing hypothesis also applied to the CNS compartment.

Our results are in line with our previous studies (Magliozzi et al., 2018, 2020), where LIGHT was strongly related with subsequent cortical thinning ($\beta = 2.6 \cdot 10^{-4}$; $p = 0.003$, Magliozzi et al., 2020).

Furthermore, molecules related to lymphoid recruitment, as CXCL13, that similarly associated to cortical atrophy accumulation were confirmed as also candidate biomarkers of PIRA, further proposing meningeal infiltrates as biological surrogates of disability progression.

The STRING pathway analysis detected an inflammatory profile characterized by high and dysregulated levels of the TNF superfamily.

It is quite established the role of TNF in the pathogenesis of MS and neuronal loss (Picon et al., 2021; James et al., 2020). Patients with progressive MS are characterized by higher TNF levels and degree of disability progression (Fresegna et al., 2019). Accordingly, increased TNF, detected in meninges and CSF in cases of post-mortem MS, highly correlated with GM demyelination both at the time of diagnosis and death (Magliozzi et al., 2020), with unbalanced levels of their receptor soluble molecules (sTNF-R1 and 2). Gene expression profiling of both lesional and normal appearing GM confirmed that increased meningeal inflammation associated with a shift in the balance of TNF signaling away from TNFR1/TNFR2, the first preferentially expressed on neurons and oligodendrocytes, the latter more expressed by astrocytes and microglia (Magliozzi et al., 2019). Finally, the meningeal persistent production in the animal model of TNF and IFN γ lead to both subpial demyelination and neuronal loss,

corroborating all these proteomic, transcriptomic and pathological evidences (James et al., 2020).

The paper is not without limitations. Particularly, the relatively low number of patients in the PIRA cohort, and in the subgroups without MRI activity could limit our conclusions. A validation cohort is necessary. Nevertheless, the approach has some intriguing aspects: using our definition of PIRA, patients with relapses were excluded, leaving space, from a biological point of view, to a ‘pure’ PIRA cohort, also avoiding recall biases due to clinical difficulties. With the above limitations, we can suggest that: i) a specific intrathecal inflammatory profile characterize PIRA since early disease phases; ii) further studies are needed to evaluate the efficacy of anti-inflammatory treatments, particularly those acting intrathecally, in preventing PIRA events and subsequent disability.

9. CONCLUSIONS

Concluding, we approached the field of intrathecal inflammation, from different points of view. All the evidences that emerged from the studies corroborate the hypothesis that chronic compartmentalized inflammation is common at time of death in patients with progressive MS, and drives disability accumulation over all disease phases. Compartmentalized perivascular inflammation, associated with meningeal infiltrates, characterize patients with a shorter time to progression, a shorter time to wheelchair need and a shorter time to death, providing evidence of clinical manifestations of persistent inflammatory waves. Another relevant finding, is that the perivascular compartment emerges as a target for therapies, subject to the ability of the treatment to cross the BBB. Perivenular inflammation could therefore be considered as a potential relevant biomarker of lesion activity, that, whether validated and assessed in early disease stages, might help to discriminate MS patients with higher lesion and disease activity that will benefit of early and more severe anti-inflammatory treatment.

Certainly, a limitation is the idea that MS heterogeneity is linked to precise patient-dependent immunopathology and may characterize individuals from the beginning of the disease, persisting during the progressive phase, nevertheless with reduced rate of lesion accumulation (Metz et al., 2021; Tobin et al., 2021). Accordingly with this hypothesis, our approach lack a fully quantitative extensive and a fully qualitative analysis that take in consideration inter individual.

Notably, both early active and increased perivenular inflammation were found in a subset of MS patients who also have a high level of meningeal infiltrates corroborating the hypothesis that a generally higher inflammatory activity in the CNS/CSFspace characterizes an MS subgroup with more rapid progression.

In line with this hypothesis we analyzed surrogates of chronic intrathecal inflammation such as cortical lesions and fluid inflammatory CSF biomarkers, being the CSF the most adjacent compartment to the parenchyma that could be assessed in vivo. Cortical damage is a good surrogate of intrathecal inflammation. It associates with early accumulation of disability even when a diagnosis of RRMS has been made, and predict a severe disease course with an earlier achievement of disability milestones of EDSS 4 and 6 and an earlier diagnosis of SPMS. Notably, these observations have implications in clinical practice. Cortical lesions, and accumulation of focal cortical damage in the first years after a diagnosis of MS, represent then a negative prognostic marker associated with persistent intrathecal inflammation.

Nevertheless, our analysis was limited by the absence of fully quantitative data on spinal cord total lesion number and area. Moreover, the cognitive evaluation, that is commonly adopted in many MS centers, was not included in the clinical evaluation. Furthermore, the number of patients who enter the progressive phase is relatively low; therefore, other studies with a larger sample size but a similar follow

up, although very difficult to be carried out, should be designed to confirm our results.

Finally, CSF inflammatory markers provide additional value in predicting disease course. Defining the patients at higher risk of disability progression remains an unmet need. Non conventional MRI is not commonly acquired, while lumbar puncture is increasingly executed, particularly according to the current diagnostic criteria (Thompson et al., 2018) that focus on CSF analysis as a criteria for dissemination in time. Notably, while pathological studies could detect the picture of MS pathology at the end of the disease, thus limiting the information that can be drawn from a retrospective study cohort, the analysis of CSF markers permit to assess the patients inflammatory profile at the time of diagnosis. Notably, from our studies, adding CSF markers to regression analysis taking in consideration conventional MRI measures, clinical and demographical parameters, provided an increasing value in the prediction of the outcome analyzed.

The study of inflammatory markers is anyway limited by the cost, the need of a laboratory for sample processation, storage and analysis, the low number of patients evaluated in different studies, the inter-individual variability. Nevertheless, it could provide insight into molecule that could contribute to MS pathology as in the case of Osteopontin. Osteopontin, and the relative gene SPP1 are upregulated in the context of chronic active lesions, OPN represents a member of SIBLING (small integrin-binding ligand, N-linked glycoproteins) family of proteins. OPN is a binding partner of $\alpha 4\beta 1$ integrin, the main homing molecule for lymphocyte entry to the brain in MS, as well as several extracellular matrix proteins, including fibronectin and vitronectin. OPN is expressed by the inflamed endothelium in the brains of patients with MS within active plaques but also in the white matter adjacent to plaques, reactive astrocytes and microglial cells. Notably, neurons have been suggested as capable of secreting OPN, a process that could lead to the inhibition of cell lysis, thus protecting the axon from degeneration during autoimmune demyelination.

Our results are in line with an initial *in vivo* report of OPN associated with long-term atrophy in patients with MS. Accordingly with initial evidence in EAE, a role of OPN in mediating neurodegeneration has been shown by a population of OPN+ microglia bearing the CD11c surface marker, that was associated with signs of Alzheimer disease neuropathology. Whether these results reflect chronic inflammatory or neurodegenerative processes occurring in active plaques in both WM and GM or microstructural changes in NAWM, remains to be elucidated in a future pathological and mechanistic study.

Along with Osteopontin, CXCL13, molecules associated to the TNF superfamily are associated with a severe disease course. Notably, these markers could provide additional and specific informations regarding intrathecal inflammatory processes, being helpful in the characterization of the patient at risk of developing early disability accumulation

Our studies expands the field of possible markers of intrathecal inflammation,

cortical atrophy and disability accumulation, emphasizing the importance of cerebrospinal fluid assessment at the time of diagnosis and its potential to provide reliable predictors of disability accumulation as well as treatment response.

Along with molecules associated with focal cortical damage that clearly emerge as reflecting chronic meningeal inflammation, we suggest OPN as a reliable marker, needing further validation in a larger and separate cohort.

10. REFERENCES

- Absinta M, Sati P, Reich DS. Advanced MRI and staging of multiple sclerosis lesions. *Nat Rev Neurol*. 2016 Jun;12(6):358-68.
- Absinta M, Maric D, Gharagozloo M, et al. A lymphocyte-microglia-astrocyte axis in chronic active multiple sclerosis. *Nature* 2021; 597: 709–14.
- Absinta, M., P. Sati, A. Fechner, M. K. Schindler, G. Nair and D. S. Reich. Identification of Chronic Active Multiple Sclerosis Lesions on 3T MRI. *AJNR Am J Neuroradiol* 2018; 39(7): 1233-1238.
- Absinta M, Sati P, Masuzzo F, et al. Association of Chronic Active Multiple Sclerosis Lesions with Disability in Vivo. *JAMA Neurol*. 2019;76(12):1474-1483.
- Absinta M, Sati P, Schindler M, et al. Persistent 7-tesla phase rim predicts poor outcome in new multiple sclerosis patient lesions. *J Clin Invest*. 2016;126(7):2597-2609.
- Ahmed SM, Fransen NL, Touil H, et al. Accumulation of meningeal lymphocytes correlates with white matter lesion activity in progressive multiple sclerosis. *JCI Insight* 2022; 7.
- Aloisi, F. and R. Pujol-Borrell. Lymphoid neogenesis in chronic inflammatory diseases. *Nat Rev Immunol* 2006; 6(3): 205-217.
- Amato MP, Fonderico M, Portaccio E, et al. Disease-modifying drugs can reduce disability progression in relapsing multiple sclerosis. *Brain*. 2020;143(10):3013-3024.
- Anand S. Essential role of TNF family molecule LIGHT as a cytokine in the pathogenesis of hepatitis. *Journal of Clinical Investigation*. 2006;116(4):1045-1051.
- Andersson, M., J. Alvarez-Cermeno, G. Bernardi, I. et al. Cerebrospinal fluid in the diagnosis of multiple sclerosis: a consensus report. *Journal of Neurology, Neurosurgery & Psychiatry* 1994; 57(8): 897-902.
- Androdias G, Reynolds R, Chanal M, Ritleng C, Confavreux C, Nataf S. Meningeal T cells associate with diffuse axonal loss in multiple sclerosis spinal cords. *Ann Neurol* 2010; 68: 465–76.
- Antel J, Antel S, Caramanos Z, Arnold DL, Kuhlmann T. Primary progressive multiple sclerosis: part of the MS disease spectrum or separate disease entity? *Acta Neuropathol*. 2012;123(5):627-638.
- Arrambide, G., M. Tintore, C. Espejo, et al., The value of oligoclonal bands in the multiple sclerosis diagnostic criteria. *Brain* 2018;141(4): 1075-1084.
- Arrambide G, Rovira A, Sastre-Garriga J, et al. Spinal cord lesions: A modest contributor to diagnosis in clinically isolated syndromes but a relevant prognostic factor. *Multiple*

Sclerosis Journal. 2018;24(3).

Bagnato F, Hametner S, Welch EB. Visualizing iron in multiple sclerosis. *Magn Reson Imaging* 2013; 31: 376–84.

Bajrami A, Pitteri M, Castellaro M, et al. The effect of fingolimod on focal and diffuse grey matter damage in active MS patients. *J Neurol*. 2018;265(9).

Bankhead P, Loughrey MB, Fernández JA, Dombrowski Y, McArt DG, Dunne PD, et al. QuPath: Open source software for digital pathology image analysis. *Sci Rep*. 2017 Dec 4;7(1):16878.

Baranzini, S. E. and J. R. Oksenberg. The Genetics of Multiple Sclerosis: From 0 to 200 in 50 Years. *Trends Genet* 2017;33(12): 960-970.

Barcellos, L. F., J. R. Oksenberg, A. J. Green, et al. Genetic basis for clinical expression in multiple sclerosis. *Brain* 2002;125(Pt 1): 150-158.

Barkhof F. The clinico-radiological paradox in multiple sclerosis revisited. *Curr Opin Neurol*. 2002;15(3)

Barro, C., P. Benkert, G. Disanto, et al. Serum neurofilament as a predictor of disease worsening and brain and spinal cord atrophy in multiple sclerosis. *Brain* 2018;141(8): 2382-2391.

Battaglia, M. A. and D. Bezzini. Estimated prevalence of multiple sclerosis in Italy in 2015. *Neurol Sci* 2018;38(3): 473-479.

Beck ES, Maranzano J, Luciano NJ, et al. Cortical lesion hotspots and association of subpial lesions with disability in multiple sclerosis. *Multiple Sclerosis Journal*. Published online 2022.

Bevan RJ, Evans R, Griffiths L, et al. Meningeal inflammation and cortical demyelination in acute multiple sclerosis: Meningeal Inflammation in MS. *Ann Neurol*. 2018;84(6):829-842.

Bhargava, P. and P. A. Calabresi. Metabolomics in multiple sclerosis. *Multiple Sclerosis Journal* 2016;22(4): 451-460.

Bjornevik K, Cortese M, Healy BC, et al. Longitudinal analysis reveals high prevalence of Epstein-Barr virus associated with multiple sclerosis. *Science* 1979; 2022; 375: 296–301.

Bielekova B, Sung M-H, Kadom N, Simon R, McFarland H, Martin R. Expansion and Functional Relevance of High-Avidity Myelin-Specific CD4+ T Cells in Multiple Sclerosis. *The Journal of Immunology* 2004; 172: 3893–904

Bitsch, A., T. Kuhlmann, C. Stadelmann, H. Lassmann, C. Lucchinetti and W. Bruck. A longitudinal MRI study of histopathologically defined hypointense multiple sclerosis

lesions. *Ann Neurol* 2001;49(6): 793- 796.

Bø, L., C. A. Vedeler, H. I. Nyland, B. D. Trapp and S. J. Mørk. Subpial demyelination in the cerebral cortex of multiple sclerosis patients. *Journal of Neuropathology & Experimental Neurology* 2003;62(7): 723- 732.

Bornsén L, Khademi M, Olsson T, Sørensen PS, Finn Sellebjerg F. Osteopontin concentrations are increased in cerebrospinal fluid during attacks of multiple sclerosis. *Mult Scler.* 2011;17(1):32-42.

Braithwaite M, Nunan R, Niepel G, Edwards LJ, Constantinescu CS. Increased osteopontin levels in the cerebrospinal fluid of patients with multiple sclerosis. *Arch Neurol.* 2008;65(5):633-635.

Bramow, S., J. M. Frischer, H. Lassmann, N. Koch-Henriksen, C. F. Lucchinetti, P. S. Sørensen and H. Laursen. Demyelination versus remyelination in progressive multiple sclerosis. *Brain* 2010;133(10): 2983-2998.

Brocke S, Piercy C, Steinman L, Weissman IL, Veromaa T. Antibodies to CD44 and integrin alpha4, but not L-selectin, prevent central nervous system inflammation and experimental encephalomyelitis by blocking secondary leukocyte recruitment. *Proc Natl Acad Sci U S A.* 1999;96(12):6896-901.

Brown JW, Coles A, Horakova D, et al. Association of Initial Disease-Modifying Therapy with Later Conversion to Secondary Progressive Multiple Sclerosis. *JAMA - Journal of the American Medical Association.* 2019;321(2).

Brownlee WJ, Altmann DR, Prados F, et al. Early imaging predictors of long-term outcomes in relapse-onset multiple sclerosis. *Brain.* 2019;142(8).

Brück, W., A. Bitsch, H. Kolenda, Y. Brück, M. Stiefel and H. Lassmann. Inflammatory central nervous system demyelination: correlation of magnetic resonance imaging findings with lesion pathology. *Annals of neurology* 1997;42(5): 783-793.

Brück W, Porada P, Poser S, Rieckmann P, Hanefeld F, Kretzschmar HA, Lassmann H. Monocyte/macrophage differentiation in early multiple sclerosis lesions. *Ann Neurol.* 1995 Nov;38(5):788-96.

Bunyan RF, Popescu BFG, Carter JL, Caselli RJ, Parisi JE, Lucchinetti CF. Childhood-onset multiple sclerosis with progressive dementia and pathological cortical demyelination. *Arch Neurol* 2011; 68: 525–8.

Cabre, P., A. Signate, S. Olindo, H. Merle, D. Caparros-Lefebvre, O. Bera and D. Smadja. Role of return migration in the emergence of multiple sclerosis in the French West Indies. *Brain* 2005;128(Pt 12): 2899-2910.

Cagol A, Schaedelin S, Barakovic M, et al. Association of Brain Atrophy With Disease

Progression Independent of Relapse Activity in Patients With Relapsing Multiple Sclerosis. *JAMA Neurol.* 2022;79(7):682.

Caillier S, Barcellos LF, Baranzini SE, et al. Osteopontin polymorphisms and disease course in multiple sclerosis. *Genes Immun.* 2003;4(4):312-315.

Calabrese M, Atzori M, Bernardi V, et al. Cortical atrophy is relevant in multiple sclerosis at clinical onset. *J Neurol.* 2007;254(9):1212-1220.

Calabrese M, Filippi M, Rovaris M, et al. Evidence for relative cortical sparing in benign multiple sclerosis: A longitudinal magnetic resonance imaging study. *Multiple Sclerosis.* 2009;15(1).

Calabrese M, Favaretto A, Poretto V, et al. Low degree of cortical pathology is associated with benign course of multiple sclerosis. *Multiple Sclerosis Journal.* 2013;19(7).

Calabrese M, Rinaldi F, Mattisi I, et al. The predictive value of gray matter atrophy in clinically isolated syndromes. *Neurology.* 2011;77(3):257-263

Calabrese M, Poretto V, Favaretto A, et al. Cortical lesion load associates with progression of disability in multiple sclerosis. *Brain.* 2012;135(10):2952-2961. doi:10.1093/brain/aws246

Calabrese M, Romualdi C, Poretto V, et al. The changing clinical course of multiple sclerosis: A matter of gray matter: Cortical Pathology and Secondary Progressive MS. *Ann Neurol.* 2013;74(1):76-83.

Calabrese M, Bernardi V, Atzori M, et al. Effect of disease-modifying drugs on cortical lesions and atrophy in relapsing-remitting multiple sclerosis. *Multiple Sclerosis Journal.* 2012;18(4):418-424.

Calabrese M, Magliozzi R, Ciccarelli O, Geurts JJG, Reynolds R, Martin R. Exploring the origins of grey matter damage in multiple sclerosis. *Nat Rev Neurosci.* 2015;16(3):147-158.

Calabrese M, Battaglini M, Giorgio A, et al. Imaging distribution and frequency of cortical lesions in patients with multiple sclerosis. *Neurology.* 2010;75(14):1234-1240.

Carassiti D, Altmann DR, Petrova N, Pakkenberg B, Scaravilli F, Schmierer K. Neuronal loss, demyelination and volume change in the multiple sclerosis neocortex. *Neuropathol Appl Neurobiol* 2018; 44: 377–90.

Cepok S, Jacobsen M, Schock S, et al. Patterns of cerebrospinal fluid pathology correlate with disease progression in multiple sclerosis. *Brain.* 2001 Nov;124(Pt 11):2169-76.

Chabas D, Baranzini SE, Mitchell D, et al. The influence of the pro-inflammatory cytokine, osteopontin, on autoimmune demyelinating disease. *Science.* 2001;294:1731–

1735.

Chang, A., W. W. Tourtellotte, R. Rudick and B. D. Trapp. Premyelinating oligodendrocytes in chronic lesions of multiple sclerosis. *New England Journal of Medicine* 2002;346(3): 165-173.

Charcot, J.-M. *Leçons sur les maladies du système nerveux: faites a la Salpêtrière*, Adrien Delahaye. 1877.

Charcot JM. *Histologie de la Sclérose en Plaques*. Paris: Imprimerie L. Pupart-Davyl; 1869.

Cheung TC, Steinberg MW, Osborne LM, et al. Unconventional ligand activation of herpesvirus entry mediator signals cell survival. *Proc Natl Acad Sci USA*. 2009;106(15):6244-6249.

Chard D, Trip SA. Resolving the clinico-radiological paradox in multiple sclerosis. *F1000Res*. 2017;6.

Chiocchetti A, Comi C, Indelicato M, et al. Osteopontin gene haplotypes correlate with multiple sclerosis development and progression. *J Neuroimmunol*. 2005;163(1- 2):172-178.

Choi S, Howell OW, Carassiti D, et al. Meningeal inflammation plays a role in the pathology of primary progressive multiple sclerosis. *Brain*. 2012;135(pt 10):2925-2937.

Chung KK, Altmann D, Barkhof F, et al. A 30-Year Clinical and Magnetic Resonance Imaging Observational Study of Multiple Sclerosis and Clinically Isolated Syndromes. *Ann Neurol*. 2020;87(1):63-74.

Chiaravalloti, N. D. and J. DeLuca. Cognitive impairment in multiple sclerosis. *The Lancet Neurology* 2008;7(12): 1139-1151.

Church ME, Ceja G, McGeehan M, et al. Meningeal B Cell Clusters Correlate with Submeningeal Pathology in a Natural Model of Multiple Sclerosis. *The Journal of Immunology*. 2021;207(1).

Comi G, Bar-Or A, Lassmann H, Uccelli A, Hartung HP, Montalban X, Sørensen PS, Hohlfeld R, Hauser SL; Expert Panel of the 27th Annual Meeting of the European Charcot Foundation. Role of B Cells in Multiple Sclerosis and Related Disorders. *Ann Neurol*. 2021 Jan;89(1):13-23.

Confavreux C, Vukusic S. Age at disability milestones in multiple sclerosis. *Brain*. 2006;129(pt 3):595-605. Confavreux C, Vukusic S, Moreau T, Adeleine P. Relapses and Progression of Disability in Multiple Sclerosis. *New England Journal of Medicine*. 2000;343(20):1430-1438.

Cooze BJ, Dickerson M, Loganathan R, et al. The association between neurodegeneration

and local complement activation in the thalamus to progressive multiple sclerosis outcome. *Brain Pathol* 2022; 32.

Cortese, I., V. Chaudhry, Y. So, F. Cantor, D. Cornblath and A. Rae-Grant. Evidence-based guideline update: plasmapheresis in neurologic disorders: report of the Therapeutics and Technology Assessment Subcommittee of the American Academy of Neurology. *Neurology* 2011;76(3): 294-300.

Crescenzo F, Marastoni D, Zuco C, et al. Effect of glatiramer acetate on cerebral grey matter pathology in patients with relapsing-remitting multiple sclerosis. *Mult Scler Relat Disord*. 2019;27:305-311.

Dal-Bianco A, Grabner G, Kronnerwetter C, et al. Long-term evolution of multiple sclerosis iron rim lesions in 7 T MRI. *Brain* 2021; 144: 833–47.

Dal-Bianco A, Grabner G, Kronnerwetter C, et al. Slow expansion of multiple sclerosis iron rim lesions: pathology and 7 T magnetic resonance imaging. *Acta Neuropathol* 2017; 133: 25–42.

Davenport, c. b.. Multiple sclerosis: from the standpoint of geographic distribution and race. *archives of neurology & psychiatry* 1922;8(1): 51-58.

Dawson, J. W. The histology of disseminated sclerosis. *Edinburgh Medical Journal* 1916;17(5): 311.

De Groot CJ, Bergers E, Kamphorst W, Ravid R, Polman CH, Barkhof F, van der Valk P. Post-mortem MRI-guided sampling of multiple sclerosis brain lesions: increased yield of active demyelinating and (p)reactive lesions. *Brain*.2001 Aug;124(Pt 8):1635-45.

Del Prete A, Scutera S, Sozzani S, Musso T. Role of Osteopontin in dendritic cell shaping of immune responses. *Cytokine Growth Factor Rev*. 2019;50:19-28.

Dendrou, C. A., L. Fugger and M. A. Friese. Immunopathology of multiple sclerosis. *Nat Rev Immunol* 2015;15(9): 545-558.

Denhardt DT, Noda M, O'Regan AW, Pavlin D, Berman JS. Osteopontin as a means to cope with environmental insults: regulation of inflammation, tissue remodeling, and cell survival. *J Clin Invest*. 2001;107(9):1055-1061.

Derfuss T, Mehling M, Papadopoulou A, Bar-Or A, Cohen JA, Kappos L. Advances in oral immunomodulating therapies in relapsing multiple sclerosis. *Lancet Neurol*. 2020;19(4):336-347.

Duddy ME, Dickson G, Hawkins SA, Armstrong MA. 2001 Monocyte-derived dendritic cells: a potential target for therapy in multiplesclerosis (MS). *Clin Exp Immunol*. 2001 Feb;123(2):280-7.

Eshaghi A, Bodini B, Ridgway GR, et al. Temporal and spatial evolution of grey matter

atrophy in primary progressive multiple sclerosis. *Neuroimage*. 2014;86:257-264.

Eshaghi A, Marinescu RV, Young AL, et al. Progression of regional grey matter atrophy in multiple sclerosis. *Brain*. 2018;141(6):1665-1677.

Fadda G, Brown RA, Longoni G, et al. MRI and laboratory features and the performance of international criteria in the diagnosis of multiple sclerosis in children and adolescents: a prospective cohort study. *The Lancet Child & Adolescent Health*. 2018;2(3):191-204.

Farina, G., R. Magliozzi, M. Pitteri, R. et al. Increased cortical lesion load and intrathecal inflammation is associated with oligoclonal bands in multiple sclerosis patients: a combined CSF and MRI study. *Journal of neuroinflammation* 2017;14(1): 40.

Filippi, M., M. A. Rocca, O. Ciccarelli, et al. MRI criteria for the diagnosis of multiple sclerosis: MAGNIMS consensus guidelines. *The Lancet Neurology* 2016;15(3): 292-303.

Filippi M, Preziosa P, Banwell BL, et al. Assessment of lesions on magnetic resonance imaging in multiple sclerosis: practical guidelines. *Brain*. 2019;142(7):1858-1875.

Filippi M, Preziosa P, Copetti M, et al. Gray matter damage predicts the accumulation of disability 13 years later in MS. *Neurology*. 2013;81(20):1759-67.

Fischl B. *NeuroImage FreeSurfer*. 2012;62:774–81.

Fisniku LK, Chard DT, Jackson JS, et al. Gray matter atrophy is related to long-term disability in multiple sclerosis. *Ann Neurol*. 2008;64(3):247-54.

Fresegna D, Bullitta S, Musella A, et al. Re-Examining the Role of TNF in MS Pathogenesis and Therapy. *Cells*. 2020;9(10):2290.

Frischer JM, Bramow S, Dal Bianco A, et al. The relation between inflammation and neurodegeneration in multiple sclerosis brains. *Brain*. 2009;132(pt 5): 1175-1189.

Frischer JM, Weigand SD, Guo Y, et al. Clinical and pathological insights into the dynamic nature of the white matter multiple sclerosis plaque. *Ann Neurol*. 2015 Nov;78(5):710-21.

Gandhi, R., A. Laroni and H. L. Weiner. Role of the innate immune system in the pathogenesis of multiple sclerosis. *J Neuroimmunol* 2010;221(1-2): 7-14.

Gaetani L, Fanelli F, Riccucci I, et al. High risk of early conversion to multiple sclerosis in clinically isolated syndromes with dissemination in space at baseline. *J Neurol Sci*. 2017;379

Gardner C, Magliozzi R, Durrenberger PF, Howell OW, Rundle J, Reynolds R. Cortical grey matter demyelination can be induced by elevated pro-inflammatory cytokines in the subarachnoid space of MOG-immunized rats. *Brain*. 2013;136(12):3596-3608.

Geurts, J. J. and F. Barkhof. Grey matter pathology in multiple sclerosis. *The Lancet*

Neurology 2008;7(9): 841-851.

Geurts JJG, Calabrese M, Fisher E, Rudick RA. Measurement and clinical effect of grey matter pathology in multiple sclerosis. *Lancet Neurol.* 2012;11(12):1082-1092.

Geurts JJG, Pouwels PJW, Uitdehaag BMJ, Polman CH, Barkhof F, Castelijns JA. Intracortical lesions in multiple sclerosis: Improved detection with 3D double inversion-recovery MR imaging. *Radiology.* 2005;236(1):254-260.

Geurts JJ, Roosendaal SD, Calabrese M, et al. Consensus recommendations for MS cortical lesion scoring using double inversion recovery MRI. *Neurology.* 2011;76(5):418–24.

Giovannoni G, Tomic D, Bright JR, et al. ‘No evident disease activity’: The use of combined assessments in the management of patients with multiple sclerosis. *Mult. Scler.* 2017;23:1179–87.

Giorgio A, Battaglini M, Rocca MA, et al. Location of brain lesions predicts conversion of clinically isolated syndromes to multiple sclerosis. *Neurology.* 2013;80(3).

Giovannoni G, Popescu V, Wuerfel J, et al. Smouldering multiple sclerosis: the ‘real MS.’ *Ther Adv Neurol Disord.* 2022;15:175628642110667.

Goldschmidt, T., J. Antel, F. König, W. Brück and T. Kuhlmann. Remyelination capacity of the MS brain decreases with disease chronicity. *Neurology* 2009;72(22): 1914-1921.

Griffiths L, Reynolds R, Evans R, et al. Substantial subpial cortical demyelination in progressive multiple sclerosis: have we underestimated the extent of cortical pathology? *Neuroimmunol Neuroinflamm.* Published online 2020.

Guyon A. CXCL12 chemokine and its receptors as major players in the interactions between immune and nervous systems. *Front Cel Neurosci.* 2014;8:65.

Haider L, Prados F, Chung K, et al. Cortical involvement determines impairment 30 years after a clinically isolated syndrome. *Brain.* 2021 Jun 22;144(5):1384-1395.

Haider L, Chung K, Birch G, et al. Linear brain atrophy measures in multiple sclerosis and clinically isolated syndromes: a 30-year follow-up. *J Neurol Neurosurg Psychiatry.* 2021;92(8):839-846.

Haider L, Zrzavy T, Hametner S, et al. The topography of demyelination and neurodegeneration in the multiplesclerosis brain. *Brain.* 2016 Mar;139(Pt 3):807-15.

Haines, J. L., H. A. Terwedow, K. Burgess, M. A. et al. Linkage of the MHC to familial multiple sclerosis suggests genetic heterogeneity. The Multiple Sclerosis Genetics Group. *Hum Mol Genet* 1998;7(8): 1229-1234.

Hametner, S., I. Wimmer, L. Haider, S. Pfeifenbring, W. Bruck and H. Lassmann. Iron and neurodegeneration in the multiple sclerosis brain. *Ann Neurol* 2013;74(6): 848-861.

Harding K, Williams O, Willis M, et al. Clinical Outcomes of Escalation vs Early Intensive Disease-Modifying Therapy in Patients With Multiple Sclerosis. *JAMA Neurol.* 2019;76(5):536.

He A, Merkel B, Brown JW, et al. Timing of high-efficacy therapy for multiple sclerosis: a retrospective observational cohort study. *Lancet Neurol.* 2020;19(4):307-316.

Heß K, Starost L, Kieran NW, et al. Lesion stage-dependent causes for impaired remyelination in MS. *Acta Neuropathol* 2020; 140: 359–75.

Heming M, Börsch AL, Wiendl H, Meyer Zu Hörste G. High-dimensional investigation of the cerebrospinal fluid to explore and monitor CNS immune responses. *Genome Med.* 2022;14(1):94.

Horwitz, N. H. Lectures on the diseases of the nervous system. Jean Martin Charcot. Lectures on the localisation of cerebral and spinal diseases. Jean Martin Charcot. *Neurosurgery* 1995;37(5): 1022- 1025.

Hensiek AE, Roxburg R, Merenian M, et al. Osteopontin gene and clinical severity of multiple sclerosis. *J Neurol.* 2003;250(8):943-947.

Howell OW, Reeves CA, Nicholas R, et al. Meningeal inflammation is widespread and linked to cortical pathology in multiple sclerosis. *Brain* 2011;134:2755-2771.

Humphries C. Progressive multiple sclerosis: The treatment gap. *Nature.* 2012 Apr 12;484(7393):S10.

Hur E, Sawsan Y, Haws ME, et al. Osteopontin induced relapse and progression of autoimmune brain disease via enhanced survival of activated T cells. *Nature Immunol.* 2007;8, 77–86.

Iaffaldano P, Lucisano G, Caputo F, et al. Long-term disability trajectories in relapsing multiple sclerosis patients treated with early intensive or escalation treatment strategies. *Ther Adv Neurol Disord.* 2021;14.

Hutchinson, M. Neurodegeneration in multiple sclerosis is a process separate from inflammation: No. *Mult Scler* 2015;21(13): 1628-1631.

International Multiple Sclerosis Genetics, C. Multiple sclerosis genomic map implicates peripheral immune cells and microglia in susceptibility. *Science* 2019;365(6460).

Jäckle K, Zeis T, Schaeren-Wiemers N, et al. Molecular signature of slowly expanding lesions in progressive multiple sclerosis. *Brain* 2020; 143: 2073–88.

James RE, Schalks R, Browne E, et al. Persistent elevation of intrathecal pro-inflammatory cytokines leads to multiple sclerosis-like cortical demyelination and neurodegeneration. *acta neuropathol commun.* 2020;8(1):66.

James Bates RE, Browne E, Schalks R, et al. Lymphotoxin-alpha expression in the

meninges causes lymphoid tissue formation and neurodegeneration. *Brain* 2022; 145: 4287–307.

Jansson, M., Panoutsakopoulou, V., Baker, J., Klein, L., Cantor, H. Attenuated experimental autoimmune encephalomyelitis in Eta-1/osteopontin-deficient mice. *J. Immunol.* 2002;168:2096–2099.

Jelicic I, Al Nimer F, Wang J, et al. Memory B Cells Activate Brain-Homing, Autoreactive CD4+ T Cells in Multiple Sclerosis. *Cell* 2018; 175: 85-100.e23.

Jersild, C., A. Svejgaard and T. Fog. HL-A antigens and multiple sclerosis. *Lancet* 1972;1(7762): 1240- 1241.

Kappos L, Bar-Or A, Cree BAC, et al. Siponimod versus placebo in secondary progressive multiple sclerosis (EXPAND): a double-blind, randomised, phase 3 study. *Lancet.* 2018 Mar 31;391(10127):1263-1273.

Kappos L, Wolinsky JS, Giovannoni G, et al. Contribution of Relapse-Independent Progression vs Relapse-Associated Worsening to Overall Confirmed Disability Accumulation in Typical Relapsing Multiple Sclerosis in a Pooled Analysis of 2 Randomized Clinical Trials. *JAMA Neurol.* 2020;77(9):1132.

Katz Sand I, Krieger S, Farrell C, Miller AE. Diagnostic uncertainty during the transition to secondary progressive multiple sclerosis. *Mult Scler.* 2014 Oct;20(12):1654-7.

Kaunzner UW, Kang Y, Zhang S, et al. Quantitative susceptibility mapping identifies inflammation in a subset of chronic multiple sclerosis lesions. *Brain* 2019; 142: 133–45.

Khademi M, Bornsen L, Rafatnia F, et al. The effects of natalizumab on inflammatory mediators in multiple sclerosis: prospects for treatment-sensitive biomarkers. *Eur J Neurol.* 2009;16(4):528-536.

Kidd D, Barkhof F, McConnell R, Algra PR, Allen I V., Revesz T. Cortical lesions in multiple sclerosis. *Brain.* 1999;122 (Pt 1)(1):17-26.

Koch-Henriksen, N. The Danish Multiple Sclerosis Registry: a 50-year follow-up. *Mult Scler* 1999;5(4): 293-296.

König FB, Wildemann B, Nessler S, et al. Persistence of immunopathological and radiological traits in multiple sclerosis. *Arch Neurol.* 2008 Nov;65(11):1527-32.

Korakas, N. and M. Tsolaki. Cognitive impairment in multiple sclerosis: a review of neuropsychological assessments. *Cognitive And Behavioral Neurology* 2016;29(2): 55-67.

Krumbholz M, Theil D, Cepok S, et al. Chemokines in multiple sclerosis: CXCL12 and CXCL13 up-regulation is differentially linked to CNS immune cell recruitment. *Brain.* 2006;129:200-11.

Kuhlmann T, Ludwin S, Prat A, Antel J, Brück W, Lassmann H. An updated histological classification system for multiple sclerosis lesions. *Acta Neuropathol.* 2017 Jan;133(1):13-24.

Kurtzke JF. Rating neurologic impairment in multiple sclerosis: An expanded disability status scale (EDSS). *Neurology.* 1983;33(11):1444-1444.

Kutzelnigg, A., J. C. Faber-Rod, J. Bauer, C. F. Lucchinetti, P. S. Sorensen, H. Laursen, C. Stadelmann, W. Brück, H. Rauschka and M. Schmidbauer. Widespread demyelination in the cerebellar cortex in multiple sclerosis. *Brain pathology* 2007;17(1): 38-44.

Kutzelnigg A, Lucchinetti CF, Stadelmann C, et al. Cortical demyelination and diffuse white matter injury in multiple sclerosis. *Brain.* 2005;128(11):2705–12.

Kutzelnigg A, Lassmann H. Pathology of multiple sclerosis and related inflammatory demyelinating diseases. *Handb Clin Neurol.* 2014;122:15-58.

Labiano-Fontcuberta, A. and J. Benito-León. Radiologically isolated syndrome: An update on a rare entity. *Multiple Sclerosis Journal* 2016;22(12): 1514-1521.

Lassmann, H. The pathology of multiple sclerosis and its evolution. *Philos Trans R Soc Lond B Biol Sci* 1998;354(1390): 1635-1640.

Lassmann, H. Multiple sclerosis pathology. *Cold Spring Harbor perspectives in medicine* 2018;8(3): a028936.

Lassmann H. Pathogenic Mechanisms Associated With Different Clinical Courses of Multiple Sclerosis. *Front Immunol* 2019;9:3116.

Lassmann, H. and J. van Horssen. The molecular basis of neurodegeneration in multiple sclerosis. *FEBS Lett* 2011;585(23): 3715-3723.

Leppert, D. and J. Kuhle. Serum NfL levels should be used to monitor multiple sclerosis evolution - Yes. *Mult Scler* 2020;26(1): 17-19.

Leray E, Yaouanq J, Le Page E, et al. Evidence for a two-stage disability progression in multiple sclerosis. *Brain.* 2010;133(7).

Li R, Patterson KR, Bar-Or A. Reassessing B cell contributions in multiple sclerosis. *Nat Immunol.* 2018 Jul;19(7):696-707.

Link, H. and Y.-M. Huang. Oligoclonal bands in multiple sclerosis cerebrospinal fluid: an update on methodology and clinical usefulness. *Journal of neuroimmunology* 2006;180(1-2): 17-28.

Lisak RP, Benjamins JA, Nedelkoska L, et al. Secretory products of multiple sclerosis B cells are cytotoxic to oligodendroglia in vitro. *J Neuroimmunol.* 2012 May 15;246(1-2):85-95.

Lisak RP, Nedelkoska L, Benjamins JA, et al. B cells from patients with multiple

sclerosis induce cell death via apoptosis in neurons in vitro. *Journal of Neuroimmunology*. 2017;309:88-99.

Lorscheider J, Buzzard K, Jokubaitis V, et al. Defining secondary progressive multiple sclerosis. *Brain*. 2016;139(9):2395-2405.

Louapre, C. and C. Lubetzki. Neurodegeneration in multiple sclerosis is a process separate from inflammation: Yes. *Mult Scler* 2015;21(13): 1626-1628.

Lovato L, Willis SN, Rodig SJ, et al. Related B cell clones populate the meninges and parenchyma of patients with multiple sclerosis. *Brain*. 2011 Feb;134(Pt 2):534-41.

Lublin, F. D. and S. C. Reingold. Defining the clinical course of multiple sclerosis: results of an international survey. National Multiple Sclerosis Society (USA) Advisory Committee on Clinical Trials of New Agents in Multiple Sclerosis. *Neurology* 1996;46(4): 907-911.

Lublin FD, Reingold SC, Cohen JA, et al. Defining the clinical course of multiple sclerosis: the 2013 revisions. *Neurology*. 2014;83(3):278-86.

Lublin FD, Häring DA, Ganjgahi H, et al. How patients with multiple sclerosis acquire disability. *Brain*. 2022;145(9):3147-3161.

Lucchinetti CF, Popescu BO, Bunyan R, et al. Inflammatory cortical demyelination in early multiple sclerosis. *NEJM*. 2011;365(23):2188-2197.

Lucchinetti C, Brück W, Parisi J, Scheithauer B, Rodriguez M, Lassmann H. Heterogeneity of multiple sclerosis lesions: implications for the pathogenesis of demyelination. *Ann Neurol*. 2000 Jun;47(6):707-17.

Luchetti S, Fransen NL, van Eden CG, Ramaglia V, Mason M, Huitinga I. Progressive multiple sclerosis patients show substantial lesion activity that correlates with clinical disease severity and sex: a retrospective autopsy cohort analysis. *Acta Neuropathol*. 2018 Apr;135(4):511-528.

Machado-Santos J, Saji E, Tröscher AR, et al. The compartmentalized inflammatory response in the multiple sclerosis brain is composed of tissue-resident CD8+ T lymphocytes and B cells. *Brain* 2018;141:2066-2082.

Maggi, P., M. Absinta, M. Grammatico, L. et al. Central vein sign differentiates Multiple Sclerosis from central nervous system inflammatory vasculopathies. *Ann Neurol* 2018;83(2): 283-294.

Maggi P, Kuhle J, Schädelin S, et al. Chronic White Matter Inflammation and Serum Neurofilament Levels in Multiple Sclerosis. *Neurology* 2021; 97: e543–53.

Magliozzi R, Howell O, Vora A, et al. Meningeal B-cell follicles in secondary progressive multiple sclerosis associate with early onset of disease and severe cortical pathology. *Brain* 2007;130:1089-1104.

Magliozzi R, Howell OW, Durrenberger P, et al. Meningeal inflammation changes the balance of TNF signalling in cortical grey matter in multiple sclerosis. *J Neuroinflammation*. 2019;16(1):259.

Magliozzi R, Howell OW, Reeves CA, et al. A Gradient of neuronal loss and meningeal inflammation in multiple sclerosis. *Ann Neurol*. 2010;68(4):477-493.

Magliozzi R, Howell OW, Nicholas R, et al. Inflammatory intrathecal profiles and cortical damage in multiple sclerosis: Intrathecal Inflammation in MS. *Ann Neurol*. 2018;83(4):739-755.

Magliozzi R, Hametner S, Facchiano F, et al. Iron homeostasis, complement, and coagulation cascade as CSF signature of cortical lesions in early multiple sclerosis. *Ann Clin Transl Neurol*. 2019;6(11):2150-2163.

Magliozzi R, Scalfari A, Pisani AI, et al. The CSF Profile Linked to Cortical Damage Predicts Multiple Sclerosis Activity. *Ann Neurol*. 2020;88(3):562-573.

Magliozzi R, Fadda G, Brown RA, et al. "Ependymal-in" Gradient of Thalamic Damage in Progressive Multiple Sclerosis. *Annals of Neurology*. 2022;92(4):670-685.

Mahad DH, Trapp BD, Lassmann H. Pathological mechanisms in progressive multiple sclerosis. *Lancet Neurol*. 2015 Feb;14(2):183-93.

Mahajan KR, Nakamura K, Cohen JA, Trapp BD, Ontaneda D. Intrinsic and Extrinsic Mechanisms of Thalamic Pathology in Multiple Sclerosis. *Ann Neurol* 2020; 88: 81–92.

Malmeström C, Gillett A, Jernås M, et al. Serum levels of LIGHT in MS. *Mult Scler*. 2013;19(7):871-876.

Mandolesi G, Grasselli G, Musella A, et al. GABAergic signaling and connectivity on Purkinje cells are impaired in experimental autoimmune encephalomyelitis. *Neurobiol Dis* 2012; 46: 414–24.

Manouchehrinia, A., O. Beiki and J. Hillert. Clinical course of multiple sclerosis: A nationwide cohort study." *Mult Scler* 2017;23(11): 1488-1495.

Marastoni D, Pisani AI, Schiavi G, et al. CSF TNF and osteopontin levels correlate with the response to dimethyl fumarate in early multiple sclerosis. *Ther Adv Neurol Disord*. 2022 Jun 21;15:17562864221092124.

Marastoni D, Magliozzi R, Bolzan A, et al. CSF Levels of CXCL12 and Osteopontin as Early Markers of Primary Progressive Multiple Sclerosis. *Neurology(R) neuroimmunology & neuroinflammation*. 2021;8(6).

Martire MS, Moiola L, Rocca MA, Filippi M, Absinta M. What is the potential of paramagnetic rim lesions as diagnostic indicators in multiple sclerosis? *Expert Review of Neurotherapeutics*. 2022;22(10):829-837.

Matthews PM. Chronic inflammation in multiple sclerosis - seeing what was always there. *Nat Rev Neurol*. 2019 Oct;15(10):582-593.

McDonald, W. I., A. Compston, G. Edan, et al. Recommended diagnostic criteria for multiple sclerosis: guidelines from the International Panel on the diagnosis of multiple sclerosis. *Ann Neurol* 2001;50(1): 121- 127.

Meinl E, Krumbholz M, Derfuss T, Junker A, Hohlfeld R. Compartmentalization of inflammation in the CNS: a major mechanism driving progressive multiple sclerosis. *J Neurol Sci*. 2008 Nov 15;274(1-2):42-4.

Metz I, Weigand SD, Popescu BF, et al. Pathologic heterogeneity persists in early active multiple sclerosis lesions. *Ann Neurol*. 2014 May;75(5):728-38.

Miller DH, Thompson AJ, Barkhof F, Berry I, Kappos L, Scotti G. Magnetic resonance imaging in monitoring the treatment of multiple sclerosis: Concerted Action Guidelines. *J Neurol Neurosurg Psychiatry*. 1991;54(8):683-688.

Miller, D., B. G. Weinshenker, M. Filippi, et al. Differential diagnosis of suspected multiple sclerosis: a consensus approach. *Multiple Sclerosis Journal* 2008;14(9): 1157-1174.

Miller, D. H., D. T. Chard and O. Ciccarelli. Clinically isolated syndromes. *The Lancet Neurology* 2012;11(2): 157-169.

Miller DH, Leary SM. Primary-progressive multiple sclerosis. *Lancet Neurol*. 2007; 6(10):903-912

Miller DH, Rudge P, Johnson G, et al. Serial gadolinium enhanced magnetic resonance imaging in multiple sclerosis. *Brain*. 1988 Aug;111 (Pt 4):927-39.

Mills, R. and C. Young. A medical definition of fatigue in multiple sclerosis. *QJM: An International Journal of Medicine* 2008;101(1): 49-60.

Monaco S, Nicholas R, Reynolds R, Magliozzi R. Intrathecal Inflammation in Progressive Multiple Sclerosis. *Int J Mol Sci*. 2020 Nov 3;21(21):8217.

Montalban X, Hauser SL, Kappos L, et al. Ocrelizumab versus Placebo in Primary Progressive Multiple Sclerosis. *N Engl J Med*. 2017 Jan 19;376(3):209-220.

Murugaiyan G, Mittal A, Weiner HL. Increased osteopontin expression in dendritic cells amplifies IL-17 production by CD41T cells in experimental autoimmune encephalomyelitis and in multiple sclerosis. *J Immunol*. 2008;181:7480-7488.

Niino M, Kikuchi S, Fukazawa T, Yabe I, Tashiro K. Genetic polymorphisms of

Osteopontin in association with multiple sclerosis in Japanese patients. *J Neuroimmunol.* 2003;136(1-2):125-129.

Okuda, D. T., E. M. Mowry, A. Beheshtian, et al. Incidental MRI anomalies suggestive of multiple sclerosis: the radiologically isolated syndrome. *Neurology* 2009;72(9): 800-805.

Olesen, J., Gustavsson, A., Svensson, M., Wittchen, H.U. and Jönsson, B. CDBE2010 study group; European Brain Council. The economic cost of brain disorders in Europe. *Eur. J. Neurol.* 2012;19:155–162.

Olsson, T., L. F. Barcellos and L. Alfredsson. Interactions between genetic, lifestyle and environmental risk factors for multiple sclerosis. *Nat Rev Neurol* 2017;13(1): 25-36.

Orsi G, Hayden Z, Cseh T, Berki T, Illes Z. Osteopontin levels are associated with late-time lower regional brain volumes in multiple sclerosis. *Sci Rep.* 2021;11(1):23604.

Orsi G, Cseh T, Hayden Z, et al. Microstructural and functional brain abnormalities in multiple sclerosis predicted by osteopontin and neurofilament light. *Mult Scler Relat Disord.* 2021;51:102923.

Orton, S. M., B. M. Herrera, I. M. Yee, et al. Sex ratio of multiple sclerosis in Canada: a longitudinal study. *Lancet Neurol* 2006;5(11): 932-936.

Pearce, J. M. Historical descriptions of multiple sclerosis. *Eur Neurol* 2005;54(1): 49-53.

Peterson JW, Bö L, Mörk S, Chang A, Trapp BD. Transected neurites, apoptotic neurons, and reduced inflammation in cortical multiple sclerosis lesions. 2001;50(3):389-400.

Pham DL, Prince JL. Adaptive fuzzy segmentation of magnetic resonance images. *IEEE Trans Med Imaging.* 1999;18(9):737-752.

Picon C, Jayaraman A, James R, et al. Neuron-specific activation of necroptosis signaling in multiple sclerosis cortical grey matter. *Acta Neuropathol.* 2021;141(4):585-604.

Pikor NB, Prat A, Bar-Or A, Gommerman JL. Meningeal Tertiary Lymphoid Tissues and Multiple Sclerosis: A Gathering Place for Diverse Types of Immune Cells during CNS Autoimmunity. *Front Immunol.* 2016;6.

Pinteac R, Montalban X, Comabella M. Chitinases and chitinase-like proteins as biomarkers in neurologic disorders. *Neurol Neuroimmunol Neuroinflamm.* 2020;8(1):e921.

Pisani AI, Scalfari A, Crescenzo F, Romualdi C, Calabrese M. A novel prognostic score to assess the risk of progression in relapsing–remitting multiple sclerosis patients. *Eur J Neurol.* 2021;28(8):2503-2512.

Planas R, Santos R, Tomas-Ojer P, et al. GDP-*f*-fucose synthase is a CD4⁺ T cell-specific autoantigen in DRB3*02:02 patients with multiple sclerosis. *Sci Transl Med* 2018; 10.

Polman, C. H., S. C. Reingold, B. Banwell, et al. Diagnostic criteria for multiple sclerosis: 2010 revisions to the McDonald criteria. *Ann Neurol* 2011;69(2): 292-302.

Polman, C. H., S. C. Reingold, G. Edan, et al. Diagnostic criteria for multiple sclerosis: 2005 revisions to the "McDonald Criteria". *Ann Neurol* 2005;58(6): 840-846.

Poser, C. M., D. W. Paty, L. Scheinberg, et al., New diagnostic criteria for multiple sclerosis: guidelines for research protocols. *Ann Neurol* 1983;13(3): 227-231.

Prineas, J. W., R. O. Barnard, E. E. Kwon, L. R. Sharer and E. S. Cho. Multiple sclerosis: remyelination of nascent lesions. *Ann Neurol* 1993;33(2): 137-151.

Ransohoff RM. Multiple sclerosis: role of meningeal lymphoid aggregates in progression independent of relapse activity. *Trends Immunol*. Published online 2023.

Reali C, Magliozzi R, Roncaroli F, Nicholas R, Howell OW, Reynolds R. B cell rich meningeal inflammation associates with increased spinal cord pathology in multiple sclerosis. *Brain Pathology* 2020; 30: 779–93.

Reynolds R, Roncaroli F, Nicholas R, Radotra B, Gveric D, Howell O. The neuropathological basis of clinical progression in multiple sclerosis. *Acta Neuropathol* 2011; 122:155-70.

Rocca MA, Mesaros S, Pagani E, Sormani MP, Comi G, Filippi M. Thalamic damage and long-term progression of disability in multiple sclerosis. *Radiology*. 2010;257(2):463-469.

Romme Christensen J, Bořnsen L, Khademi M, et al. CSF inflammation and axonal damage are increased and correlate in progressive multiple sclerosis. *Mult Scler*. 2013; 19(7):877-884.

Rotstein D, Montalban X. Reaching an evidence-based prognosis for personalized treatment of multiple sclerosis. *Nat Rev Neurol*. 2019 May;15(5):287-300.

Rotstein D, Solomon JM, Sormani MP, et al. Association of No Evidence of Disease Activity With No Long-term Disability Progression in Multiple Sclerosis: A Systematic Review and Meta-analysis. *Neurology*. 2022;10.1212/WNL.0000000000200549.

Rudick RA, Lee JC, Simon J, Fisher E. Significance of T2 lesions in multiple sclerosis: A 13-year longitudinal study. *Ann Neurol*. 2006;60(2):236-242.

Sawcer S. The complex genetics of multiple sclerosis: pitfalls and prospects. *Brain*. 2008;131(12):3118-3131.

Sawcer, S., R. J. Franklin and M. Ban. Multiple sclerosis genetics. *Lancet Neurol* 2014;13(7): 700-709.

Scalfari A, Neuhaus A, Degenhardt A, et al. The natural history of multiple sclerosis, a geographically based study 10: relapses and long-term disability. *Brain*.

2010;133(7):1914-1929.

Scalfari A, Neuhaus A, Daumer M, Muraro PA, Ebers GC. Onset of secondary progressive phase and long-term evolution of multiple sclerosis. *J Neurol Neurosurg Psychiatry*. 2014;85(1):67-75.

Scalfari A, Lederer C, Daumer M, Nicholas R, Ebers GC, Muraro PA. The relationship of age with the clinical phenotype in multiple sclerosis. *Mult Scler*. 2016;22(13):1750-1758.

Scalfari A, Neuhaus A, Daumer M, DeLuca GC, Muraro PA, Ebers GC. Early relapses, onset of progression, and late outcome in multiple sclerosis. *JAMA Neurol*. 2013;70(2).

Scalfari A, Romualdi C, Nicholas RS, et al. The cortical damage, early relapses, and onset of the progressive phase in multiple sclerosis. *Neurology*. 2018;90(24):e2107-e2118.

Serafini B, Rosicarelli B, Magliozzi R, Stigliano E, Aloisi F. Detection of Ectopic B-cell Follicles with Germinal Centers in the Meninges of Patients with Secondary Progressive Multiple Sclerosis. *Brain Pathology* 2004; 14: 164–74.

Schirmer L, Albert M, Buss A, et al. Substantial early, but nonprogressive neuronal loss in multiple sclerosis (MS) spinal cord. *Ann Neurol* 2009; 66: 698–704.

Schmierer K, Parkes HG, So PW, et al. High field (9.4 Tesla) magnetic resonance imaging of cortical grey matter lesions in multiple sclerosis. *Brain*. 2010;133(3):858-867.

Schumacher, G. A., G. Beebe, R. F. Kibler, et al. Problems of experimental trials of therapy in multiple sclerosis: report by the panel on the evaluation of experimental trials of therapy in multiple sclerosis." *Annals of the New York Academy of Sciences* 1965;122(1): 552-568.

Seewann A, Kooi EJ, Roosendaal SD, et al. Postmortem verification of MS cortical lesion detection with 3D DIR. *Neurology*. 2012;78(5):302-308.

Seewann A, Vrenken H, Kooi EJ, et al. Imaging the tip of the iceberg: Visualization of cortical lesions in multiple sclerosis. *Multiple Sclerosis Journal*. 2011;17(10):1202-1210.

Serafini B, Rosicarelli B, Magliozzi R, Stigliano E, Aloisi F. Detection of ectopic B-cell follicles with germinal centers in the meninges of patients with secondary progressive multiple sclerosis. *Brain Pathol*. 2004 Apr;14(2):164-74.

Shechter R, London A, Schwartz M. Orchestrated leukocyte recruitment to immune-privileged sites: absolute barriers versus educational gates. *Nat Rev Immunol*. 2013 Mar;13(3):206-18.

Sinclair C, Mirakhur M, Kirk J, Farrell M, McQuaid S. Up-regulation of osteopontin and alphaBeta-crystallin in the normal-appearing white matter of multiple sclerosis: an

immunohistochemical study utilizing tissue microarrays. *Neuropathol Appl Neurobiol.* 2005;31:292-303.

Singh, S., T. Dallenga, A. Winkler, et al. Relationship of acute axonal damage, Wallerian degeneration, and clinical disability in multiple sclerosis. *Journal of neuroinflammation* 2017;14(1): 1-15.

Solomon, A. J., R. T. Naismith and A. H. Cross. Misdiagnosis of multiple sclerosis: Impact of the 2017 McDonald criteria on clinical practice. *Neurology* 2019;92(1): 26-33.

Sorensen PS, Fox RJ, Comi G. The window of opportunity for treatment of progressive multiple sclerosis. *Curr Opin Neurol.* 2020 Jun;33(3):262-270.

Sormani MP, Li DK, Bruzzi P, Stubinski B, Cornelisse P, Rocak S, De Stefano N. Combined MRI lesions and relapses as a surrogate for disability in multiple sclerosis. *Neurology.* 2011 Nov 1;77(18):1684-90.

Sormani MP, Calabrese M, Signori A, Giorgio A, Gallo P, de Stefano N. Modeling the distribution of new MRI cortical lesions in multiple sclerosis longitudinal studies. *PLoS One.* 2011;6(10):6-10.

Soroosh P, Doherty TA, So T, et al. Herpesvirus entry mediator (TNFRSF14) regulates the persistence of T helper memory cell populations. *Journal of Experimental Medicine.* 2011;208(4):797-809.

Starost L, Lindner M, Herold M, et al. Extrinsic immune cell-derived, but not intrinsic oligodendroglial factors contribute to oligodendroglial differentiation block in multiple sclerosis. *Acta Neuropathol* 2020; 140: 715–36.

Stathopoulos P, Dalakas MC. Evolution of Anti-B Cell Therapeutics in Autoimmune Neurological Diseases. *Neurotherapeutics.* Published online 2022.

Steinman, L. A molecular trio in relapse and remission of multiple sclerosis. *Nat. Rev. Immunol.* 2009;9:440–448.

Steinman L, Zamvil SS. Beginning of the end of two-stage theory purporting that inflammation then degeneration explains pathogenesis of progressive multiple sclerosis. *Curr Opin Neurol.* 2016;29(3):340-4.

Stern, J. N., G. Yaari, J. A. Vander Heiden, et al. B cells populating the multiple sclerosis brain mature in the draining cervical lymph nodes. *Sci Transl Med* 2014;6(248): 248ra107.

Stilund M, Reuschlein AK, Christensen T, Møller HJ, Rasmussen PV, Petersen T. Soluble CD163 as a marker of macrophage activity in newly diagnosed patients with multiple sclerosis. *PLoS One.* 2014;9(6):e98588.

Tamada K, Shimozaki K, Chapoval AI, et al. Modulation of T-cell-mediated immunity in

tumor and graft-versus-host disease models through the LIGHT co-stimulatory pathway. *Nat Med.* 2000;6(3):283-289.

Tardif CL, Bedell BJ, Eskildsen SF, Collins DL, Pike GB. Quantitative magnetic resonance imaging of cortical multiple sclerosis pathology. *Mult Scler Int.* 2012;2012:1-13.

Teunissen CE, Petzold A, Bennett JL, et al. A consensus protocol for the standardization of cerebrospinal fluid collection and biobanking. *Neurology.* 2009;73(22):1914-1922.

Thompson AJ, Banwell BL, Barkhof F, et al. Diagnosis of multiple sclerosis: 2017 revisions of the McDonald criteria. *The Lancet Neurology.* 2018;17(2):162-173.

Thompson AJ, Baranzini SE, Geurts J, Hemmer B, Ciccarelli O. Multiple sclerosis. *Lancet.* 2018;391(10130):1622-1636

Tillack, K., P. Breiden, R. Martin and M. Sospedra. T lymphocyte priming by neutrophil extracellular traps links innate and adaptive immune responses. *J Immunol* 2012;188(7): 3150-3159.

Tintore M, Rovira A, Arrambide G, et al. Brainstem lesions in clinically isolated syndromes. *Neurology.* 2010;75(21).

Tintore M, Rovira À, Río J, et al. Defining high, medium and low impact prognostic factors for developing multiple sclerosis. *Brain.* 2015;138(7).

Tobin WO, Kalinowska-Lyszczarz A, Weigand SD, et al. Clinical Correlation of Multiple Sclerosis Immunopathologic Subtypes. *Neurology.* 2021 Nov 9;97(19):e1906-e1913.

Trapp BD, Vignos M, Dudman J, et al. Cortical neuronal densities and cerebral white matter demyelination in multiple sclerosis: a retrospective study. *Lancet Neurol* 2018; 17: 870–84.

Treaba CA, Herranz E, Barletta VT, et al. The relevance of multiple sclerosis cortical lesions on cortical thinning and their clinical impact as assessed by 7.0-T MRI. *J Neurol.* 2021;268(7):2473-2481.

Truyen, L., J. H. van Waesberghe, M. A. van Walderveen, et al. Accumulation of hypointense lesions ("black holes") on T1 spin-echo MRI correlates with disease progression in multiple sclerosis. *Neurology* 1996;47(6): 1469-1476.

University of California, S. F. M. E. T., B. A. Cree, P. et al. Long-term evolution of multiple sclerosis disability in the treatment era. *Annals of neurology* 2016;80(4): 499-510.

University of California, San Francisco MS-EPIC Team, Cree BAC, Hollenbach JA, et al. Silent progression in disease activity-free relapsing multiple sclerosis. *Ann Neurol.* 2019

May;85(5):653-666.

Valencia-Vera, E., A. M.-E. Garcia-Ripoll, A. Enguix, C. Abalos-Garcia and M. J. Segovia-Cuevas. Application of κ free light chains in cerebrospinal fluid as a biomarker in multiple sclerosis diagnosis: development of a diagnosis algorithm. *Clinical Chemistry and Laboratory Medicine* 2018;56(4): 609- 613.

van Olst L, Rodriguez-Mogeda C, Picon C, et al. Meningeal inflammation in multiple sclerosis induces phenotypic changes in cortical microglia that differentially associate with neurodegeneration. *Acta Neuropathol.* 2021;141(6).

Vercellino M, Plano F, Votta B, Mutani R, Giordana MT, Cavalla P. Grey matter pathology in multiple sclerosis. *J Neuropathol Exp Neurol.* 2005;64(12):1101-1107.

Vercellino, M., S. Masera, M. Lorenzatti, et al. Demyelination, inflammation, and neurodegeneration in multiple sclerosis deep gray matter." *Journal of Neuropathology & Experimental Neurology* 2009;68(5): 489-502.

Vittinghoff E, Glidden DV, Shiboski SC, McCulloch CE. *Regression Methods in Biostatistics: Linear, Logistic, Survival, and Repeated Measures Models*, 2nd ed. Springer; 2011.

Wang J, Foster A, Chin R, et al. The complementation of lymphotoxin deficiency with LIGHT, a newly discovered TNF family member, for the restoration of secondary lymphoid structure and function. *Eur J Immunol.* 2002;32(7):1969.

Wattjes, M. P., A. Rovira, D. Miller, et al. Evidence-based guidelines: MAGNIMS consensus guidelines on the use of MRI in multiple sclerosis--establishing disease prognosis and monitoring patients. *Nat Rev Neurol* 2015;11(10): 597-606.

Willing, A., O. A. Leach, F. Ufer, et al. CD8(+) MAIT cells infiltrate into the CNS and alterations in their blood frequencies correlate with IL-18 serum levels in multiple sclerosis. *Eur J Immunol* 2014;44(10): 3119-3128.

Zrzavy T, Hametner S, Wimmer I, Butovsky O, Weiner HL, Lassmann H. Loss of 'homeostatic' microglia and patterns of their activation in active multiple sclerosis. *Brain* 2017; 140: 1900–13.